Order Number 8920160

Chemical-biochemical process and ventilation study of the change in gaseous pollutants in ventilated swine buildings

Liao, Chung-Min, Ph.D.

Iowa State University, 1989

U·M·I
300 N. Zeeb Rd.
Ann Arbor, MI 48106

Chemical-biochemical process and ventilation study of the change in gaseous pollutants in ventilated swine buildings

by

Chung-Min Liao

A Dissertation Submitted to the
Graduate Faculty in Partial Fulfillment of the
Requirements for the Degree of
DOCTOR OF PHILOSOPHY

Major: Agricultural Engineering

Approved:

Signature was redacted for privacy.

In Charge of Major Work

Signature was redacted for privacy.

For the Major Department

Signature was redacted for privacy.

For the Graduate College

Iowa State University
Ames, Iowa

1989

TABLE OF CONTENTS

LIST OF TABLES

LIST OF FIGURES

LIST OF SYMBOLS

A	surface area of swine manure pit, cm^2
$A(k)$	constants account to the general solution of gas concentration
A_o	effective area of the stream at discharge from an open end duct or at contracted section, cm^2
A_{ij}	cofactor of the flow matrix $\underline{Q}$
B_{ij}	element of the inverse flow matrix $\underline{Q}^{-1}$
$C(s,s)$	equilibrium concentration of gaseous pollutant, ppm
$C(t)$	time-dependent concentration profile
$\underline{C}(t)$	column matrix (vector) whose elements are the airspace concentrations
C_e	extract concentration, ppm
C_g	concentration of the compound in gas phase, mol/l
$C_g(s)$	interfacial concentration in gas phase, mol/l
C_i	concentration of the compound i in liquid phase, mg/l
C_o	a reference concentration in age distribution measurement
C_s	concentration of gas in the supply air, ppm
C_w	concentration of the compound in liquid phase, mol/l
$C_w(s)$	interfacial concentration in liquid phase, mol/l
C_w^*	soluble concentration of the compound in equilibrium with the partial pressure P_g of the compound in gas phase, mol/l
d_g	thickness of diffusion boundary of gas phase, cm
D_g	molecular diffusion coefficient of gas phase, cm^2/s
D_i	molecular diffusion coefficient of the compound i, cm^2/s

D_o	diffusion coefficient of oxygen, cm^2/s
d_w	thickness of diffusion boundary of liquid phase, cm^2/s
D_w	molecular diffusion coefficient of liquid phase, cm^2/s
E(t)	probability density function for exit age
e	nominal air-exchange rate, e=Q/V, 1/hr
ey(k)	eigenvalues of $\underline{T}^{-1}$
$e_{y_{max}}$	maximum eigenvalue of $\underline{T}^{-1}$
F	the rate of transfer of the compound per unit area, mol/cm^2-s
F(t)	cumulative distribution function for exit age of fluid element
H	depth of swine manure pit, m
H_i	Henry's law constant of the compound i, atm-m^3/g-mole
H_o	width of long shot, cm
$\underline{I}$	unit matrix
I(t)	probability density function for internal age
$I_p(t)$	local probability density function for internal age
K	Henry's law constant, $K=C_g(s)/C_w(s)$
K'	proportionality constant
K_g	transfer coefficient for gas phase, cm/s (or, g-mole/cm^2-s)
K_i	fraction of the total air volume
K_o	overall transfer coefficient, cm/s (or, g-mole/cm^2-s)
K_w	transfer coefficient for liquid phase, cm/s (or, g-mole/cm^2-s)
K_1	coefficient used in temperature correlation for Henry's law, kg/m^3-atm
K_2	coefficient used in temperature correlation for Henry's law, °K

m_i	the amount of tracer injected in space i, g
$\dot{m}(i)$	equilibrium generation rate for the compound i, g/s
$\dot{m}(s,s)$	equilibrium generation rate of the gaseous pollutant, g/s
$\dot{m}(t)$	time-dependent generation rate of gaseous pollutant, g/s
$\bar{M}$	average molecular weight of the liquid swine manure, g/g-mole
M_i	molecular weight of the compound i, g/g-mole
$M^{(n)}$	nth moment about the origin of concentration or age distribution function
$\underline{M}^{(n)}$	nth moment matrix
P	total pressure in gas phase, atm
$\underline{P}$	transition probability matrix
Pg	equilibrium partial pressure of gas above a solution, atm
P_{ij}	transition probability of gaseous pollutant released at space j to pass space i
Q	total volumetric flow rate of air supplied to system, m^3/hr
$\underline{Q}$	flow matrix
$\underline{Q}^{-1}$	inverse of flow matrix
$\underline{Q}^T$	transported flow matrix
$\underline{Q}_e$	extract airflow column matrix (vector)
$\underline{Q}_s$	diagonal supply airflow matrix
r	entertainment ratio
R_f	relative response factor
S_c	Schmidt Number
S_e	slope of the decay concentration profile
T	temperature, °C

$\underline{T}$	$\underline{T}$ matrix, $\underline{T}=\underline{Q}^{-1}\ \underline{V}$
$\underline{T}^{-1}$	inverse of $\underline{T}$ matrix
t	generic symbol for time
t_i	internal age of a fluid element, hr
t_n	mean-holding time of airflow, $t_n=V/Q$, hr
t_o	a sufficiently long period of time
t_r	residence time of a fluid element, hr
t_{rl}	residual life time of a fluid element, hr
t_p	mean-holding time of gaseous pollutant, hr
U	air velocity, m/s
U_i	local purging flow rate, m^3/hr
V	total volume of the ventilated system, m^3
$\underline{V}$	diagonal volume matrix
x	distance from the face of the outlet, m
X_i	concentration of the compound i in liquid phase, mole fraction
X_i^*	equilibrium concentration of the compound i in gas phase, mole fraction
$\underline{X}(k)$	eigenvectors of $\underline{T}^{-1}$
Z	the length of swine manure surface, m
ß	cleanness factor
g	mixing factor
$\Phi(t)$	total cumulative distribution function for internal age
$\Phi_p(t)$	local cumulative distribution function for internal age
$\Psi(t)$	total cumulative distribution function for residual life time
$\Psi_p(t)$	local cumulative distribution function for residual life time

$\psi(t)$ total probability density function for residual life time

$\psi_p(t)$ local probability density function for residual life time

$X(t)$ cumulative distribution function for residence time

$\chi(t)$ probability density function for residence time

subscripts

e refers to extract

g refers to gas phase

s refers to supply

w refers to liquid phase

superscripts

* refers to dimensionless form

- refers to averaged quantity

INTRODUCTION

The increased use of confinement buildings has resulted from an economic need for increased productivity. Enclosing and concentrating swine, however, meant concentrating their waste products and pollutants. Potential health hazards to the workers and swine occur when they are exposed to these agents. Swine producers are concerned about gases produced in liquid manure storage pits in buildings with partially or totally slatted floors. The main gaseous pollutants contained in a swine confinement building with known physiological effects include ammonia, carbon dioxide, hydrogen sulfide, and methane.

There is ample evidence that several of the gaseous pollutants released during the decomposition of excreta, if concentrated, can cause injury or even death to swine. Prolonged exposure to low levels of those gaseous pollutants may be of considerable importance, although health effects are largely unknown.

The most common remedy for decreasing gaseous pollutant levels is to increase ventilation rates above values needed for limiting swine exposure to gaseous pollutants. This implies, at least for a steady gaseous pollutant source, that its spread and residence time within a ventilated enclosure shall be minimized; i.e., the sooner the gaseous pollutants reach the exhaust duct, the better is the ventilation.

Gaseous pollutants spread is characterized by the gaseous pollutants themselves and the distribution of the supplied airflow within the ventilated enclosure. Thus, proper air distribution is essential in a ventilated enclosure. Although theoretically speaking,

the Navier-Stokes equation can be used to represent airflow and distribution in such a system, it is extremely difficult, if not impossible, to solve it exactly. The problems are more difficult for ventilation systems with multiple inlets and outlets. A method to define the local flow rate does not presently exist. Velocity profiles can yield a solution, but these are usually hard to obtain.

From the physical point of view, the transportation and mixing process in any flow system often is conceptually divided into a systematic part, represented by the fluid velocity, and a random part. The latter is due to molecular diffusion and turbulent movement. The molecular diffusion is represented by a molecular diffusion coefficient. It also uses the turbulent mixing coefficient to represent the phenomena of turbulence (Csanady, 1973).

There are two main approaches to modeling a turbulent flow system. One approach is the so-called advection-diffusion model (i.e., distributed-parameter model). The diffusion coefficients in this model usually are estimated by tracer experiments. The concentration of tracers are measured, and the diffusion coefficients are calculated by finding a solution to the advection-diffusion equation.

This approach, mainly used in the flow systems, becomes a one-dimensional equation in the main flow. Pollutant transported in rivers is an example of a flow system using this approach. In a three-dimensional flow system, e.g., in a ventilated enclosure, the meaning of turbulent mixing coefficient always will become ambiguous.

The other approach is the lumped-parameter model. In this model, the internal-flow in a ventilated enclosure can be represented by a number of interconnected perfect mixing spaces. When it comes to formulating an airflow model in an enclosure and to deriving the terms that constitute the model, the total volumetric flow rate of outdoor air to each mixing airspace is important.

Therefore, it is possible to assume that the airflow in a ventilated enclosure is like a box filled with turbulent air with almost no net flow rate. Thus, at any point within the enclosure, there are air and gaseous pollutants of different ages. The net flow rate at which gaseous pollutants will be removed from the ventilated systems cannot be easily determined from velocity data. The optimum way to purify the air to an acceptable air quality may be obtained if the age distribution of the polluted air is known. Also, the concept of age, or residence time, is applicable to characterize how the supplied air or gaseous pollutant is spread within a ventilated enclosure and how quickly a gaseous pollutant is removed.

Another method for controlling gaseous pollutants in swine confinement buildings is the chemical-biochemical process. Several studies have pursued the possibility of applying chemical-biochemical additives to the manure pit. These additives tend to suppress the gaseous pollutants released. Generally, such chemical-biochemical additives owe their effectiveness to the ability to act as a digestive (bacteria enzyme) agent, or as a strong oxidizing agent.

The effect of a chemical-biochemical process to reduce the generation rate of gaseous pollutants is unpredictable. Because air sampling and analysis for gaseous pollutants are complex, costly, and time-consuming, the emission rate models are useful in predicting the emission rate of gaseous pollutants and assessing air quality near manure waste disposal sites in an economical, simple, and quick manner. Therefore, emission models have been developed and gradually accepted to estimate toxic emissions from hazardous wastes and land disposal sites. Although many published emission models are based on a well-established mass transfer theory, each model is unique. Most of the available emission models deal with complex equations which cannot be applied easily to practical engineering solutions. Therefore, it is important that an emission model be developed which is capable of predicting the emission rate of gaseous pollutants from a manure pit and of assessing air quality simply and quickly.

OBJECTIVES

In specific terms, the purposes of this thesis are:

1. to determine the effect of chemical-bacteria additives on the production of gases from the surface of swine manure,
2. to model the dynamic behavior of gaseous pollutants in ventilated airspaces, and
3. to evaluate the concentration distribution of gaseous pollutants with data from research literature and field chamber tests.

LITERATURE REVIEW

The Formation of Volatile Compounds

Volatile compounds identified in swine confinement building

To characterize the smell of swine wastes, a great number of volatile compounds have been identified in the air of swine confinement units. Most researchers have identified compounds in the atmosphere of swine buildings. Some researchers, however, have identified volatile compounds in the liquid manure. Compounds identified by different researchers are listed in Table 1. Some volatile compounds that have been found only in the wastes can be explained by:

1. volatile compounds present in the wastes are undetectable in the air because of chemical reactions in the atmosphere, forming compounds not in the wastes; and
2. discrepancies appear because of the use of different analytical techniques by researchers analyzing air and waste samples.

Overall processes leading to accumulations of volatile compounds

The conversion of feed to wastes as stored in manure pits can be divided into two stages: (1) the passage through the swine, producing urine and feces; and (2) the anaerobic degradation of the mixture of feces and urine during storage.

In the alimentary canal, the feed is partially absorbed by swine, and partially subjected to microbial activity in the intestine. Here, interrelations exist between microbial catabolism and mammalian metabolism. Some products of microbial activity are absorbed and

TABLE 1. Literature review of volatiles identified in the air of swine confinement units and in anaerobically stored swine manure wastes

Components	AIR	WASTE
Methanol	1, 2 [a]	
Ethanol	1, 2	
1-propanol	2	
2-propanol	1, 2	
1-Butanol	2, 10	
2-Butanol	10	
2-Methyl-1-propanol	2	
3-Methyl-1-butanol	10	
2-Ethoxy-1-propanol	10	
2,3-Butanediol	10	
3-Hydroxy-2-butanone	10	
Propanone	8	
3-Pentanone	8	
2-Octanone	10	
2,3-Butanedione	7, 10	
Ethanal	2, 8	
Methanal	2	

[a] Note:

1. Bethea and Narayan (1972)
2. Merkel et al. (1969)
3. White et al. (1971)
4. Miner and Hazen (1969)
5. Burnett (1969)
6. Mosier et al. (1973)
7. Hammond et al. (1979)
8. Hartung et al.(1971)
9. Day et al. (1965)
10. Miner et al. (1975)
11. Banwart and Bremner (1975b)
12. Elliott and Travis (1973)
13. Yasuhara and Fuwa (1977a)
14. Avery et al. (1975)
15. Yasuhara and Fuwa (1977b)

TABLE 1. (continued)

Components	AIR	WASTE
Propanal	2, 8	
Butanal	2	
Pentanal	2	
Hexanal	2, 7	
Heptanal	2, 7	
Octanal	2	
Nonanal	7	
Decanal	2	
2-Methyl-1-propanal	2	
Ethanoic acid	10	
Propanoic acid	5, 10	
Butanoic acid	5, 7, 10	
2-Methylpropionic acid	5	
2-Methylbutanoic acid	10	
Pentanoic acid	10	
Heptanoic acid	10	
Phenol	7, 10	13
3-Methylphenol	13	
4-Methylphenol	7, 10	13
4-Ethylphenol	10	
Toluene	10	
Xylene	10	
Indane	10	
Benzaldehyde	10	
Benzoic acid	10	13
Methylphthalene	10	
Acetophenone	10	
Phenylacetic acid	7	13
3-Phenylpropionic acid	7	13
Ammonia	6, 10	
Indole	15	
Skatole	7	15
Methylamine	6, 4	
Ethylamine	6, 4	
Trimethylamine	6, 10	
Triethylamine	4	
Carbonylsulphide	11, 12	
Hydrogen sulfide	3, 5, 9, 11, 12, 14	
Methanethiol	11	
Methyl mercaptan	5, 11	
Ethyl mercaptan	5, 11	
Dimethyl sulfide	3	
Diethyl sulfide	3	
Dimethyldisulphide	10, 11	
Dimethyltrisulphide	10	

transformed by the pig and excreted with the urine. Other products, endogenous secretions, and unchanged constituents are excreted in the feces. In general, the urinary constituents are products of mammalian origin, while the volatile compounds in the feces are products of anaerobic microbial catabolism. During storage, many constituents are transformed by microbial activity. Fresh swine manure contains 50 percent to 70 percent biodegradable materials, including carbohydrates, proteins, and fats from which microorganisms obtain energy for growth by metabolizing these substrate sources into simple compounds. The types of compounds produced depends on the oxygen (O_2) levels during waste decomposition.

When O_2 is not limited, organic waste decomposes primarily into CO_2 and H_2O and will result in only a few gaseous pollutants being accumulated (see Figure 1). Some water-soluble inorganic compounds of nitrogen (N) and sulfur (S) also will accumulate. Under anaerobic conditions, waste decomposes more slowly, many intermediate gaseous pollutants are released, and less CO_2 is released per unit of substrate consumed.

Partial processes leading to the formation of volatile compounds

The volatile fatty acids are the most common in swine manure. Total amounts in the waste range from 4 to 25 g/l (McGill and Jackson, 1977; Cooper and Cornforth, 1978). Acetic acid and propionic acid represent about 60 percent and 25 percent respectively of the total amount of volatile fatty acids. Butyric, isobutyric, branched valeric and n-valeric acids range from 3 percent to 10 percent each. Synthesis of

acetic acid from CO_2 and H_2 seems to be a common pathway in anaerobic ecosystems (Balch et al. 1977).

Adamson et al. (1975) and Francis et al. (1975) could identify a great number of volatile products after the addition of glucose to soils under anaerobic conditions. The identified products in the headspace consist of two aldehydes, four ketones, nine alcohols, and 15 esters.

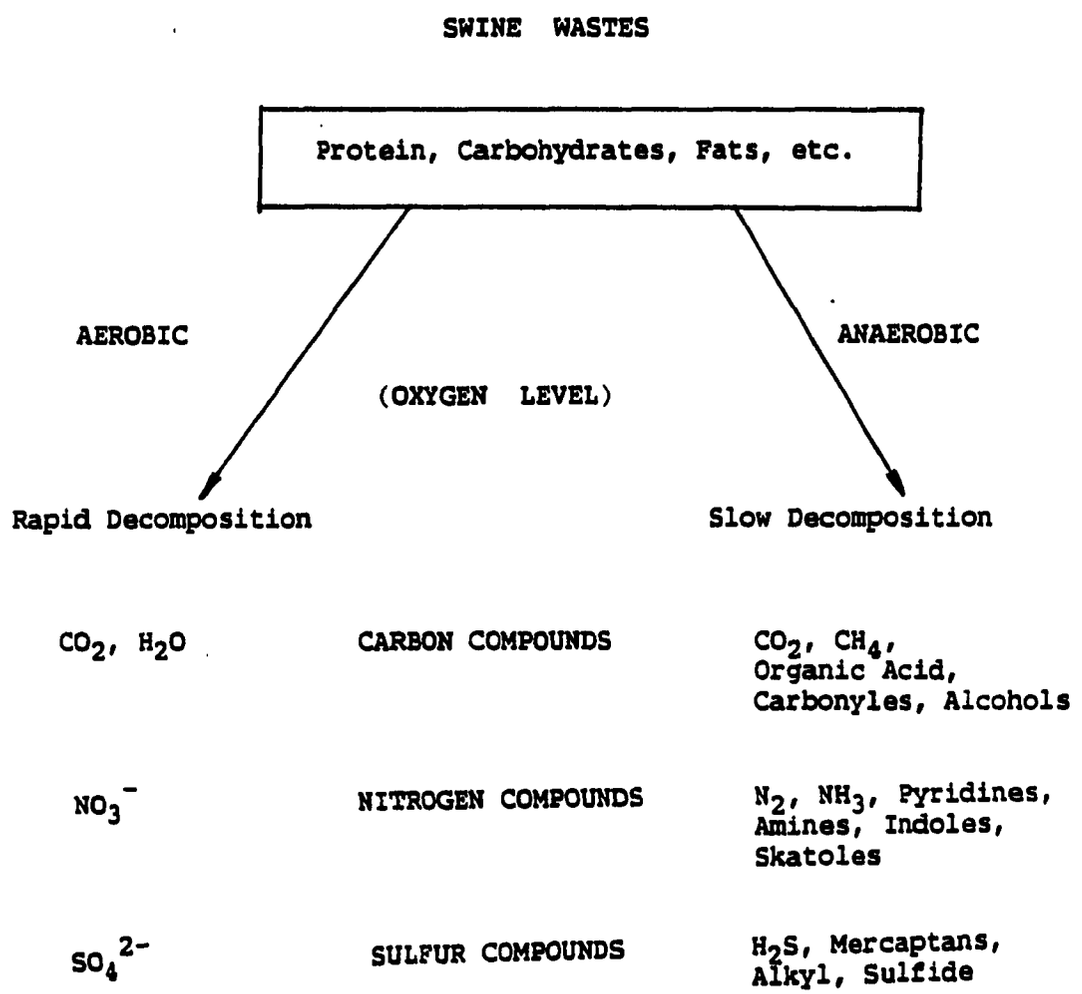

FIGURE 1. Gaseous pollutants from stored swine manure wastes subjected to aerobic and anaerobic decomposition (Parr, 1974)

Specific Volatile Compounds

N-containing volatile compounds

Many N-containing compounds have been detected in the headspace of swine wastes (Table 1). Ammonia is the most frequently reported as a constituent of swine manure.

A schematic diagram delineating the conversion of the nitrogenous swine manure into atmospheric NH_3 is shown in Figure 2 (Hutchinson et al. 1982; Hoff et al. 1981). Operationally, the overall process was subdivided into four steps: (1) bacterial ammonification (uric acid → NH_4^+/NH_3); (2) gaseous ammonia production within the pits; (3) mass transfer of pits NH_3 gas to the overlying atmosphere; and (4) establishment of ambient NH_3 levels through mixing and ventilation space.

The average concentration of NH_3 during storage was directly proportional to the initial solid concentration (Janni et al. 1980). Ammonia in water can be either in the form of ammonium ion or ammonia. In the ammonia form, it is readily released into the atmosphere. Ammonia in solution is a weak base that can take up H^+ to form ammonium ions,

$$NH_3 + H^+ \Leftrightarrow NH_4^+ \qquad pH = 9.2 \text{ (1 atm, 20°C)} \qquad (1)$$

This means that at pH 9.2, 50 percent of the ammonia solution is in the form of ammonium ions and 50 percent is in the form of ammonia. At high pH levels, more of the ammonia in the manure is in the volatile ammonia form. The higher concentration of volatile ammonia means that the partial pressure of ammonia would be higher.

S-containing volatile compounds

Many sulfur-containing compounds have been detected in the headspace of swine wastes (Table 1). Most of these compounds are present only in trace amounts (ng/l) (Banwart and Bremner, 1975a). Hydrogen sulfide (H_2S) and methyl mercaptan (CH_3SH) are most frequently reported:

In the ventilation air, only traces of these compounds have been reported (Avery et al. 1975). This is due to the oxidation of mercaptan to the less volatile disulfides by air (Kadota and Ishida, 1972) and possibly by adsorption. Hydrogen sulfide most likely will originate mainly from the microbial reduction of sulfate. Urine contains about 1100 mg/l of sulfur, mainly as sulfate, which originates from the animals' metabolism (Loehr, 1974; p. 519). Sulfate reducing organisms have been found to be present in swine manure of 1000 - 10000 per ml (Riviere et al. 1974). Sulphate reducing bacteria have been shown to produce trace amounts of carbon disulfide, carbonyl sulfide, and methyl, ethyl, and propyl mercaptans (Freney, 1967; Riviere et al. 1974).
In solution, hydrogen sulfide behaves as a weak acid to yield H^+ and sulfhydryl ions (SH^-),

$$H_2S \Leftrightarrow H^+ + SH^- \quad pH = 6.9 \text{ (1 atm, 20°C)} \qquad (2)$$

Therefore, increased pH levels depressed the dissociation of H_2S. According to Banwart and Bremner (1975a), the amounts of sulfur volatilized in one month at 23°C incubated under anaerobic conditions represented 1 percent of the total sulfur in the swine manure.

Addition of plant residues to soils leads to volatilization of methyl mercaptan, dimethyl sulfide, dimethyl disulfide, carbonyl sulfide and carbon disulfide (Bremner and Banwart, 1976). Hydrogen sulfide does not evolve because this gas is strongly absorbed by soil (Banwart and Bremner, 1975b).

Physiological Response to Volatile Compounds

Human responses to volatile compounds

Donham (1982) found that current levels of volatile compounds in swine confinement buildings may present a lung-disease threat in 20 years that may rival "Coal Miner's Lung" of the fifties. Donham (1982) and Donham et al. (1977) have recorded symptoms of respiratory stress in more than 50 percent of the operators surveyed.

Government agencies charged with maintaining safe working environments have adopted two measures of safe exposure to gases. The Time Weighted Average (TWA) averages exposure over an 8 hr. period and the Short Term Exposure Limit (STEL) averages exposure over a 15 min. period. The "Iowa Occupational Safety and Health Standards for General Industry" (IOSH) (Iowa Bureau of Labor, 1981) and literature from the American Conference of Governmental Industrial Health Hygienists (ACGIH) (1982) were reviewed for TWAs. In 1982, ACGIH had TWAs equal to or lower than the ones listed in IOSH. Some selected values of TWAs and STELs are presented in Table 2.

The Water Pollution Control Federation (1967) listed 1.4 to 1.6×10^5 ppm O_2 as the minimum safe 8 hr. exposure concentration, and 1.0×10^5 ppm as the limit below which life would be endangered.

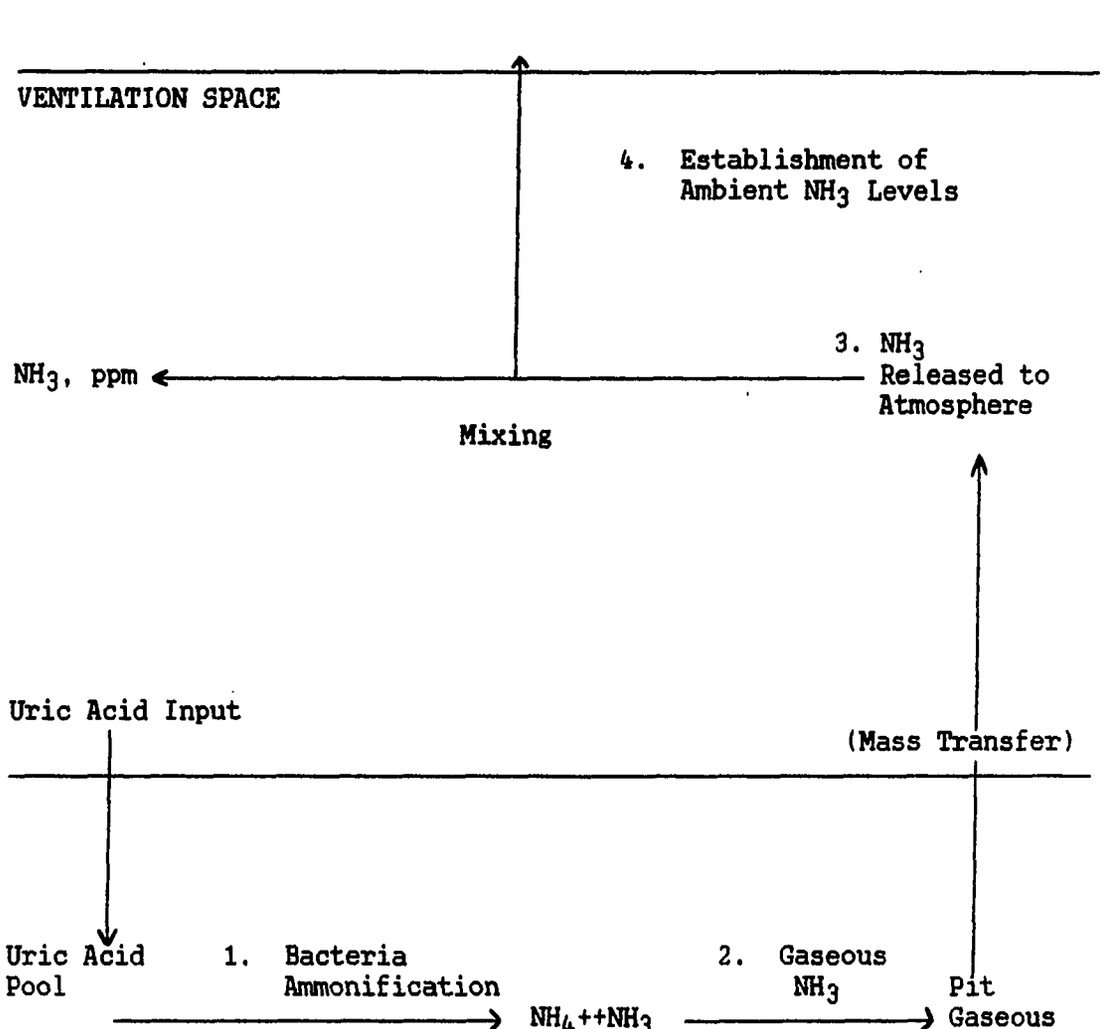

FIGURE 2. A Schematic diagram delineating the conversion of the nitrogenous swine manure into atmospheric ammonia

TABLE 2. Time-weight average (TWA) and short-term exposure limit (STEL) for humans (Anderson et al. 1987)

Compounds	TWA, ppm	STEL, ppm
Carbon dioxide	5,000	15,000
Ammonia	25	35
Hydrogen sulfide	10	15

Taiganides and White (1969) have summarized the important properties of major volatile compounds along with their threshold odor level, maximum allowable concentrations and adult human physiological responses to different levels of concentrations (Table 3).

Pig responses to volatile compounds

Many signs and symptoms in swine of short-term exposure to individual noxious substances of manure gases are known, but long-term exposure of swine to low levels of these gases has received little attention and may pose different problems. In many cases, the short-term toxic effects of H_2S and NH_3 may occur from agitating waste before or during pumping. Chronic poisoning from manure gases also may occur where liquid manure is recirculated. Chronic poisoning develops slowly, and much time may elapse until clear signs of illness are visible.

Muehling (1969) has shown the response of swine to various volatile compounds (Table 4). Curtis et al. (1975) found that up to 75 ppm NH_3 and 8.5 ppm H_2S had no effect on the rate of gain or on the respiratory

TABLE 3. Properties of gaseous pollutants and their physiological effects to human (Taiganides and White, 1969)

Gas	Odor	MIO[a] ppm	MAC[b] ppm	CONCEN ppm	Exposure[c] period	Physiological[d] effects
NH_3	sharp pungent	5.3	100			IRRITANT
				400	---	Irritation of throat
				700	---	Irritation of eyes
				1700	---	Coughing & frothing
				3000	30 min	Asphyxiating
				5000	40 min	Could be fatal
CO_2	none	--	5500			ASPHYXIANT
				20000	---	Safe
				30000	---	Increased breathing
				40000	---	Drowsiness, headaches
				60000	30 min	Heavy, asphyxiating breathing
				300000	30 min	Could be fatal
H_2S	rotten egg smell	.7	20			POISON
				100	hours	Irritation of eyes & nose
				200	60 min	Headaches, dizziness
				500	30 min	Nausea, excitement, insomnia
				1000	---	Unconsciousness, death
CH_4	none	--	--			ASPHYXIANT
				500000	---	Headaches, non-toxic

[a]MIO = Minimum Identifiable Odor, the threshold odor; i.e., the lowest concentration from which an odor is detected.

[b]MAC = Maximum Allowable Concentration.

[c]Exposure period: the time during which the effects of noxious gas are felt by an adult human and an animal (especially pig) of about 68 kg in weight.

[d]Physiological Effects: those found to occur in adult human; similar effects would be felt by animals weight 68 kg; lighter animals will affected sooner and at lower levels; heavier animals at later times and higher concentrations.

TABLE 4. Response of pigs to various atmospheric compounds (Muehling, 1969)

Compounds	Concentration (ppm)	Animal response
Carbon dioxide	40,000	An increase in depth and rate of respiration
Methane	50,000	No response from animal, but explosive
Ammonia	100 - 200	Induce sneezing, salivation and loss of appetite
Hydrogen sulfide	20	Develops photophobia, anorexia and nervousness
Oxygen	100,000	Critically dangerous condition

tracts of pigs. Drummond et al. (1980) found that 50 ppm of NH_3 slowed growth and caused mild respiratory disorders. Kovacs et al. (1967) found that the incidence and severity of pneumonic lesions in swine could be related to the volatile compound levels to which they were subjected in closed houses. It has been suggested that swine raised in confinement with under-floor waste pits have depressed rate of gain (Day et al. 1965).

The overall causal relationship of volatile compounds, "Source--airspace--effect", is illustrated in Figure 3.

Chemical-biochemical Control

There are two main categories of chemical-biochemical gaseous pollutants control additives used in livestock wastes:

1. digestive additives contain bacteria or enzymes that

eliminate odors and suppress gaseous pollutants and are released through biochemical digestive processes, and

2. chemical additives are strong oxidizing agents or germicides that alter or eliminate bacteria action responsible for gaseous pollutants or odor production.

Digestive additives

Some digestive additives contain only enzymes or bacteria while others are a combination of enzymes and anaerobic and facultative bacteria. Research data have indicated limited success with digestive additives. Ritter et al. (1975) found that a product sold under the trade name Agri-gest was effective in controlling odors in manure. Cole et al. (1975) found that digestive additives were not effective in reducing odors, ammonia, or sulfides (for long-term and short-term experiments). Miner and Stroh (1976) found that "Odor Control Plus" reduced the rate of ammonia released from a feedlot, but just for short-term operations. Another digestive additive used in the same trial did not reduce the odor intensity or ammonia. Ulich and Ford (1975) tested Formula 2 and found that it was not effective in reducing the rate of ammonia, sulfurous compounds or amines released from beef cattle feedlots. Sweeten et al. (1977) found that a bacteria culture did not decrease the odor when sprayed on a feedlot. Jensen (1977) reported effective odor control with bacteria products. Several commercial companies have reported some case examples where good gaseous pollutant control has been obtained by digestive additive products in both liquid manure tanks and feedlots (Bergdoll, 1975).

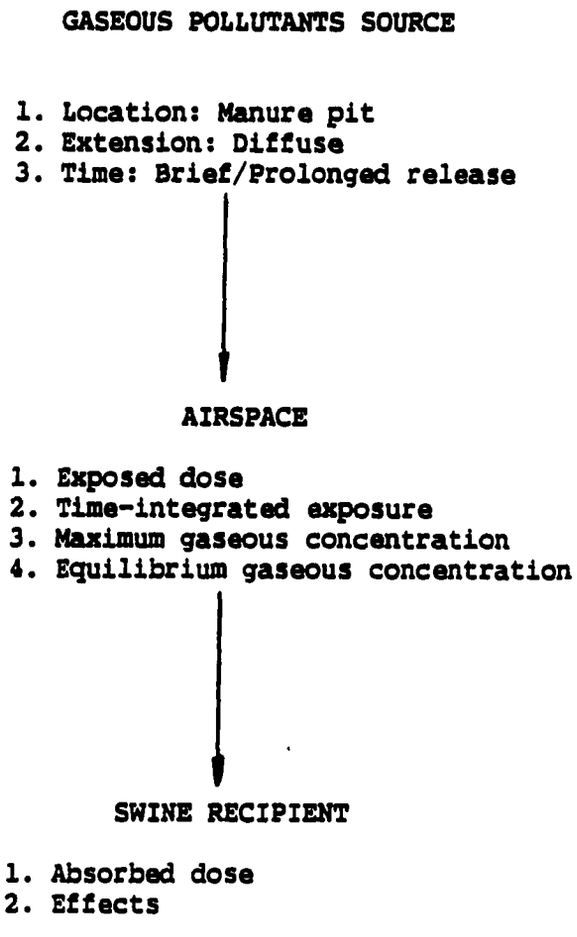

FIGURE 3. The causal relationship of gaseous pollutants in ventilated swine buildings (source-ventilation system-effect)

Chemical additives

Oxidizing agents Potassium permanganate ($KMnO_4$) is a strong oxidizing agent that is the most effective, in a practical sense, in neutral solutions because it is noncorrosive (Miner, 1974). Potassium permanganate is effective in reducing sulfide gases by the following reaction;

$$8KMnO_4 + 2H^+ + 3H_2S(aq) \rightarrow 8MnO_2 + 4H_2O + 3SO_4^{2-} + 8K^+ \quad (3)$$

For amines the reaction is:

$$16KMnO_4 + 4H^+ + 6NH_4^+ \rightarrow 16MnO_2 + 14H_2O + 6KNO_3 + 10K^+ \quad (4)$$

The reaction of $KMnO_4$ with amines is kinetically quite slow. This probably accounts for its lack of effectiveness in controlling ammonia (Warburton et al. 1980).

Faith (1964) was the first to report successful use of $KMnO_4$ to control feedlot odors. Cole et al. (1975) found that $KMnO_4$ at a dosage of 100-500 ppm, was effective in controlling sulfide odors in swine manure. Ritter et al. (1975) reported that $KMnO_4$ was effective in controlling odors for 72 hours in liquid manure at a dosage of 240 ppm-480 ppm.

Ulich and Ford (1975) reported that $KMnO_4$ was the most economical of six control agents tested in totally suppressing the release of important gaseous pollutants from feedlot manure when added at a rate of 28 g/kg. Miner and Stroh (1976) reported that $KMnO_4$ did not reduce ammonia evolution when applied at a rate of 22 g/ha.

Hydrogen peroxide has been used to control gaseous pollutants in

swine, dairy, and poultry manure. Reaction of H_2S with H_2O_2 can be described as follows;

$$H_2S(g) + H_2O \rightarrow H_2S(aq) + H_2O \text{ (absorption)} \quad (5)$$

The gas dissolves to a small extent in water.

$$H_2S(aq) \rightarrow H^+ + HS^- \quad (6)$$

$$HS^- \rightarrow H^+ + S^{2-} \quad (7)$$

Finally, the H_2O_2 which is added to the liquid manure, ionizes as follows;

$$4H_2O_2 \rightarrow 4H^+ + 4HO_2^- \quad (8)$$

and the oxygen rich ion reacts with the sulfide ion according to,

$$S^{2-} + 4HO_2^- \rightarrow SO_4^{2-} + 4OH^- \quad (9)$$

So that the overall reaction is given by

$$H_2S + 4H_2O_2 \rightarrow 4H_2O + H_2SO_4 \quad (10)$$

$$[34 \text{ kg} + 136 \text{ kg} \rightarrow 72 \text{ kg} + 98 \text{ kg}]$$

in which 136 kg of H_2O_2 can remove 34 kg of H_2S and convert it to dilute sulfuric acid which has no significant harmful properties.

Miner (1974) found that H_2O_2 was effective in controlling H_2S in swine and dairy manure. Cole et al. (1975) found that H_2O_2 was effective in reducing sulfide levels in liquid swine manure during short-term tests when dosed at 100 ppm. Sulfide levels were reduced from 120 ppm to 4 ppm. Ritter et al. (1975) reported that H_2O_2 was effective in reducing sulfide levels in liquid dairy manure within two hours when added at 100 ppm. Dosage rates from 100-125 ppm of H_2O_2 have been reported as the most economical (Warburton et al. 1980).

Disinfectants Ulich and Ford (1975) found that ozene was effective in controlling feedlot odors. Cole et al. (1975) found that orthodichlorobenzene was not effective in reducing sulfide or other odors in long-term dairy and swine manure tests.

Day (1966) reported that chlorine has been effective in reducing odors in liquid swine manure. Formaldehyde (CH_2O) and paraformaldehyde (90% - 99% of CH_2O) have been used to control odors and reduce ammonia evolution in animal wastes. Seltzer et al. (1969) found paraformaldehyde to be effective in reducing the evolution of ammonia and hydrogen sulfide from poultry manure because the number of viable bacteria were reduced. Cole et al. (1975) found that CH_2O slightly reduced the sulfide, but did not reduce the odor of dairy manure in long-term tests.

A summary of published references to chemical-biochemical gaseous pollutants control of livestock wastes is illustrated in Table 5.

Ventilation Control

The gaseous pollutants with known physiological effects, e.g., CO_2, NH_3, CH_4, and H_2S have been measured in ventilated swine building systems by several investigators.

Robertson and Galbraith (1971) showed that the gases' concentrations might vary along the length of the building in the high sidewall continuous inlet with exhaust fans in the pit. Grub et al. (1974) found that a large difference in CH_4, NH_3, and H_2S concentration in air exhausted through high sidewall exhaust fan vs. pit fan, and

TABLE 5. A summary of chemical-biochemical control of livestock wastes

AUTHOR	PRODUCTS	TYPE	MEDIUM TREATED	POLLUTANT	DOSAGE	EFFECTS
Bergdoll 1975	bacteria	D[a]	liquid manure	odors		G[a]
Cole et al. 1975	bacteria	D	swine manure	NH_3,H_2S		B
	$KMnO_4$	O	swine manure	H_2S	100-500 ppm	G
	H_2O_2	O	swine manure	H_2S	100 ppm	G
	orthodi-chloro-benzene	DI	dairy & swine manure	H_2S		G
	paraform-aldehyde	DI	dairy manure	H_2S		B
Day 1966	Chlorine	DI	swine manure	odors		G
Faith 1964	$KMnO_4$	O	feedlots	odors		G

[a] Note:
D = Digestive Deodorants.
DI = Disinfectants.
O = Oxidizing Agents.
G = Good Effects.
B = Bad Effects.

Table 5 (continued)

AUTHOR	PRODUCTS	TYPES	MEDIUM	POLLUTANTS TREATED	DOSAGE	EFFECTS
Jensen 1977	Bacteria	D	pounds	odors		G
Miner 1974	$KMnO_4$	O	swine dairy manure	H_2S		G
	H_2O_2	O	swine and dairy manure	H_2S		G
Miner & Stroh 1976	bacteria	D	feedlots	NH_3		G
	$KMnO_4$	O	feedlots	NH_3	22 kg/ha	B
Ritter et al. 1975	bacteria	D	dairy manure	odors		G
	$KMnO_4$	O	dairy manure	odors	480-240 ppm	G
	H_2O_2	O	dairy manure	odors	100 ppm	G
Seltzer et al. 1969	paraform-aldehyde	DI	poultry manure	NH_3, H_2S		G
Sweeten et al. 1977	bacteria	D	feedlots	odors		B
Ulich & Ford 1975	bacteria	D	feedlots	odors		B
	$KMnO_4$	O	feedlots	odors	28 g/ha	G
	Ozone	DI	feedlots	odors		G
Warburton et al. 1980	bacteria	D	swine manure	odors		G
	H_2O_2	O	swine manure	odors	100-250 ppm	G
	Tel II	DI	swine manure	odors		G

Skarp (1975) observed that the concentration of CO_2, CH_4, and H_2S varied with height in the building.

Lebeda et al. (1964) attempted unsuccessfully to correlate CO_2, NH_3, and H_2S generation rates with a large number of management, pit and

ventilation parameters. Avery et al. (1975) showed that H_2S production was correlated with outside air temperature, pit-to-room volume, and air retention time in the high sidewall exhaust fan buildings, but no mathematical expressions were derived.

A summary of reported concentrations of CO_2, CH_4, NH_3, and H_2S in different ventilation systems of swine confinement buildings are illustrated in Table 6. The selected components of unpolluted background atmospheric air concentrations are presented in Table 7.

Therasse and Sine (1974) in their studies of ventilation for livestock buildings, interpreted the results of tracer gas experiments in terms of concept related to the residence time of air. Therasse and Sine indicated that in livestock buildings the air inlet and exhaust locations are important for air quality.

Furry (1965) used a similitude model incorporating the Navier-Stokes equation to explain the changing CO_2 concentration by velocity analysis in a ventilated enclosure. The conclusion of this study indicated that the model design and operation system just based on one system parameter, i.e., air-exchange number (Qt/V), and the Froude Number and Reynolds Number did not appear to influence the ventilation-dilution phenomena. However, the static descriptions do not explain the dynamic relationship between gaseous pollutants and air distribution.

Therefore, a more sophisticated and comprehensive description of the ventilation process is needed, and the substantial research work has been carried out in this area during the last five years. Two

approaches have been used: (1) multi-cell air diffusion theory (Malmstrom and Ahlgren, 1982; Sandberg, 1981; Skaaret and Mathisen, 1982, 1983; NRC, 1981; Wadden and Scheff, 1983), and (2) age distribution function theory (Sandberg, 1981; Sandberg, 1983; Skaaret, 1986).

The concept of age distribution has been used successfully in the study of mixing in a chemical reactor (Danckwerts, 1953; Levenspiel and Bischoff, 1963). According to Himmelblau and Bischoff (1968), the meaning of residence time and age can be defined as follows: "The residence time of a fluid element is the time that elapses from the time the element enters the vessel to the time it leaves it. The age of a fluid element at a given instant of time is the time that elapses between the element's entrance into the vessel and the given instant, and is, of course, less than or equal to the residence time."

The main conclusions of the research works cited can be stated as follows:

<u>The ventilation airflow</u>

1. Airflow and gaseous pollutants are distributed differently in a ventilated airspace.
2. The mean-holding time for the ventilation airflow through the enclosure (average age of the air in the exhaust, taken as the time elapsed from the moment the air entered the enclosure) is always equal to "t_n" ($t_n = V/Q$) (Sandberg, 1981, 1983).

TABLE 6. Reported concentration of CO_2, CH_4, NH_3, and H_2S in different ventilation systems of swine confinement building

Source	Component	Concen (ppm)	Ventilation systems	Sampling location
Lebeda et al. 1964	CO_2 NH_3 H_2S	779 8.1 0.27	high sidewall inlet with a positive pressure fan	475mm, 914mm 1617mm above the floor
McAllister & McQuitty 1965	CO_2 CH_4 NH_3 H_2S	Trace 14,000 0 - 84,000 4 - 124 0 - 8	not indicated	Floor level in house outlet to slurry tank
Robertson & Galbraith 1971	CO_2 NH_3 H_2S	350-1200 8.5-17.5 7 - 59	High sidewall continuous inlet with exhaust fans in the pit	100mm & 1670mm above floor
Grub et al. 1974	CH_4 NH_3 H_2S	35-43 16-54 0.02-0.226	Continuous pit vent with high sidewall exhaust fans & circulation	pit fan inlet 152mm above floor & at ceiling
Sallvik, 1974	H_2S	0.3	High sidewall exhaust fans with cont. inlet	350mm above manure channel
Skarp, 1975	CO_2 NH_3	1250-2150 20-75		Various heights above waste
Avery et al. 1975	H_2S	0.42-0.85	High sidewall exhaust fans	1.2m above floor and 0.3m behind exhaust fans

TABLE 7. The compositions of dry air at sea level and concentrations of atmospheric trace gases (Seinfeld, 1975, pp. 5, 94)

Gas components	Background concentration, ppm
Nitrogen	780,900
Oxygen	209,500
Argon	9,300
Carbon dioxide	300
Neon	20
Helium	5
Methane	2
Hydrogen sulfide	0.002 - 0.02
Ammonia	0.006 - 0.02

3. The average air-exchange time for the total volume of air in the enclosure is twice the average age for the air in the enclosure taken as the time elapsed after the air entered the enclosure. (The time for filling the whole room with new air is equal to the time necessary for the air to leave the enclosure.) The airflow patterns become important and are obviously dependent on the type of ventilation system (Skaaret, 1986).

In fact, only when the airflows are a piston through the enclosure (plug flow), the mean-holding time for the air in the enclosure is equal to the average air-exchange time for the air flowing through the enclosure. The average exchange time is greater, increasing to the double at complete mixing between enclosure and ventilation airflow.

The gaseous pollutants

1. The concept of moments of concentration histories of gaseous pollutants (i.e., multiplying concentration reading by time

of reading, then integrating with regard to time) is applicable to characterize either the diffusion of the supplied air or gaseous pollutant released within the ventilation system (Sandberg, 1983).

2. The mean-holding time for the gaseous pollutants is contrary to the situation for the ventilation air, dependent on the flow patterns for the total system. It can be shown that the average concentration of gaseous pollutant in the enclosure,

   $\bar{C}_i$, is proportional to its mean-holding time t_p, obeying the following rule at steady state conditions (Skaaret, 1986):

   $$\bar{C}_i \; / \; C_e(s,s) = t_p \; / \; t_n \qquad (11)$$

   where

   $C_e(s,s) = \dot{m}/Q$ = steady state concentration of exhaust air.

   $\dot{m}$ = generation rate of gaseous pollutant

   Q = total volumetric flow rate of outdoor to the system

3. The more the polluted air is short-circuited to the exhaust, the lower the mean holding time. Displacement airflow promotes short-circuiting of gaseous pollutants. Local concentrations may vary considerably, so air quality finally can be determined only from measurements of the concentration of all the actual gaseous pollutants in the enclosure.

Pollutant removal and air exchange performance

1. Criteria for effective ventilation and behavior of airflow in a ventilation system can be defined through the age distribution theory. That is to say, a useful approach to evaluate air quality in a ventilation system is based on the determination of the local age of the supplied air and polluted air. The local ages then are compared to the nominal time constant of the system (Sandberg, 1981; Skaaret, 1986).

2. The average performance or effectiveness of ventilation systems at steady state, $\bar{E}_v$, can be expressed as a ratio between the mean-holding time for the ventilation air flow and the mean-holding time for the polluted airflow (Skaaret, 1986):

$$\bar{E}_v = t_n / t_p = C_e(s,s) / \bar{C}_i \qquad (12)$$

The local air quality index can be expressed as (Skaaret, 1986):

$$AQI = C_e(s,s) / C_i(s,s) \qquad (13)$$

where

$C_i(s,s)$ = local steady state concentration.

The average air-exchange efficiency, $\bar{E}_e$, can be expressed as the ratio between the mean-holding time for the ventilation air and the mean-holding time for the air in the enclosure (Skaaret, 1986):

$$\bar{E}_e = t_n / 2t_i \qquad (14)$$

where t_i = mean age of air in the enclosure.

CHEMICAL-BIOCHEMICAL CONTROL EXPERIMENT

Experimental Procedure

Materials

Columns Eight columns 0.4 m in diameter by 1.8 m high were used to evaluate the different chemical-bacteria additives. The experimental columns were filled with 0.8 m of swine wastes from under a slatted floor nursery building. Wastes were added weekly at the rate of 4 cm to each column. Each of the five columns contained a different additive. Three columns were used for control (blanks). Each column had a plexiglas window, 7.6 cm wide by 1.5 m high to observe the settling of the solids in the waste.

Swine manure Swine manure was collected daily from approximately 240 feeder pigs (nursery). The animals were at the Swine Nutrition Station, West 1/2 of Unit C, ISU, Ames, IA. The animals were fed a 16 percent ration, which was available for nutrient content.

The animal pens have raised crates with a sloped solid floor for cleaning or collection purposes. Farm workers cleaned and washed the floor daily.

Twenty-four hours before the waste was collected, the two drains under the pens were covered. After 24 hours, the floor was scraped and liquids were collected. The collected waste was mixed thoroughly in one container. The appropriate amounts then were added to the columns and the remainder of waste was discarded. Amounts were determined by weight and by measurement (volume).

After loading each column, the quantity of treatments were calculated, then weighed on a Mettler AC100 balance. Fifty milliliters of deionized H_2O was used to suspend treatments for ease of adding to them each week. Twenty-four hours before loading the columns, the columns were covered and sealed with a polyethylene sheet.

Sampling techniques

A 250 ml Fisher, Septum-port gas sample tube was filled with a retaining fluid (saturated sodium chloride solution containing 5 percent H_2SO_4 and methyl orange) from a leveling bottle. Once filled with fluid, the gas sample tube was connected to the treated column. The retaining fluid would flow back to the leveling bottle, drawing out of the treated column to allow a gas sample to be taken. The gas sample then was analyzed on GC/MS within two hours.

Temperature was maintained at approximately 15°C in the room where the columns were situated. The chemical sampling was done each week.

Treatment descriptions

- Waste treatment #1 (No. 6806 405) directions; one kg. per 83270 liters, repeat every week by 1/10th 37850 liters or 0.2 kg every 3 or 4 weeks.
- Waste treatment #2 (Specimen) directions; same as treatment #1.
- Waste treatment #3 (No. 6806 405) directions; same as treatment #1 + Insta. pro. In addition, add 0.04 kg per m^3 of waste material per week (Insta Pro).
- Waste treatment #4 directions; up to 94625 liters of waste. The

first day add 8 liters treatment. Next 8 weeks add 2 liters per week. Thereafter, add 1/2 liter per week.

- Waste treatment #5 directions; add 5.5 kg per 190000 liters waste for odor control.
- Waste treatment #6 -- No additives.
- Waste treatment #7 -- No additives.
- Waste treatment #8 -- No additives.

Headspace Screening of Gases

Equipment

A VARIAN AEROGRAPH SERIES -- 1250 Gas Chromatography and a 5970 SERIES mass selective detector with a HEWLETT PACKARD model 9133 GC/MS -- equipped with an HP 200 computer system was used for all analysis in this study. The GC/MS was equipped with a heated on-column injection port, and modified to accept a gas-phase sample from a HEWLETT PACKARD model 7675A purge and trap instrument. The GC/MS was run under the nominal conditions given in Table 8. Qualitative and quantitative measurements were made from the ion chromatogram and mass spectra obtained from GC/MS analysis.

Data analysis

Qualitative analysis The GC/MS analysis provides information for the initial identification of gases generated from manure. The total mass scan for each of the major peaks in the total ion chromatogram (TIC) was interpreted with the aid of computer searching, comparison to the mass spectra of known compounds available in the

NBS/REVE/L library of mass spectra, and comparison to the retention index (RI).

Quantitative analysis Reverse library search techniques using acquired reference spectra were used to find the target compounds. The retention time of a compound determines a window within which the search was performed. A compound is confirmed when fragment ions in the total ion chromatogram maximize at a preselected match probability with the reference spectra. The target ion peak height or relative abundance

TABLE 8. GC/MS conditions for gases screening analysis

Initial temperature	45 - 55°C
Time at initial temperature	2 - 3 min.
Oven ramp rate	10°C/min.
Final temperature	200 - 250°C
Time at final temperature	40 - 45 min.
Mass range for scan	5 - 50 m/z
Run time	10.00 min.
Equilibration time	0.5 min.
Splitless on time	0.5 min.

values should be predetermined using standards. Each compound is quantified by comparing the ratio of an ion peak area in the unknown to its relative abundance with the ratio of the peak area and relative abundance of a quantitative internal standard. The major compounds identified during GC/MS screening is illustrated in Table 9. The results of the typical mass spectra and total ion chromatogram of headspace GC/MS screening from air sample and eight waste treatment samples are illustrated in Appendix A (Figure A-1 -- Figure A-9). The

overall quantitative results of the experiment (peak area) are illustrated in Appendix B (Table B-1).

Determination of the concentrations of gaseous pollutant in headspace

Choice of calibration method In this study, the external calibration method was chosen to determine the concentration of gas in headspace. This method gives a direct response for known amounts of a pure compound analyzed. It is assumed there is no significant change in

TABLE 9. Components identified during GC/MS screening

Components	m/z
Nitrogen	14.05
Oxygen	32.05 & 32.15
Carbon dioxide	44.05
Hydrogen sulfide	34.05
Methane	16.05 & 16.15
Ammonia	17.05 & 17.15
Water vapor	18.05 & 18.15

mass spectrometer response between sample and standard analysis. The ratio of the response for the sample and the standard is used for quantification. A number of factors may influence quantification, including variations in injection volume and the effect of the sample matrix on the response of individual components.

In this experiment, the ambient air in the laboratory was selected as the external quantitative standard. Therefore, immediately before GC/MS analysis of gases sampled, 50 µl of ambient air was collected to serve as the external quantitative standard. The mass spectra, total ion chromatogram, and peaks for each selected gas compound of the

external quantitative standard, i.e., ambient air, for this experiment are listed in Appendix C.

Relative response factors, R_f, were calculated for each compound.

The relative response factor can be calculated by the following equation (Schuetzle and Hampton, 1985):

$$R_f = \frac{\text{(Area Analate)} \quad \text{(Amount Standard)}}{\text{(Area Standard)} \quad \text{(Amount Analate)}} \qquad (15)$$

Cornu and Massot (1975) have listed R_f for hundreds of compounds determined on various instruments. These values are referenced to butane, hexadecane, and toluene. The R_f values for N_2, O_2, CH_4, NH_3, CO_2, and H_2S are illustrated in Table 10. Therefore, from the equation of R_f, the amount of analyte can be expressed as;

$$\text{Amount Analyte} = \frac{\text{(Area Analate) (Amount Standard)}}{\text{(Area Standard)} \times R_f} \qquad (16)$$

TABLE 10. Relative response factor value for different gaseous compounds (Cornu and Massot, 1975)

Components	R_f
Nitrogen	0.64
Oxygen	0.53
Methane	0.54
Ammonia	0.32
Carbon dioxide	0.81
Hydrogen sulfide	0.75

Here, the unpolluted background atmospheric air concentrations were chosen as the ambient air in the laboratory. The concentrations of ammonia, carbon dioxide, methane, and hydrogen sulfide for the external

TABLE 11. Concentration (ppm) of gaseous pollutants released from swine manure in experimental columns

GASES	DATE (1987)	GAS SAMPLES, ppm 1	2	3	4	5	6	7	8
	2/23	2.40	6.20	6.20	9.00	6.00	2.60		
CH_4	3/04	0.40	5.80	6.60	9.20	61.40	2.00		
	3/12	3.20	6.40	6.20	9.20	6.40	2.40		
	3/19	3.00	6.20	7.40	4.80	2.80	2.20		
	4/09	0.88	1.80	5.60	1.40	1.10	2.80	0.08	0.66
	4/16	0.60	1.30	4.60	1.10	1.00	2.80	0.24	0.70
	4/23	2.80	2.20	6.40	1.70	1.00	1.00	1.00	0.60
	4/30	3.80	2.40	4.80	1.10	1.00	1.10	0.90	0.60
	5/28	1.80	2.00	4.40	1.00	1.10	2.80	0.80	0.70
	6/11	1.80	1.80	5.00	1.00	1.00	2.20	1.00	0.80
	6/18	1.70	1.70	4.60	1.00	1.00	1.40	0.90	0.70
	7/02	0.53	1.20	1.70	1.30	1.00	0.81	0.82	1.30
	2/23	0.01	0.005	0.008	0.008	0.008	0.006		
	3/04	0.19	0.31	0.35	0.29	0.29	0.10		
	3/12	0.14	0.31	0.31	0.35	0.29	0.10		
NH_3	3/19	0.14	0.37	0.33	0.36	0.007	0.10		
	4/09	1.25	0.06	0.39	0.17	0.56	0.11	0.11	0.19
	4/16	0.04	0.29	0.42	0.27	0.47	0.10	0.10	0.20
	4/23	2.20	0.38	0.42	0.54	0.54	0.25	0.12	0.05
	4/30	0.54	0.29	0.33	0.33	0.47	0.11	0.10	0.07
	5/28	0.36	0.27	0.36	0.29	0.44	0.10	0.11	0.08
	6/11	0.35	0.29	0.33	0.33	0.47	0.10	0.10	0.07
	6/18	0.36	0.27	0.33	0.27	0.42	0.10	0.10	0.08
	7/02	0.15	0.51	0.56	0.23	0.40	0.10	0.10	0.08
CO_2	2/23	1360	1550	1510	2300	1920	490		
	3/04	1280	1430	1470	2220	1810	600		
	3/12	1390	1360	1470	2290	1850	570		
	3/19	320	1210	320	1020	110	530		
	4/09	570	980	2030	900	530	450	3	3
	4/16	530	900	980	790	530	490	11	26
	4/23	200	320	900	410	120	140	15	30
	4/30	530	720	900	530	340	410	11	26
	5/28	570	800	980	640	300	530	11	28
	6/11	520	570	980	570	370	530	17	30
	6/18	450	600	900	600	340	490	15	28
	7/02	570	520	1280	940	300	340	15	30

H_2S : Trace Concentration, $\leq$ 0.01 ppm

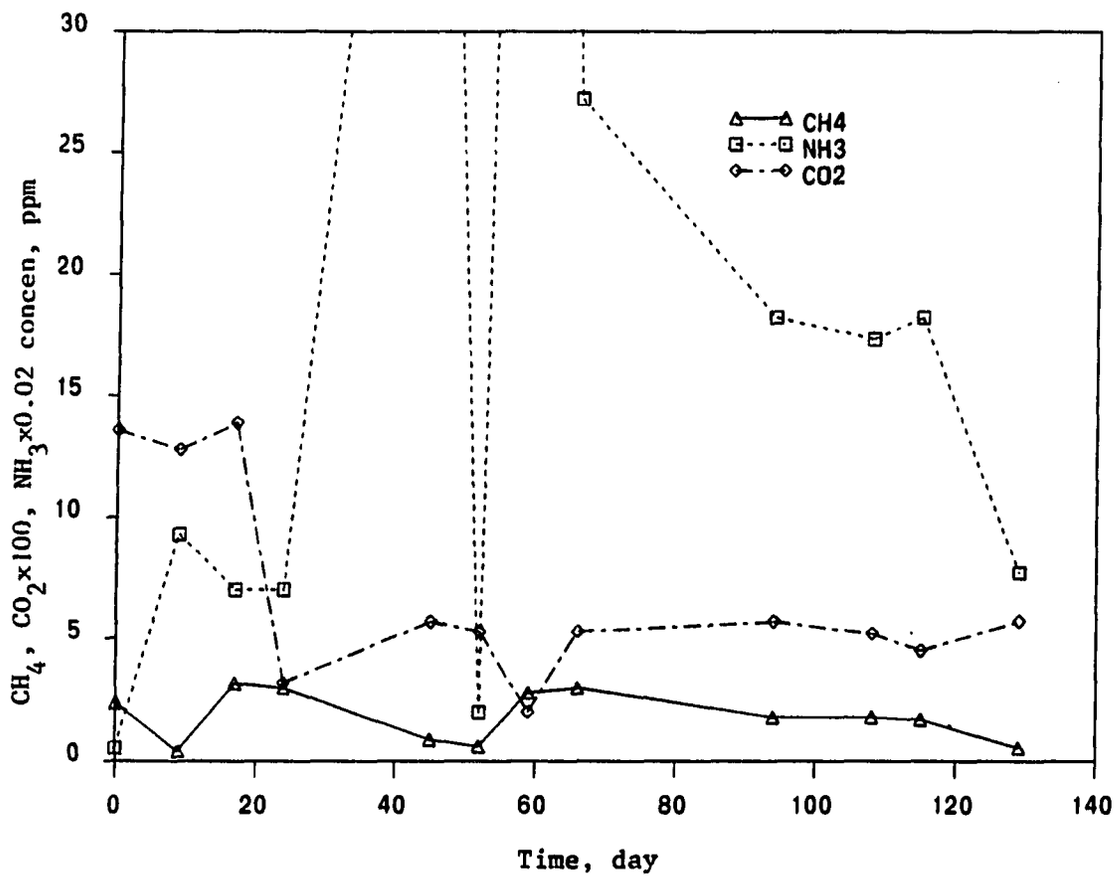

FIGURE 4. Gas concentration change with time for waste treatment #1

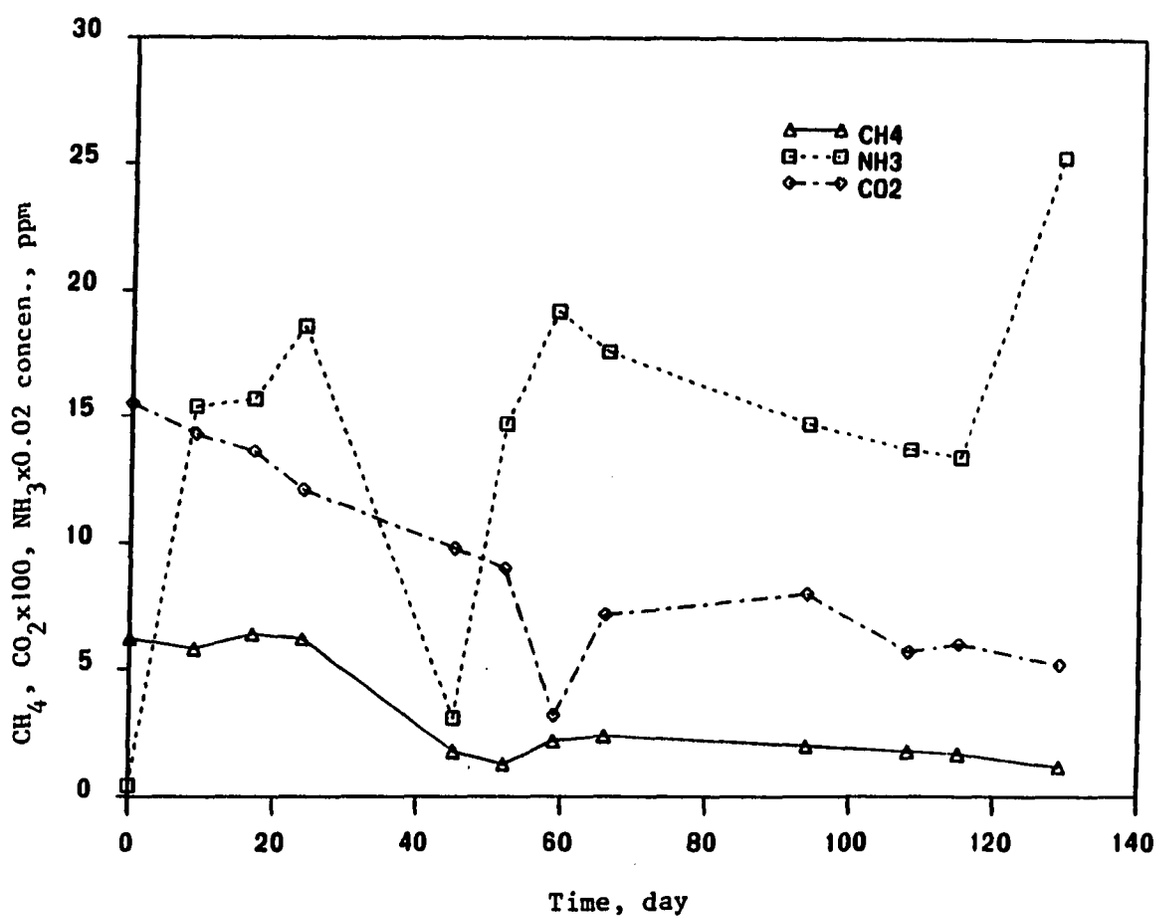

FIGURE 5. Gas concentration change with time for waste treatment #2

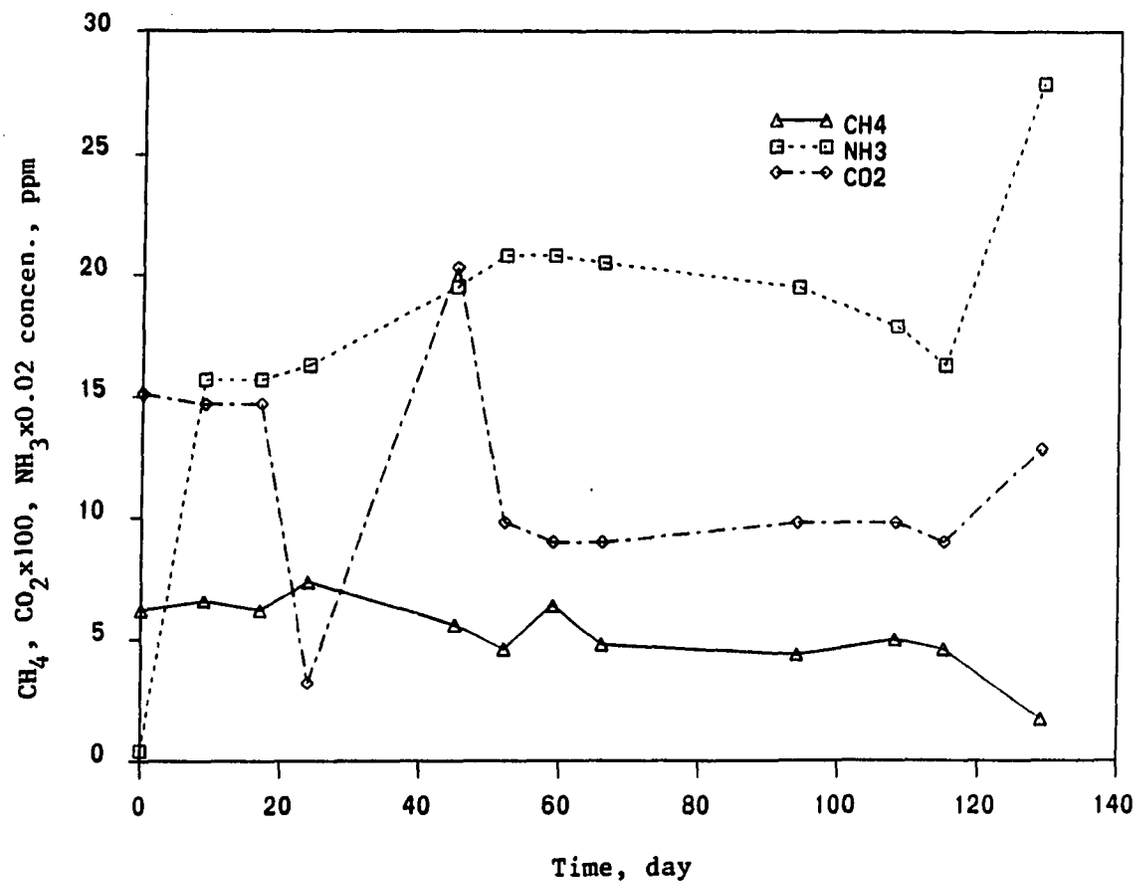

FIGURE 6. Gas concentration change with time for waste treatment #3

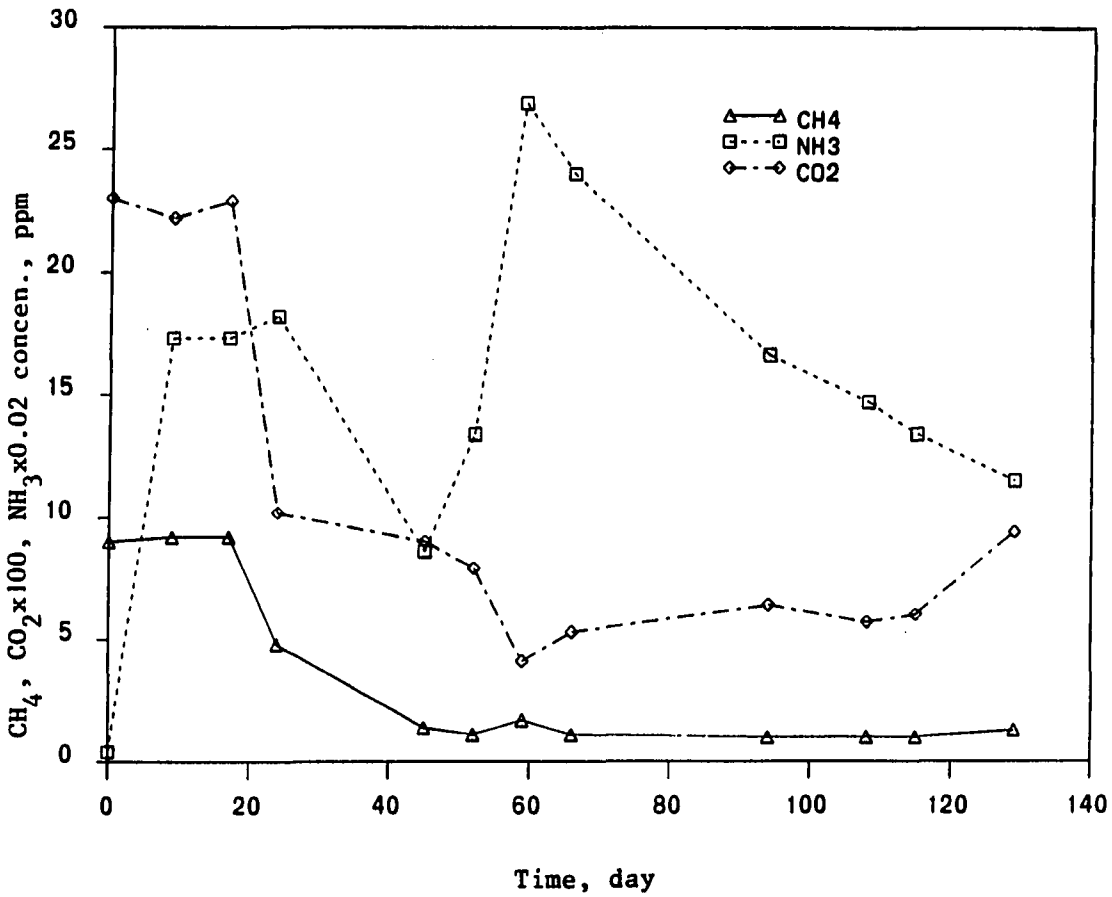

FIGURE 7. Gas concentration change with time for waste treatment #4

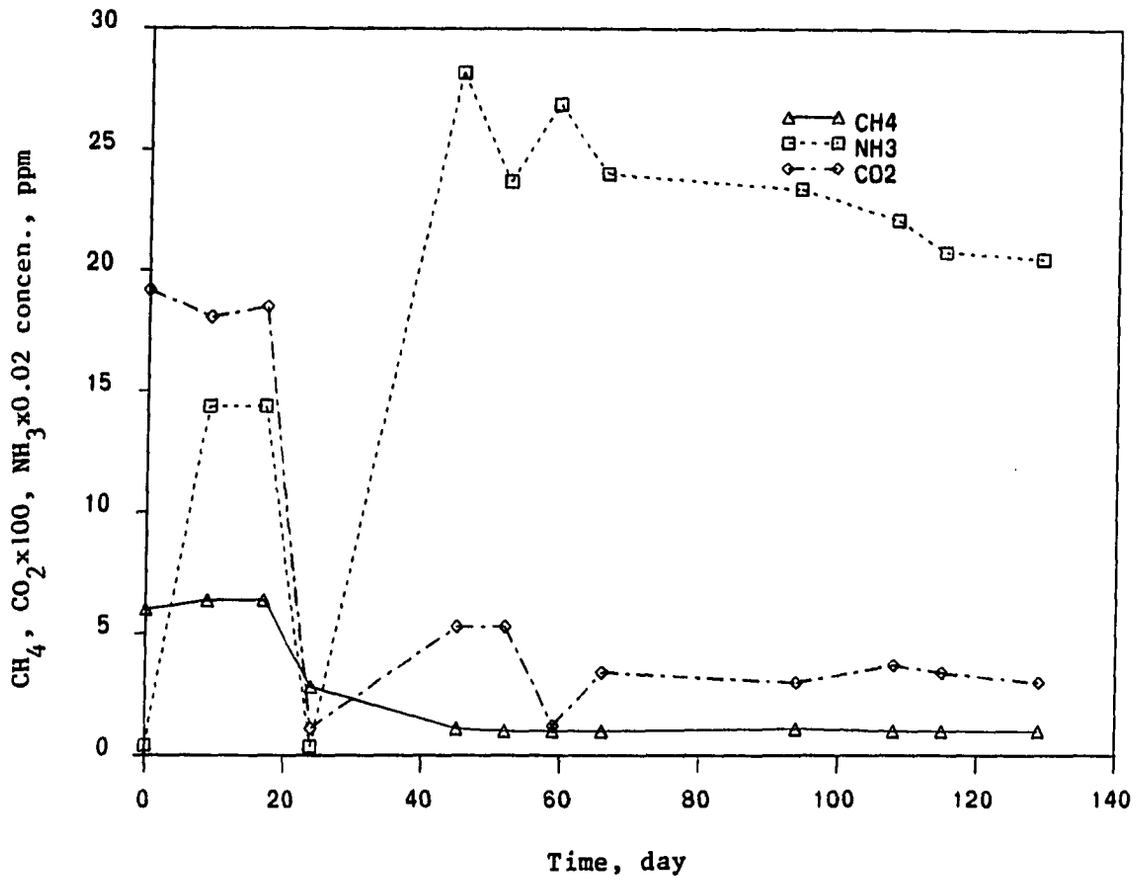

FIGURE 8. Gas concentration change with time for waste treatment #5

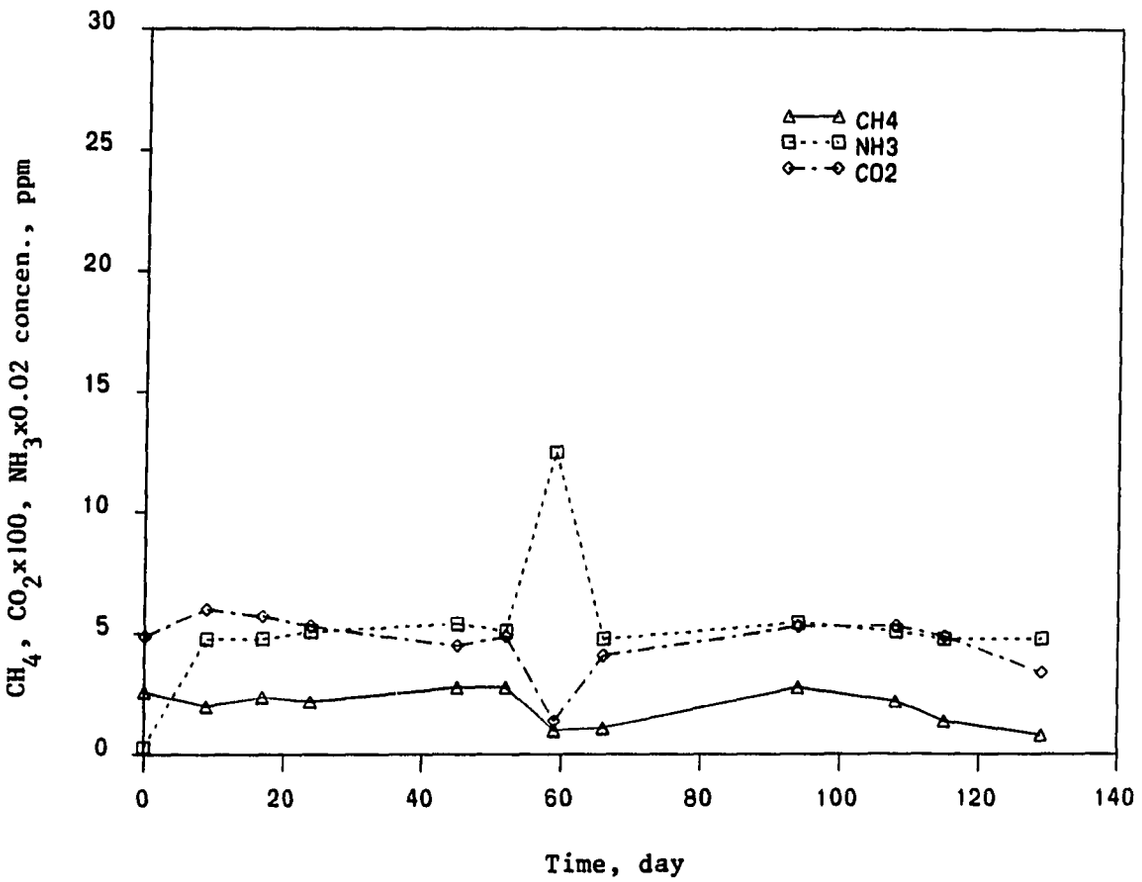

FIGURE 9. Gas concentration change with time for waste treatment #6

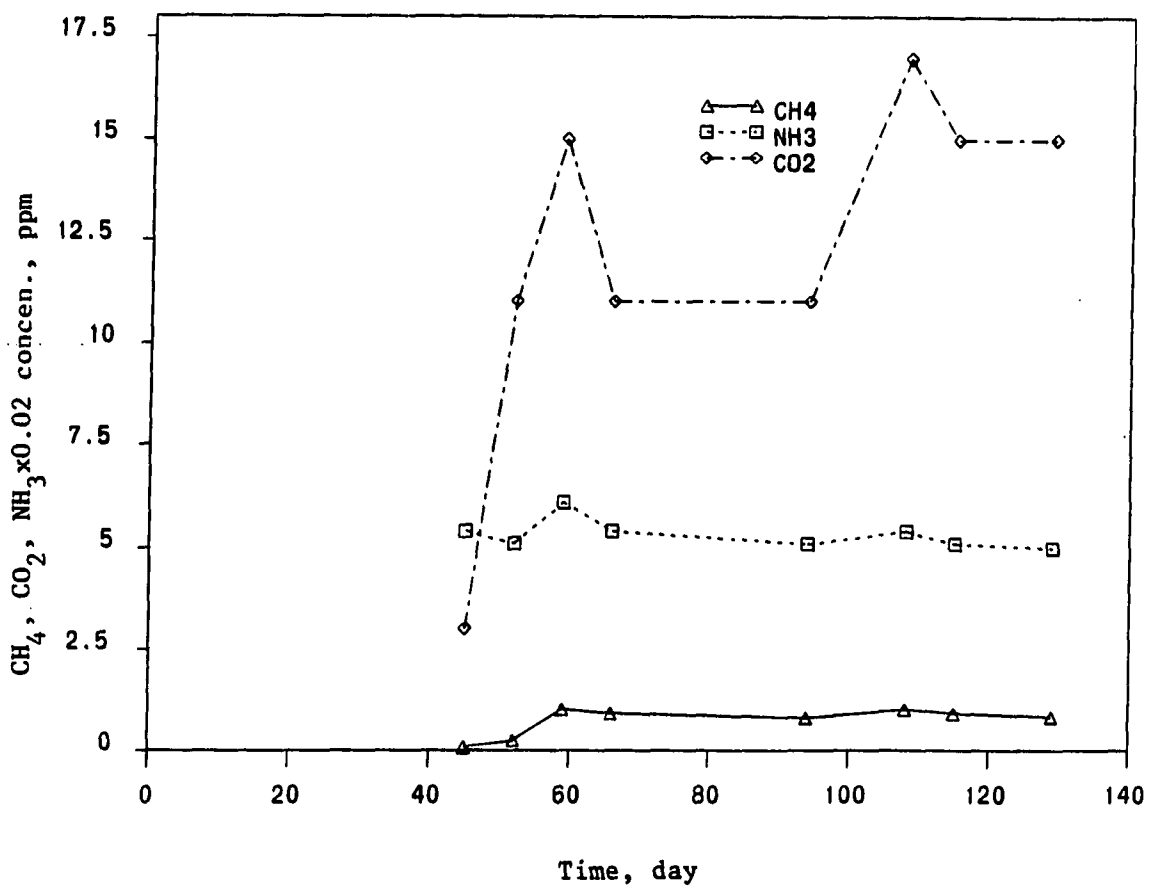

FIGURE 10. Gas concentration change with time for waste treatment #7

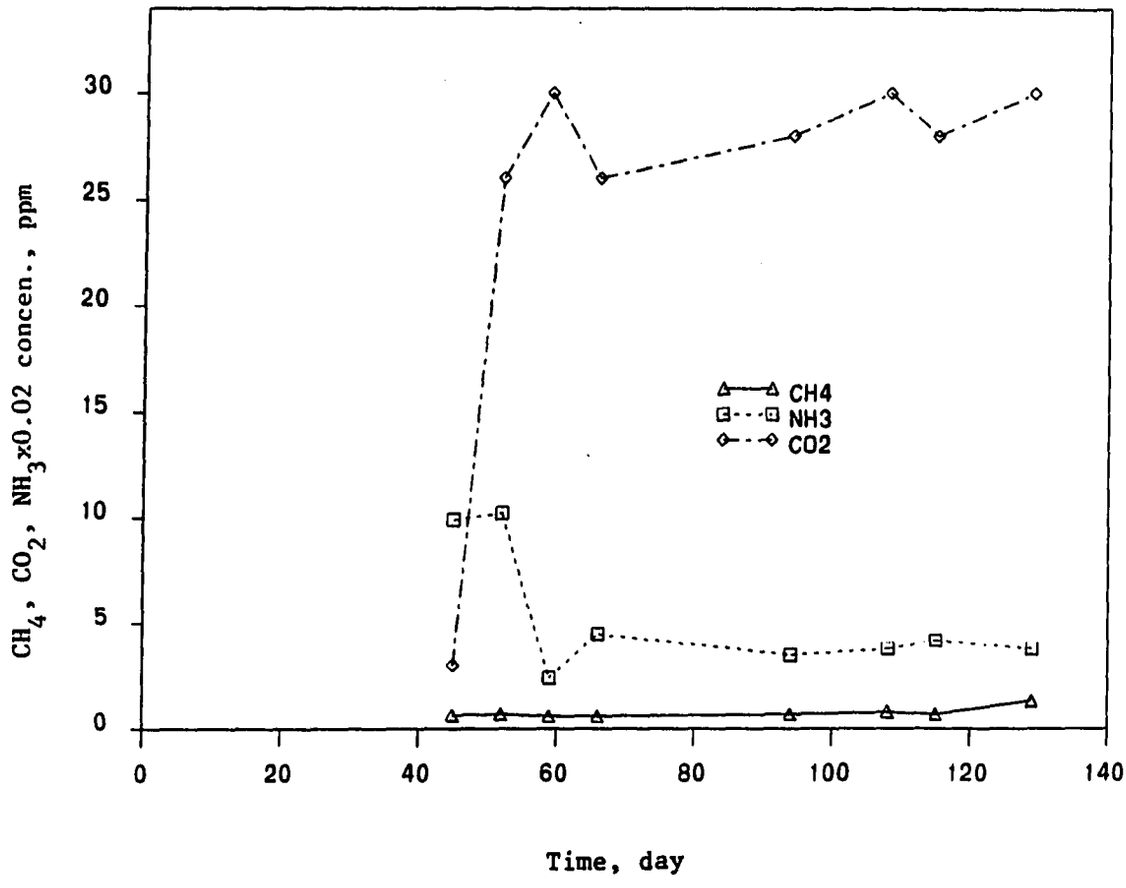

FIGURE 11. Gas concentration change with time for waste treatment #8

standard (wet basis) were taken to 0.01ppm, 305ppm, 1.1ppm, and 0.01ppm, respectively (Seinfeld, 1975).

Results

Table 11 presents the levels of gas samples that were observed for each of the experiments. Figures 4, 5, 6, 7, 8, 9, 10, and 11 present the relationship of gaseous pollutants vs. date of analysis. The ammonia data were too low because some reacted with H_2SO_4 in the retaining fluid.

Emission Rate Determination

Two-film resistance theory

The emission rate of a gas compound from the swine manure to the atmospheric environment is dependent on the physical and chemical properties of the compound, the presence of other chemical compounds, and other physical properties of the swine manure pit, and the physical properties of the atmosphere above the swine manure. The physical and chemical properties of gas compounds affecting emission may include molecular diameter, molecular weight, Henry's law constant, and the diffusion coefficient. The physical properties of the manure pit include width and depth. The atmospheric properties of concern include air velocity, stability, and other factors. Temperature affects the vapor pressure and solubility, and thus, influences the emission rate of chemicals.

Theoretical concepts of the emission of gas compounds from liquid phase to the atmosphere have been presented by various researchers and can be found elsewhere (Mackay and Wolkoff, 1973; Liss and Slater, 1974;

Mackay and Leinonen, 1975; Cohen et al. 1978; Smith et al. 1980; Mackay and Yuen, 1981; Lunney et al. 1985; Anderson et al. 1987). The review covers the assessment of air quality at waste disposal sites which are summarized in Table 12.

Lewis and Whitman's (1924) two-film resistance theory is generally used to describe the emission rate of gas compounds from liquid phase. Whenever a concentration gradient of a chemical compound exists between a solid-air or liquid-air interface, mass transfer phenomena occur across the interface and approaches an equilibrium within the system. Each phase is regarded as well-mixed by turbulence to within a small distance of the interface. The schematic representation of the two-film resistance model is illustrated in Figure 12.

The main resistance to gas transport of the exchanging gas is within these two films. The transport of the exchanging gas is assumed to take place by molecular diffusion. Thus, application of Fick's first law of diffusion for gas transport through each layer leads to

$$F = K_g(C_g(s)-C_g) = K_w(C_w-C_w(s)) \qquad (17)$$

where

F = the rate of transfer of the compound per unit area, mol/cm^2-s

K_g, K_w = the mass transfer coefficient for the gas and liquid phase, cm/s

$C_g(s)$, $C_w(s)$ = the interfacial concentrations in each phase, mol/liter.

TABLE 12. Review of the state-of-the-art emission models for waste disposal sites

Model	Applicability	Remarks
Mackay & Wolkoff (1973)	Nonaerated unsteady State	Not based on two-film theory
Liss & Slater (1974)	Nonaerated unsteady state	Based on two-film theory
Mackay & Leinonen (1975)	Nonaerated unsteady state	Only unsteady state based on two-film theory
Smith et al. (1980)	Nonaerated steady state	Based on two-film theory, but require complex lab. experiment
Mackay & Yuen (1981)	Nonaerated unsteady state	Based on two-film theory, a brief but enlightening of the survey of mechanism emission phenomena
Lunney et al. (1985)	Nonaerated steady state	Based on two-film theory, but requires complex procedure to determine K_w
Anderson et al. (1987)	Nonaerated unsteady state	Based on two-film theory, but relevant parameters considered in the K_w and K_g are not sufficiently defined

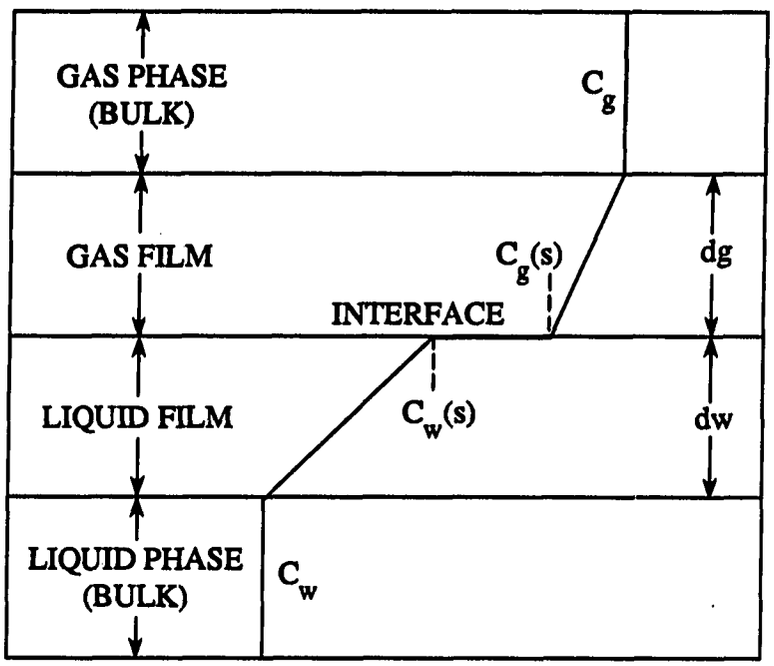

FIGURE 12. Schematic representation of two-film resistance model

C_g, C_w = the concentration of the compound in the gas or liquid phase, mol/liter.

The mass transfer coefficients are defined by the general relation,

$$K_g = D_g/d_g, \quad K_w = D_w/d_w \tag{18}$$

where

D_g, D_w = the molecular diffusion coefficients of gas and liquid phases, cm^2/s

d_g, d_w = the thickness of diffusion boundary of gas and liquid phases, cm

The two-phase equilibrium condition for the compounds being transported can be expressed by a variation on Henry's law (Stumm and Morgan, 1981);

$$\frac{C_g(s)}{C_w(s)} = K \text{ (dimensionless)} \tag{19}$$

Substituting equation (19) into (17) and rearranging it, we can obtain;

$$F = K_O (C_w - C_g/K) = K_O (C_w - C_w^*) \tag{20}$$

and

$$K_O = [1/K_w + 1/(K K_g)]^{-1} \tag{21}$$

where

K_O = overall mass transfer coefficient, cm/s.

C_w^* = the soluble concentration of the compound(mol/liter) in equilibrium with the partial pressure P_g of the compound in the gas phase.

Rewrite the equation (20) in terms of mole fractions and molecular weight of the compound, the emission rate of gaseous pollutants from manure pit can be expressed by the following equation:

where $$\dot{m}(i) = K_o A (X_i - X_i^*) M_i \quad (22)$$

$\dot{m}(i)$ = equilibrium emission rate of a compound i, g/s.

A = area of manure pit, cm^2

X_i = concentration of the compound i in the liquid manure, mole fraction.

X_i^* = equilibrium concentration of gas phase of the compound i, mole fraction.

M_i = molecular weight of the compound i, g/g-mole.

K_o = overall transfer coefficient, g-mole/cm^2-sec.

Because X_i^* is negligible compared to X_i, equation (22) reduces to;

$$m(i) = K_o A X_i M_i \quad (23)$$

Because the swine manure contained 85 percent of solid, and the moles of H_2O presented is approximately equal to the total moles presented, therefore, the g-moles of H_2O presented in swine manure can be calculated as [(100-85% of solids)10g H_2O/1000g of manure]/18 g/g-mole = 8.33 g-moles of H_2O. The average molecular weight of liquid manure then is equal to (1/8.33)1000 = 125 g/g-mole. Therefore, Xi in equation (23) can be expressed as:

$$Xi = \frac{C_i}{10^6} \quad \frac{1/M_i}{1/125} = 64.31 \times 10^{-4} \, C_i/M_i \quad (24)$$

in which

C_i = concentration of the compound i in liquid manure, mg/l.

Substituting equation (24) into equation (23), the emission rate becomes

$$m(i) = (1.25 \times 10^{-4})\ K_o\ A\ C_i \qquad (25)$$

In equation (19), the K value can be determined by the following equation;

$$K = [\ H_i/(P\ \bar{M}\ )] \times 10^6 \qquad (26)$$

where

H_i = Henry's law constant of the compound i,
atm/(g-mole/m^3)

P = total pressure, atm

M = average molecular weight of the liquid manure,
is equal to 125 g/g-mole.

It should be noted that the factor of 10^6 is derived from conversion of liquid weight into volume. It may be shown on theoretical grounds that the coefficient H_i is a function of absolute temperature and should obey a relationship of the form (Daniels and Alberty, 1966);

$$H_i = [1/(K_1 \exp(K_2/T))]\ M_i \qquad (27)$$

Values of K_1 and K_2 coefficients for CH_4, NH_3, H_2S, and CO_2 are shown in Table 13 (Anderson et al. 1987).

Equation (21) represents the addition of two-phase resistances in series to yield the overall transfer coefficient. Most of the resistance lies in the few millimeters above or below the gas-liquid interface. In many situation, either liquid phase resistance or gas resistance controls, but in some cases, both resistances control. If K_w is very small compared with K_g, the liquid phase resistance controls and K_g may be ignored, and vice versa.

TABLE 13. Coefficient for predicting the variation of Henry's law coefficient with temperature according to $H_i = /K(K_1 \exp(K_2/T))] M_i$ (Anderson et al. 1987)

Compounds	K_1 (mg/l-atm)	K_2 (°K)
Carbon dioxide	0.3280	2517
Methane	0.04197	1863
Ammonia	0.8650	4151
Hydrogen sulfide	0.01994	2226

The distribution of resistance depends on K_w, K_g and K , which must be quantified. To determine K_w is difficult because it depends on the degree of turbulence which exists at and under the liquid surface. Most researchers have measured mass flux for a system such as oxygen transfer. Several determinations have been made of K_w for lakes, rivers, oceans, and in wind wave tanks, but no determinations have been made of K_w for the types of waste lagoons. In the absence of field data of mass transfer coefficients of volatile compounds, it seems logical to apply the same basic theory and approach for calculating K_w values. According to stream studies conducted by Owens et al. (1964) K_w can be calculated by;

$$K_w = 1731.11\ (1.024)^{(T-20)}\ U^{0.67}\ H^{-0.85}\ D_i/D_o \quad (lb\text{-}mole/ft^2\text{-}h) \qquad (28)$$

where

T = temperature, °C

U = air velocity, m/hr

H = depth of the manure pit, m

D_i = diffusivity of the compound, cm^2/sec, and

D_o = diffusivity of oxygen ($2.2x10^{-5}$ cm^2/sec)

Because the ratio of diffusivity of D_i/D_o in water that was suggested by Liss and Slater (1974) is a function of molecular weight in the form of $(M_o/M_i)^{0.5}$ and M_o = 32, the term D_i/D_o can be rewritten by $(32/M_i)^{0.5}$. For consistency of units, the K_w value can be converted from lb-mole/ft^2-h to g-mole/cm^2-sec by using a multiplying conversion factor of 1/7350 and therefore that equation (28) can be simplified as follows:

$$K_w = 0.24\ M_i^{-0.5}(1.024)^{(T-20)}\ U^{0.67}\ H^{-0.85} \quad (g\text{-mole}/cm^2\text{-sec}) \qquad (29)$$

The gas mass transfer coefficient, K_g, depends on air velocity, the roughness of the manure pit surface, the length of the generating surface, and the nature of the diffusing compound. Mackay and Matsugu (1973) developed the following correlation:

$$K_g = 0.029\ U^{0.78}\ Z^{-0.11}\ S_c^{-0.67}, \quad (m/hr) \qquad (30)$$

where

U = air velocity, m/hr

Z = length of manure pit surface, m

S_c = gas phase Schmidt Number

Again, for consistency of units, the K_g value can be converted from m/hr to g-mole/cm^2-sec by using a multiplying conversion factor of (1/36 M_i) and therefore, that equation (30) can be expressed as follows;

$$K_g = 8.05 \times 10^{-4} M_i^{-1} U^{0.78} Z^{-0.11} S_c^{-0.67}$$

(g-mole/cm^2-sec) (31)

The Schmidt Number can be determined from (gas kinematic viscosity)/(molecular diffusivity) of the compound. The Schmidt Numbers of CO_2, CH_4, NH_3, and H_2S at different temperatures are listed in Table 14.

TABLE 14. The Schmidt Number of gases in air (Thibodeaux, 1979)

Gases	Temperature, °C	S_c
Ammonia	0	0.61
	25	0.78
Carbon dioxide	25	0.94
Methane	0	0.84

The emission rates of gaseous pollutants depend much on the ventilation conditions occurring at the gas-liquid interface which may vary appreciably with time. Thus, only seasonal-term emission rates should be used for estimation. Furthermore, the rates can be greatly influenced by the presence of surface materials, such as floating solids and/or liquids, which accumulated at the gas-liquid interface. The effect of such surface materials is complicated and sensitive to K_g, not K_w.

In this model, the available theoretical and experimental K_w and K_g data were mostly derived from studies of lakes, rivers, and oceans. These K_w and K_g values may be too high to apply to animal waste water as a result of the absorptive effect of floating solids and other surface

materials in the manure pit. Such an effect could reduce emission rate significantly, because such effects have some capability of exerting the vapor pressure which drives the emission process. The lack of quantitative data on this effect represents the major uncertainty in calculating K_w and K_g and may introduce a large margin of error. According to the prediction model of gaseous contaminants in swine confinement buildings, Anderson et al. (1987) indicated that this variation has been achieved by introducing a factor ß ranging in values from 0 to 1 that is used to multiply the value of the clean water mass transfer coefficient as calculated from equations (29) and equation (31).

Results of emission rate determination in experimental columns

To determine the emission rates of gases from swine manure in experimental columns, we have to use the waste treatment #6 (blank sample) to derive the emission rates. That is, we want to develop the calibration curves using the observed concentrations from waste treatment #6.

Input data

1. Geometrical parameters of experimental columns

   H = depth of the swine manure in column (0.8 m)

   Z = length of manure surface (0.4 m)

   A = area of manure (1140 cm^2)

2. Environmental parameters

   Temperature = 15°C

   Air velocity = 0

Cleanness factor, $\beta = 0.25$

Results

From equations (26), (27), (29), and (31) combined with above input data we can calculate K_w, K_g, K, H_i. The results can be tabulated as follows:

Gases	K_w (g-mole/cm^2-s)	K_g (g-mole/cm^2-s)	H_i (atm/g-mole/m^3)	K (dimensionless)
NH_3	1.1×10^{-4}	1.6×10^{-5}	3.42×10^{-5}	0.27
CH_4	1.3×10^{-4}	1.6×10^{-5}	0.99	7923
CO_2	0.68×10^{-4}	0.53×10^{-5}	0.0432	346

Thus, by substituting the values of K, K_w, and K_g into equation (21), the value of K_o can be obtained. The values of the bulk concentration of each gas compound in liquid phase, C_i, can be taken from the research literature by Anderson et al. (1987) for predicting the concentration of carbon dioxide, methane, ammonia, and hydrogen sulfide in the swine manure at the end of the pit-filling periods. Therefore, the average values for each gas compound at the condition of cleanness factor β=0.25 are; CO_2=17.2 mg/l, CH_4=0.39 mg/l, NH_3=864.5 mg/l and H_2S=0.008 mg/l, respectively. Finally, equation (23) can be used to calculate emission rates for each gaseous pollutant in experimental column #6. The results can be tabulated as follows:

Gases	K_o (g-mole/cm^2-s)	C_i (mg/l)	m(i) (g/min)
NH_3	$4.2x10^{-6}$(gas phase control)	864.5	1.52
CH_4	$1.3x10^{-4}$(liquid phase control)	0.39	0.02
CO_2	$6.6x10^{-5}$(both resistances control)	17.2	0.50

Once the emission rates of column #6 have been known, the emission rates for the other waste treatment columns can be calculated using the headspace concentrations listed in Table 11. The results of average gaseous pollutant concentrations and average emission rates of swine manure by different chemical-biochemical additives treatments in experimental columns are listed in Table 15.

Discussion of Results

Water in air samples is a big problem when sampling and analyzing gaseous pollutants (see Appendix B). According to Schuetzle (1980), no one technique can eliminate water and a related problem. In the gas analysis, the response of hydrogen sulfide in total ion chromatogram (TIC) or mass spectrum is small (see Appendix A, Figure A-1 to A-9) and no peak area appears in peak processing. Maybe we can say the hydrogen sulfide content of the swine manure was initially low.

Table 12 and Figure 4 through Figure 11 indicated that in the first two weeks after adding additives, the gaseous level of CH_4, NH_3, and CO_2 were higher than the blank sample because the chemical-bacteria additives would break up the accumulation of organic matter on the column bottom. After three weeks, the additive treatments, CH_4, of the treatments #1, #2, #4, and #5 were reduced slightly below the gaseous

TABLE 15. Average gaseous pollutant concentrations and emission rates of swine manure by different treatment of chemical-bacteria additives in experimental columns

Gaseous Pollutant		Gas Samples 1	2	3	4	5	6	7	8
CH_4	$\bar{C}$[a]	2.0	3.8	5.8	4.3	2.9	2.2	0.6	0.7
	S.D.	1.1	2.2	1.0	3.8	2.5	0.7	0.4	0.05
	$(\dot{m})$[b]	0.02	0.04	0.05	0.04	0.03	0.02	0.01	0.01
NH_3	$\bar{C}$	0.48	0.28	0.35	0.30	0.36	0.11	0.10	0.11
	S.D.	0.35	0.14	0.13	0.15	0.22	0.05	0.001	0.05
	$(\dot{m})$	6.59	4.05	4.56	4.05	5.07	1.52	1.52	1.52
CO_2	$\bar{C}$	750	1010	1170	1230	804	470	10	24
	S.D.	460	414	490	790	78	140	4	12
	$(\dot{m})$	0.78	1.01	1.24	1.29	0.84	0.50	0.02	0.004
H_2S	Not Detected								

[a] $\bar{C} \pm 1$ S.D. = Mean $\pm$ standard deviation, ppm; in which N = 12 observations for the former 6 samples, and N = 8 observations for the other 2 samples.

[b] $(\dot{m})$ = Average emission rate; g/min.

level of the blank sample #6, while CO_2 level was just reduced to the same gaseous level of the blank sample #6. For waste treatment #3, the chemical-bacteria additives were not effective in reducing CO_2 and CH_4 concentration levels. For waste treatment #1 through #5, the additives were not effective in reducing the ammonia concentration level.

Table 15 indicated that quantitative analysis of the CH_4, NH_3, and CO_2 released from stored swine waste in the experimental column gave an average value of 3.76 ppm and 2.2 ppm of CH_4; 0.35 ppm and .11 ppm of NH_3; and 1000 ppm and 470 ppm of CO_2 for treated and untreated swine

waste, respectively. The theoretical emission rates of CH_4, NH_3, and CO_2 at 15°C for the waste treatment #6 were 0.02 g/min, 1.52 g/min, and 0.50 g/min, respectively. As can be seen in Table 15, almost all the waste treatment emission rates of gaseous pollutant were greater than that of untreated swine manure samples.

The emission rate model indicated that with the exception of NH_3, which was extremely soluble, the gases of interest in the manure pit system (O_2-N_2-CO_2-H_2S-CH_4) were sufficiently volatile so that no boundary layer in the gas phase needed to be considered, i.e., $K_O \tilde{} K_W$.

By using the two-film resistance theory, the current inadequacies in applying empirical equations for emission rates estimation of gaseous pollutants from swine manure arise from a lack of data for mass transfer coefficients, K_W and K_g, for such compounds. Therefore, to increase accuracy and to reduce uncertainty of gaseous pollutant emission rates estimation, more laboratory and field studies are required to determine K_W and K_g values.

Based on the emission rates of carbon dioxide, methane, and ammonia, it seems logical to conclude that for most gaseous pollutants of environmental concern, K_W controls the rate of volatile compounds generated from swine manure, and K_g has insignificant effect in the calculation of K_O. K_g can be influenced greatly by turbulence and surface film, and these effects are not included in the equation.

MULTIPLE AIRFLOW REGIONS MODEL

Model Development

Space air distribution

A knowledge of airflow pattern is important for gaseous pollution control in a ventilated enclosure. The distribution of gaseous pollutants in an enclosure depends not only on the characteristics of the pollutants themselves, and the volumetric flow rates of clean air, but also on the flow field. The flow field in a ventilated enclosure is usually complex. The flow field can be defined in terms of supplied airflow, pollutants flow, infiltration flow, and recirculation airflow, etc. Furthermore, turbulent flow is a typical feature of the airflow in a ventilated enclosure.

The pattern of air distribution in a livestock building can form a link between the ventilation system and the microclimate around the animals. According to a study by Bundy (1984) on dust decay in a ventilated chamber, an increase in air circulation would change the airborne dust concentration with time by removing the particles from the airflow.

Randall (1977), and Randall and Battans (1979), gave some general rules that can be used to predict qualitatively the form of pattern to be expected with a system of forced ventilation in livestock buildings;

1. Primary air paths are established from the inlet to the outlet in the direction of airflow.
2. Air moves in a series of rotary motions.

3. Secondary paths are induced by the primary paths to complete one or more rotary motions.

In those references, it has been noted that the space air distribution is dependent on:

1. Different types of air inlet, outlet, and its location.
2. Whether the incoming air is used for heating or cooling.

By examining the air distribution patterns, it has been shown that we can roughly divide the airspace into the following zones (ASHRAE Handbook of Fundamentals, 1985):

1. The primary air zone. This is the part of the space close to the air inlet. This includes the air envelope where the air velocity is greater than 46 m/min.
2. The total air zone. This is the space comprising the air distribution from the primary air zone and entrained air from the general air motion zone. The air velocity in this zone is still high as it is influenced by the primary air, but less than 46 m/min.
3. The stagnant zone. This is the space where the air velocity is usually low, 5-6 m/min. It exchanges mass and heat with other zones mainly by natural convection.
4. The general building air motion zone. This is the part of space in which there is a gentle drift toward the total air zone (i.e., entrainment). Air motion in this space is attributed to total air recycling.

As an example, let us take the air distribution in this case; inlets mounted in or near the ceiling and discharging air horizontally, which is shown schematically in Figure 13. The side view is shown in Figure 14, where "A" denotes the space of volume V_a composed of the primary air and total air zones, and "B" denotes the space of volume V_b corresponding to the general building air motion zone. Below zone "B" is the stagnant zone. This picture can be represented by an airflow model, which is schematically shown in Figure 15.

In this model, "Q" is the volumetric flow rate of discharged fresh air and exit duct air under steady-state condition, "rQ" is the recycle flow rate or secondary flow rate, "r" is the entrainment ratio, and V_d is the volume of the stagnant zone which exchanges mass and heat with V_b by natural convective currents. The dotted arrows between V_a and V_b indicate recirculation streams between these two zones. To clarify the discussion, each air zone V_a and V_b is assumed to be divided into n-interconnected perfect mixing airspaces. The solid arrows between each airspace indicate secondary or tertiary flow rate, in which a tertiary flow is one induced by primary and secondary flow rates. According to Barber and Ogilvie's studies (1982), it has been indicated that the completely stagnant zones are unlikely to exist in livestock buildings, and the multiple flow regions were considered to be the most likely reason for departure from complete mixing in slot-ventilated airspace. Therefore, in this model we will assume V_d is zero.

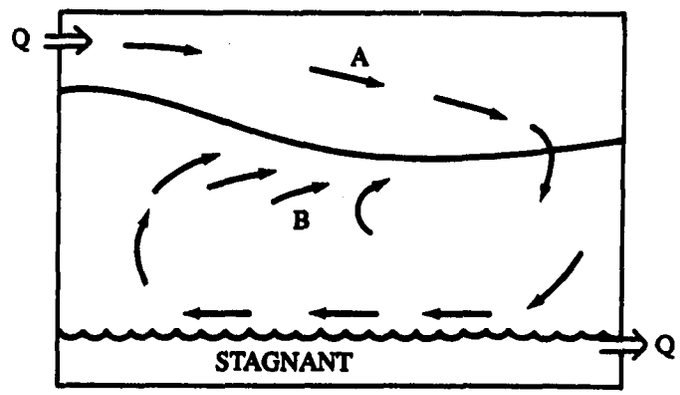

FIGURE 13. Typical airflow pattern in a ventilated enclosure

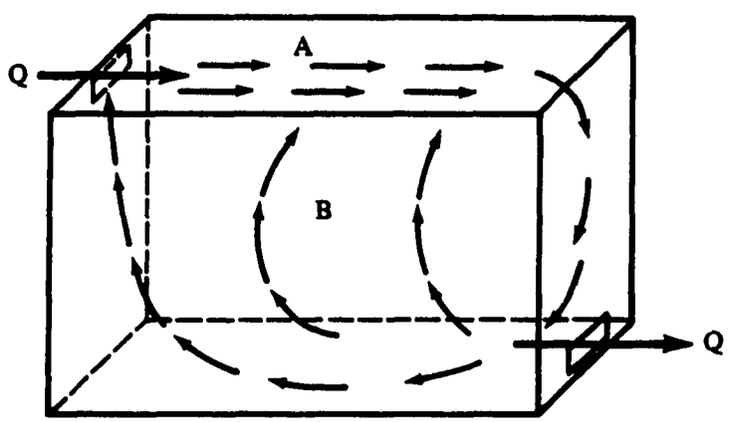

FIGURE 14. Typical airflow pattern in a ventilated enclosure (side view)

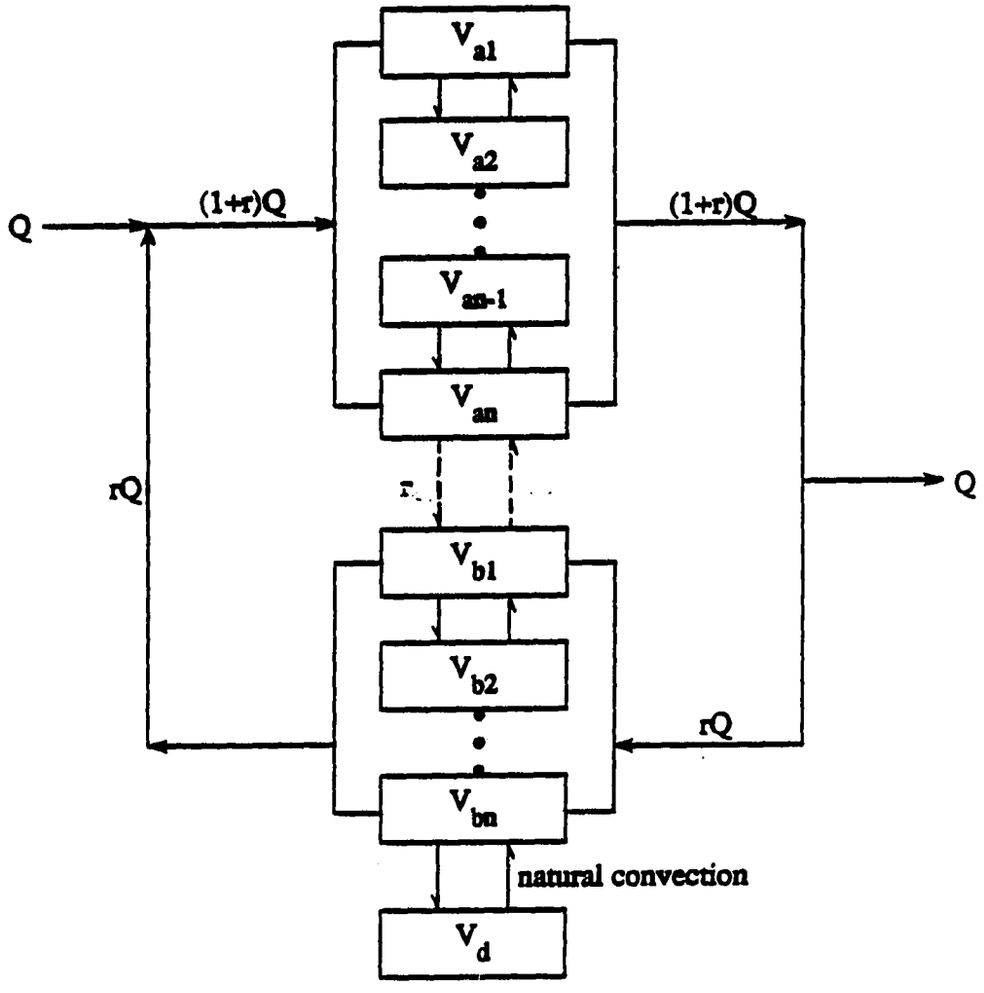

FIGURE 15. The schematic diagram of a ventilation airflow system model in an enclosure (regions in parallel)

Model formulation and mass balance equation

As shown in Figure 15, a ventilated swine building can be divided into N arbitrary subairspaces. In each airspace, the mixing state is assumed to be uniform and instantaneous. The system boundary is taken as the walls, floor and ceiling of building. The multiple airflow regions model is illustrated in Figure 16.

Generally, there are two types of spaces involved:

1. Directly linked to the outdoors, i.e., supply air spaces or exhaust air spaces.

   model in an enclosure (regions in parallel)
2. Indoor spaces which are only in contact with the outdoors via other spaces.

The assumptions throughout the model are:

1. Gaseous pollutants are dynamically passive, i.e.,there are no chemical reactions between primary pollutants and normal atmospheric components, and the motion of gaseous pollutant is totally dependent on the local airflow motion.
2. The emission rate of gaseous pollutants is much smaller than the supply airflow rate.
3. All physical quantities computed from the model represent ensemble properties and presuppose an ergodic hypothesis.
4. The uniform mixing state in airspace is in the sense of local meaning but not of global meaning.
5. No concentration gradients across the system boundary.

In this ventilation system, it is assumed that the emission rates of gaseous pollutants from the manure pit are at a time dependent rates $\dot{m}(t)$. Therefore, by applying the mass balance equation to this system, and the conservation of mass in an arbitrary space i will become (see Figure 16);

$$V_i \frac{dC_i}{dt} = -Q_{ii} C_i + \sum_{\substack{j=1 \\ (i \neq j)}}^{n} Q_{ij} C_j + Q_{is} C_s + m_i(t) \qquad (32)$$

where

Q_{ii} = overall volumetric flow rate of air leaving the space i,

Q_{ij} = transfer airflow rate from space j to space i,

Q_{is} = supplied airflow rate from outdoors to space i

V_i = air volume of space i,

C_i = concentration of gaseous pollutant leaving the space i,

C_s = concentration of supplied air.

Thus,

$$Q_{ii} = \sum_{\substack{p=1 \\ (p \neq i)}}^{n} Q_{pi} \qquad (33)$$

The exhaust concentration C_e has the following relationship;

$$Q\ C_e = \sum_{i=1}^{n} Q_{ei}\ C_i \qquad (34)$$

where Q = total volumetric flow rate of outdoors to the whole system. That is,

$$C_e = \sum_{i=1}^{n} Q_{ei}\, C_i \,/\, Q \tag{35}$$

By using the matrix notation, equations (32) and (35) can be expressed as;

$$\underline{V}\,\frac{d\underline{C}(t)}{dt} = -\underline{Q}\,\underline{C}(t) + \underline{Q}_s\,\underline{C}_s + \underline{m}(t) \tag{36}$$

$$C_e(t) = \frac{\underline{Q}_e^{T}\,\underline{C}(t)}{Q} \tag{37}$$

where $\underline{V}$ and $\underline{Q}s$ are diagonal matrices and $\underline{C}$, $\underline{C}s$, $\underline{m}(t)$, and $\underline{Q}e$ are column matrices (vectors) with nonnegative elements; and $\underline{Q}$ is a square flow matrix defined by:

$$\underline{Q} = \begin{bmatrix} Q_{11} & -Q_{12} & \cdots & -Q_{1n} \\ -Q_{21} & Q_{22} & \cdots & -Q_{2n} \\ \cdot & \cdot & & \cdot \\ \cdot & \cdot & & \cdot \\ \cdot & \cdot & & \cdot \\ -Qn_1 & -Qn_2 & \cdots & Q_{nn} \end{bmatrix} \tag{38}$$

The properties of the flow matrix $\underline{Q}$

1. From equation (38) the flow matrix $\underline{Q}$ has positive diagonal elements and nonpositive off-diagonal elements. Furthermore, there is always an exchange of airflow between the ventilation system and outdoors; and therefore that the

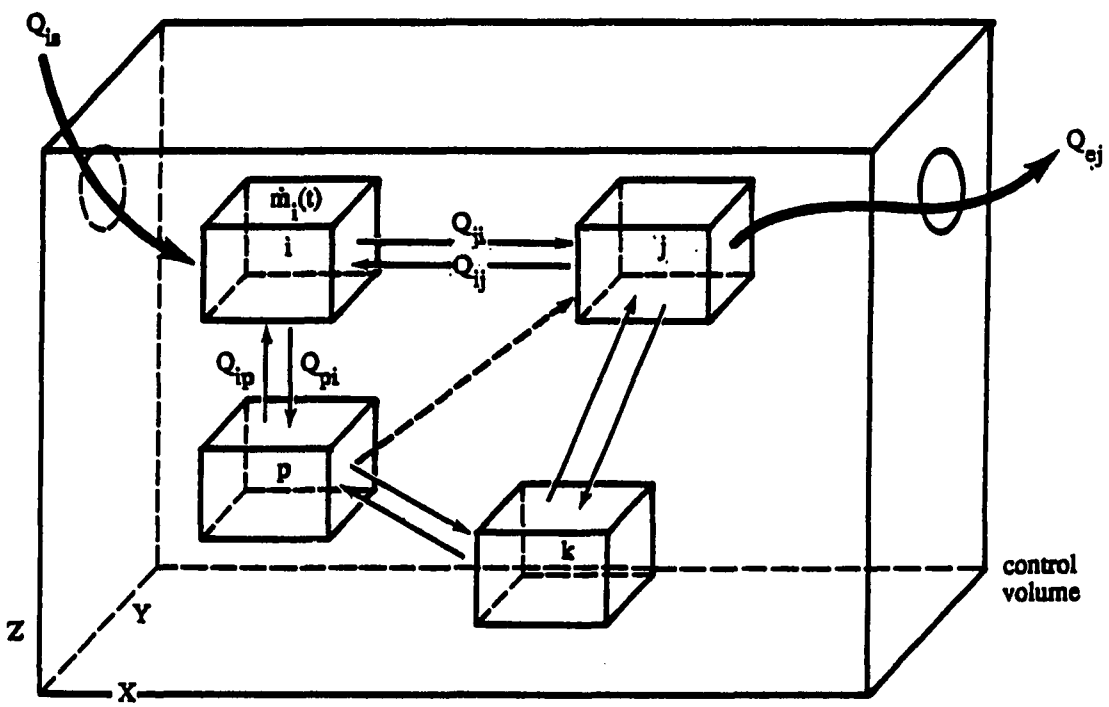

FIGURE 16. The multiple airflow regions model in a ventilated enclosure

whole system is open (a minimal model for the meaning of flow matrix is listed in Appendix G):

$$\underline{Q}s\ \underline{1} = \underline{0}, \text{ and } \underline{Q}e = \underline{0} \tag{39a}$$

This implies that at least one row sum, or one column sum in the flow matrix $\underline{Q}$ is greater than zero. Thus, the whole system has the following constraints;

(i) $\underline{Q}_S\ \underline{1} = \underline{Q}\ \underline{1} = \underline{0}$, i.e.,

$$Q_{is} = Q_{ii} + \sum_{\substack{p=1 \\ (p\neq i)}}^{n} (-Q_{ip}) \geq 0\ ,\ 1 \leq i \leq n \tag{39b}$$

(ii) $\underline{Q}e = \underline{Q}^T\ \underline{1} = \underline{0}$, i.e.,

$$Q_{ej} = Q_{jj} + \sum_{\substack{p=1 \\ (p\neq j)}}^{n} (-Q_{pj}) \geq 0\ ,\ 1 \leq j \leq n \tag{39c}$$

where $\underline{1}$ is a column matrix whose elements are unity and $\underline{0}$ is a column matrix whose elements are zero. Equation (39b) implies that the sum of all elements, say in row i, is equal to the total airflow rate of outdoor air supplied directly to space i. In an exactly analogous manner, equation (39c) implies that the sum of the total flow rate of air is transferred directly from space j to outdoors.

2. Equation (39b) can be rewritten as,

$$Q_{ii} \geq \sum_{\substack{p=1 \\ (p\neq i)}}^{n} (Q_{ip}) \tag{40}$$

According to the theory of matrices (Graham, 1987; Fiedler and Ptak, 1962) if the elements in any matrix can hold the inequality (40), the matrix is quasi-diagonally dominant.

Therefore, equation (40) implies that the flow matrix $\underline{Q}$ is quasi-diagonally dominant. Similarly, equation (39b) implies that the flow matrix is quasi-diagonally dominant with regard to the column sums. Again, from the theory of matrices (Graham, 1987), if a matrix is quasi-diagonally dominant, then the matrix is nonsingular and thus the flow matrix $\underline{Q}$ is nonsingular, i.e., its determinant is nonzero;

$$\text{Det } \underline{Q} \neq 0 \tag{41}$$

This implies that the inverse of the flow matrix, $\underline{Q}^{-1}$ exists. Thus, the elements in the inverse matrix are given by;

$$\underline{Q}^{-1} = \frac{[A_{ij}]}{\text{Det } \underline{Q}} = [B_{ij}] \tag{42}$$

where A_{ij} = cofactor of the matrix $\underline{Q}$.

3. If the matrices having the structure of equation (38) are called M-matrices, according to the theorem of nonsingular M-matrices (Plemmons, 1977), the inverse of the flow matrix $\underline{Q}^{-1}$, is larger than or is equal to zero, i.e.,

$$\underline{Q}^{-1} \geq \underline{0} \tag{43}$$

Thus, the inverse flow matrix, $\underline{Q}^{-1}$, is a nonnegative matrix.

The general solution of model

Knowing that $\underline{Q}^{-1}$ always exists and, therefore, multiplying both sides in equation (36) by $\underline{Q}^{-1}$ we can obtain:

$$\underline{Q}^{-1}\,\underline{V}\,\frac{d\underline{C}(t)}{dt} = -\underline{C}(t) + \underline{Q}^{-1}\,\underline{Q}s\,\underline{C}s + \underline{Q}^{-1}\,\dot{\underline{m}}(t) \qquad (44)$$

The physical dimension of the elements in the matrix $\underline{Q}^{-1}\,\underline{V}$ is time unit and let

$$\underline{T} = \underline{Q}^{-1}\,\underline{V} \qquad (45)$$

Its inverse always exists because all elements on the leading diagonal of $\underline{V}$ are nonzero, thus $\underline{V}^{-1}$ is always nonsingular and is equal to:

$$\underline{T}^{-1} = \underline{V}^{-1}\underline{Q} \qquad (46)$$

After substituting the $\underline{T}$ into equation (44) it becomes;

$$\underline{T}\,d\underline{C}/dt = -\underline{C}(t) + \underline{Q}^{-1}\underline{Q}_{sCs} + \underline{Q}^{-1}\dot{\underline{m}}(t) \qquad (47)$$

Here, assuming that the concentration of supply air is equal to zero, then $\underline{c}_s = \underline{0}$.

So, the time-varying gaseous pollutants' concentrations are governed by;

$$\underline{T}\,\frac{d\underline{C}(t)}{dt} = -\underline{C}(t) + \underline{Q}^{-1}\,\dot{\underline{m}}(t) \qquad (48)$$

By multiplying both sides of equation (48) by $\underline{T}^{-1}$, we can see that the

dynamics of the lumped-parameter system can be represented by the first-order vector-matrix differential equation:

$$\frac{d\underline{C}(t)}{dt} = -\underline{T}^{-1}\underline{C}(t) + \underline{V}^{-1}\,\dot{\underline{m}}(t) \qquad (49)$$

and subjected to the initial condition, $\underline{C}(t) = \underline{C}(0)$ at $t=0$.

The general solution of equation (49) subject to the initial condition is (Lancaster, 1969):

$$\underline{C}(t) = (\exp(-\underline{T}^{-1} t))\,\underline{C}(0) + \int_0^t \exp(-\underline{T}^{-1}(t-t'))\,\underline{V}^{-1}\,\underline{\dot{m}}(t')\,dt' \qquad (50)$$

In equation (50), $\exp(-\underline{T}^{-1}t)$ is the matrix exponential defined by Taylor series (Lancaster, 1969):

$$\exp(-\underline{T}^{-1} t) = \sum_{n=1}^{\infty} \frac{1}{n!} (-\underline{T}^{-1} t)^n$$

$$= \underline{I} - \underline{T}^{-1} t + \frac{1}{2!} t^2 (\underline{T}^{-1})^2 + \ldots. \qquad (51a)$$

in which $\underline{I}$ is the identity matrix:

$$\underline{I} = [\ \delta_{ij}\ ] \qquad (51b)$$

where δij is the Kronecker delta defined by

$$\delta ij = \begin{cases} 1 \text{ if } i = j \\ 0 \text{ if } i = j \end{cases} \qquad (51c)$$

If time increases, the first term in equation (50) decreases and becomes negligible compared with the pollution source term. So, with a constant emission rate of gaseous pollutant, $\underline{m}(s,s)$, equation (50) will become:

$$\underline{C}(t) = (\exp(-\underline{T}^{-1} t))(\underline{C}(0)-\underline{Q}^{-1}\,\underline{\dot{m}}(s,s)) + \underline{Q}^{-1}\,\underline{\dot{m}}(s,s) \qquad (52)$$

The equilibrium concentration attained is given by;

$$\underline{C}(s,s) = \underline{Q}^{-1}\,\underline{\dot{m}}(s,s) \qquad (53)$$

In the case of no pollution source term, equation (50) will become:

$$\underline{C}(t) = (\exp(-\underline{T}^{-1} t))\,\underline{C}(0) \qquad (54)$$

Equation (50) shows that with a time-dependent emission rate of gaseous pollutant, the pollution source term contains the terms dependent on both the flow rate of air and the volume of the space. However, equation (52) shows that in the case of a constant emission rate of gaseous pollutant, the pollution source term is dependent only on flow terms.

When the $\underline{T}^{-1}$ has j different eigenvalues, then equation (52) can be expressed in a form as:

$$\underline{C}(t) = \sum_{k=1}^{j} A(k)\ \underline{X}(k)\ \exp(-ey(k)t) + \underline{Q}^{-1}\dot{\underline{m}}(s,s) \qquad (55)$$

where

A(k) = constants, depend on the initial conditions,

$\underline{X}(k)$ = eigenvectors of $\underline{T}^{-1}$,

ey(k) = eigenvalues of $\underline{T}^{-1}$,

e = Q/V, the nominal air-exchange rate, 1/hr.

The initial conditions can be expressed as a linear combination of eigenvectors:

$$\underline{C}(0) = \sum_{k=1}^{j} A(k)\ \underline{X}(k) + \underline{Q}^{-1}\ \dot{\underline{m}}(s,s) \qquad (56)$$

Here, the background concentration in the airspace was used as the initial conditions for calculating A(k) to lead to the values of $\underline{C}(t)$ by equation (55), e.g., $\underline{C}(0)$ = 0.01 ppm for NH_3, and $\underline{C}(0)$ = 300 ppm for CO_2.

The moments of concentration profiles

The objective of this subsection is to derive a relation between the moments of concentration histories in internal spaces and the moments of concentration histories in the extract air spaces. From the moments, we can deduce the age distributions of both the supplied air and gaseous pollutants generated from swine manure.

From the statistical point of view, the moments about the origin of concentration profile are;

$$M_C^{(n)} = \int_0^{\infty} t^n C(t)\, dt \quad n = 1,2,3, \ldots, n \tag{57}$$

where M_C is the area under the concentration profile. After use of the formula of Laplace Transform, the application of equation (57) on the relation of equation (54) we can obtain:

$$\begin{aligned} \underline{M}_C^{(n)} &= n!\ (\underline{T}^{-1})^{-(n+1)}\ \underline{C}(0) \\ &= n!\ \underline{T}^{n+1}\ \underline{C}(0) \end{aligned} \tag{58}$$

After inserting equation (54) into the equation (37) of the exhaust concentration, we can obtain:

$$C_e(t) = \frac{1}{Q}\ \underline{Q}_e^T\ (\exp\ (-\underline{T}^{-1}\ t)\underline{C}(0)) \tag{59}$$

Because

$$\underline{Q}_e^T = \underline{1}^T\ \underline{Q} \tag{60}$$

By inserting equation (60) into equation (59) and calculating the moments in accordance with equation (57) we can obtain:

$$M_{C_e}^{(n)} = n!/Q\ (\underline{1}^T\ \underline{Q}\ \underline{T}^{n+1})\ \underline{C}(0)$$

$$= n!/Q\ (\underline{1}^T\ \underline{V}\ \underline{V}^{-1}\ \underline{Q}\ \underline{T}^{n+1})\ \underline{C}(0)$$

$$= n!/Q\ (\underline{1}^T\ \underline{V}\ \underline{T}^{-1}\ \underline{T}^{n+1})\ \underline{C}(0)$$

$$= n!/Q\ (\underline{1}^T\ \underline{V}\ \underline{T}^{n})\ \underline{C}(0) \qquad (61)$$

where $\underline{T}^0 = \underline{I}$.

From equation (58) it is shown that equation (61) can be expressed as;

$$M_{C_e}^{(n)} = n/Q\ (\underline{1}^T\ \underline{V}\ \underline{M}_C^{(n-1)}) \qquad (62)$$

By dividing each side in equation (62) by total volume V, and rearranging the terms, we can obtain:

$$\frac{1}{V}\ (\underline{1}^T\ \underline{V})\ \underline{M}_C^{(n-1)} = \frac{Q}{V}\ \frac{1}{N}\ M_{Ce}^{(n)} \qquad (63)$$

The matrix multiplication in equation (63) yields a summation of the moment, $M^{(n-1)}$, in each airspace weighted by the corresponding space's C_i fraction of the total volume, i.e.,

$$\sum_{i=1}^{n} \left(\frac{V_i}{V}\right) M_{C_i}^{(n-1)} = (Q/V)(1/n)\ M_{C_e}^{(n)} \qquad (64)$$

The left-hand side in equation (64) is the system's average (n-1)th moment, i.e., $\bar{M}_C^{(n-1)}$, and therefore equation (64) can be rewritten as;

$$\bar{M}_C^{(n-1)} = (Q/V)(1/n)\ M_{C_e}^{(n)} \qquad (65)$$

Residence Time Distribution

The definition of age distribution function

Consider the ventilated swine building in Figure 17; the gaseous pollutants are shown in their path through the building from manure pit surface until their departure. Each air and gaseous pollutant entering the ventilated airspace will spend some time in the airspace before leaving. It is obvious that the exit time of one gaseous pollutant is different from that of another not only because of the circulation of air flow in a ventilated enclosure but because of the internal mixing (due to the molecular diffusion and turbulent movement, etc.) in each airspace. Therefore, there is an exit age distribution in the leaving air flow. This exit age distribution function will be denoted by E(t). Intimately related to the exit age distribution function, E(t), is internal age distribution function, I(t), which accounts for the distribution of the ages (the length of time which has elapsed since the gaseous pollutant generated from the manure pit surface) of air and gaseous pollutants at any moment in a ventilated enclosure.

There are three concentrations of gaseous pollutants that are considered in terms of age distribution (Zwietering, 1959);

1. A total internal concentration consisting of all gaseous pollutants within the building.
2. A local internal concentration at any arbitrary airspace within the building.
3. An external concentration consisting of gaseous pollutants leaving the building.

Each concentration of gaseous pollutant may be characterized by its statistical cumulative age distribution function, i.e., CDF, and corresponding probability density function, i.e., PDF. The CDF is dimensionless, and the magnitude of the function at a particular time, t, gives the fraction of the considered concentration with an age less than or equal to t. The magnitude of PDF, whose dimension is one over time (1/time), is the derivation of the CDF at time t. For example, for the exit age distribution function, E(t), the general relationship between a CDF, F(t), and corresponding PDF, E(t), is

$$\frac{dF(t)}{dt} = E(t), \quad \text{or} \quad \int_0^t E(t)\, dt = F(t) \tag{66}$$

Here, E(t)dt, represents the fraction of the fluid elements in the exit stream having spent the time between t to t+dt in a ventilated enclosure, and also I(t)dt, represents the fraction of fluid elements with internal age between t and t+dt; therefore,

$$\int_0^\infty E(t)\, dt = \int_0^\infty I(t)dt = 1 \tag{67}$$

Because age cannot be negative, F(t) is defined over $(0,\infty)$. The range of F(t) is 0 to 1 with $F(-0) = 0$ and $F(\infty) = 1$ (Nauman, 1981). And with an example of exit age distribution function, the moments about the origin are:

$$M_E^{(n)} = \int_0^\infty t^n E(t)\, dt = \int_0^1 t^n\, dF(t) \tag{68}$$

The variance σ^2 can be expressed as,

$$\sigma_E^2 = \int_0^\infty (t-M_E^{(1)})^2 \, E(t) \, dt = M_E^{(2)} - (M_E^{(1)})^2 \qquad (69)$$

The moment $M^{(n)}$ also can be calculated from the CDF, F(t), by integrating by parts[1] and applying equation (68) leads to

$$M_E^{(n)} = n \int_0^\infty t^{(n-1)} \, (1-F(t)) \, dt \qquad (n > 0) \qquad (70)$$

Furthermore, for gaseous pollutants within a ventilated swine building, the following ages can be defined (Zwietering, 1959), see Figure 17;

1. The internal age, t_i, is the travel time for component to move from a point on the manure surface to a specific subvolume.
2. The residual life time, t_{rl}, is the travel time from a specific volume to the exhaust.
3. The residence time, t_r, is the average time of release to time of exhaust.

1

$$\int_{F(a)}^{F(b)} t^n \, dF(t) = b^n F(b) - a^n F(a) - n \int_a^b t^{n-1} \, F(t) dt$$

$$= F(b)(b^n - a^n) - n \int_a^b t^{n-1} F(t) dt - a^n [F(a)-F(b)]$$

$$= n \int_a^b t^{n-1} [F(b)-F(t)] dt - a^n [F(a)-F(b)]$$

Because F(a)=0, F(b)=1; and a=0, b=∞; therefore,

$$\int_0^1 t^n \, dF(t) = n \int_0^\infty t^{n-1} [1-F(t)] dt.$$

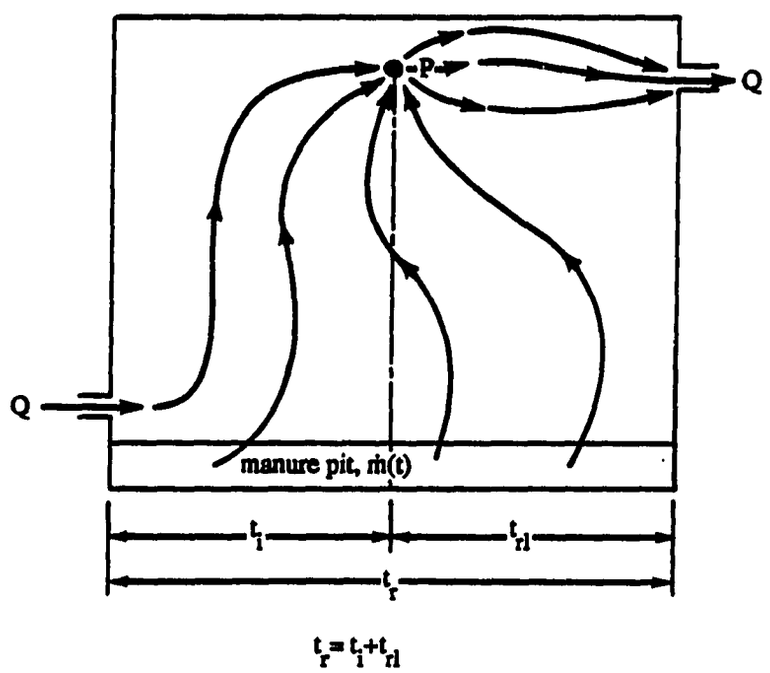

FIGURE 17. Definition of different ages of gaseous pollutants and airflow

The CDF and PDF for the total internal gaseous pollutants and for the local at arbitrary airspace or point p at different ages are illustrated in Table 16. To aid in gaining an appreciation of the several ages, an analogy to human populations may be helpful. The age corresponds to the common use of the word, while the residence time is the life span. The mean internal age is the average age of the population living at any time. The mean residence time is the average age at the time of death.

Therefore, at any time t, a mass balance of the second air flow over

a ventilated enclosure gives (Danckwerts, 1953);

$$Q\ tr = V \int_0^{t_r} I(t)\ dt + Q \int_0^{t_r} F(t)\ dt \qquad (71)$$

[entered the system]=[still in the system]+[left the system]

Differentiating equation (71) with respect to t yields

$$1 - F(t) = [V/Q]\ I(t) \qquad (72)$$

TABLE 16. The cumulative distribution function and probability density function for different age distribution

Age	cumulative distribution function		probability density function	
	total	local	total	local
t_i	Φ	Φ_p	I	I_p
t_{rl}	Ψ	Ψ_p	Ψ	Ψ_p
t_r	X		X	

where

$$V/Q = t_n = \text{mean-holding time of the ventilation air}$$

For the air or gaseous pollutants in the multiple airflow regions system, on leaving the system, the mean-holding time is always equal to t_n. This can be shown by making use of definition of the mean and equation (67) and expressed as follows,

$$t_n = \int_0^\infty t\, E(t)\, dt \tag{73}$$

According to equation (70) and applying equation (72) leads to

$$tn = \int_0^\infty (1-F(t))\, dt = t_n \int_0^\infty I(t)\, dt = tn \tag{74}$$

Each of the age distribution functions also can be expressed in dimensionless form, which is often convenient to use in analysis. With the superscript asterisk (*) to indicate a dimensionless time, t^* becomes

$$t^* = t/t_n \tag{75}$$

Thus $E(t^*)dt^* = E(t)dt$, $I(t^*)dt^* = I(t)dt$, and so forth, so that

$$E(t^*) = t_n\, E(t) \tag{76}$$

$$I(t^*) = t_n\, I(t) \tag{77}$$

Also, differentiating equation (72) once more and applying equation (67) to obtain

$$E(t^*) = -\frac{dI(t^*)}{dt^*} \tag{78}$$

The experimental measurement of age distribution

There are two perfectly equivalent methods of obtaining experimentally or numerically, the age distribution functions (Himmelblau and Bischoff, 1968);

1. Step-up, at time = 0, a fraction of the supplied air is labeled with gaseous pollutant, and the concentration of gaseous pollutant is measured at the point(s) in the system (enclosure) where the local age distribution is to be obtained.
2. Step-down, the system is initially filled with a known homogeneous concentration of gaseous pollutant and is then supplied fresh air; the decay of concentration is recorded at point(s) where the local age distribution is to be obtained.

The equation for the local age in a step-up simulation is now derived. At time t = 0, a fraction, C_o, of all the entering molecules in the system are labeled. Consider an arbitrary point (control volume) p within the system at time t where the concentration is $C_p(t)$. A fraction $C_p(t)/C_o$ of the molecules at point p thus have an age less than or equal to t. Because $C_p(t)/C_o$ has the characteristics of a cumulative distribution function, $\Phi_p(t) = C_p(t)/C_o$ is defined as the cumulative distribution function of the local age at point p (see Table 16).

From equation (70), the local age $M_{I_p}^{(1)}$ can be calculated as;

$$M_{I_p}^{(1)} = \int_0^\infty (1 - \Phi_p(t))dt$$

$$= \int_0^\infty (1 - C_p(t)/C_o)dt \qquad (79)$$

For step-down simulation with $\Phi_p(t)=1-C_p(t)/C_o$ then

$$M_{I_p}^{(1)} = \int_0^\infty (1 - \Phi_p(t))dt$$

$$= 1/C_o \int_0^\infty C_p(t)\, dt$$

$$= 1/C_o \, M_{C_p}^{(0)} \qquad (80)$$

The age distribution of airflow

From the definition of experimental measurement of age distribution functions by step-down simulation, i.e., equation (80), it is possible to determine the internal age of airflow in a ventilated enclosure by starting from the same initial concentration of air in each airspace as the reference concentration C_o, in which $C_o = C(0)$; and from the definition of the theory of matrices,

$$\underline{C}(0) = C(0)\, \underline{1} \qquad (81)$$

Therefore, by the definition of equation (80), and the recorded concentration-time relations of airflow, the mean-age of the airflow in a ventilated enclosure airspace i, can be obtained by divided the 0th moment, i.e., the area under the recorded concentration-time curve by the initial concentration, C(0); and using the matrix notation, it becomes,

$$\underline{M}_I^{(1)} = \frac{1}{C(0)} \underline{M}_C \qquad (82)$$

According to equation (58),

$$\underline{M}_C^{(0)} = \underline{T}\, \underline{C}(0) \qquad (83)$$

Combining equation (81) and equation (83) leads to;

$$\underline{M}_C^{(0)} = \underline{T}\ \underline{1}\ C(0) \tag{84}$$

Inserting equation (84) into equation (82) gives the important relations;

$$\underline{M}_I^{(1)} = \underline{T}\ \underline{1} \tag{85}$$

Equation (85) means the row sum in $\underline{T}$ matrix, say the ith row, is the local mean age of airflow in space i.

The mean age of the air when it leaves the ventilated enclosure, $M_E^{(1)}$ can be obtained from the concentration reading in the exhaust duct as;

$$M_E^{(1)} = M^{(0)} / C(0) \tag{86}$$

According to equation (61) the 0th moment is;

$$M_{C_e}^{(0)} = 1/Q\ (\ \underline{1}^T\ \underline{V}\ \underline{I}\ )\ C(0)$$

$$= V / Q\ C(0) \tag{87}$$

and equation (86) becomes;

$$\bar{M}_E^{(1)} = V / Q = t_n \tag{88}$$

The mean age of air in the whole ventilated enclosure, $\bar{M}_I^{(1)}$, is equal to;

$$\bar{M}_I^{(1)} = M_{C_e}^{(1)} / M_{C_e}^{(0)} \tag{89}$$

The first moment, $M_{C_e}^{(1)}$, according to equation (61) is equal to;

$$M_{C_e}^{(1)} = 1/Q \ (\underline{1}^T \ \underline{V} \ \underline{T} \ \underline{1}) \ C(0) \tag{90}$$

Using equation (87), (90) and equation (85) in equation (89) the following expression for the mean age of air in the whole ventilation systems can be obtained as;

$$\bar{M}_I^{(1)} = [\underline{1}^T \ \underline{V} \ \underline{T} \ \underline{1}] \ / \ V = [\underline{1}^T \ \underline{V} \ \underline{M}_I^{(1)}] \ / \ V \tag{91}$$

The matrix multiplication in the denominator of equation (91) gives rise to a summation of the mean age, $M_{I_i}^{(1)}$, in each space i, weighted by the corresponding volume fraction of the total volume of space in the systems,

$$\bar{M}_I^{(1)} = \sum_{i=1} \left(\frac{V_i}{V}\right) M_{I_i}^{(1)} \tag{92}$$

The age distribution of gaseous pollutants

The mean age of gaseous pollutants generated from manure pit surface can be obtained by the same procedure as for the airflow. The only difference is that it starts from an equilibrium concentration, C(s,s), caused by gaseous pollutants sources. The equilibrium concentration is given by equation (55) and which concentration is not necessarily the same in each space.

The mean age of the gaseous pollutants in space i is calculated from the concentration reading in that space as:

$$M_{I_i}^{(1)} = M_{C_i}^{(0)} \ / \ C_i(0) \tag{93}$$

The mean age of the whole gaseous pollutants present in the

ventilation systems, $\bar{M}_{I_i}^{(1)}$, can be calculated from the concentration reading in the exhaust duct as;

$$\bar{M}_I^{(1)} = M_{C_e}^{(1)} / M_{C_e}^{(0)} \tag{94}$$

From equation (61) the following expression of the 0th moment in the exhaust duct can be obtained as;

$$\bar{M}_{C_e}^{(0)} = 1/Q \ (\underline{1}^T \ \underline{V} \ \underline{C}(0)) \tag{95}$$

By carrying out the matrix multiplication in equation (95) it becomes;

$$M_{C_e}^{(0)} = V / Q \ \bar{C}(0) \tag{96}$$

where $\bar{C}(0)$ is the average concentrations of gaseous pollutant in the systems. By using equation (62) the 1st moment in the exhaust can be written as;

$$M_{C_e}^{(1)} = 1/Q \ (\underline{1}^T \ \underline{V} \ \underline{M}_C^{(0)}) \tag{97}$$

By inserting equation (96) and equation (97) into equation (94) to obtain following expression for the mean age of the gaseous pollutants present in a ventilated enclosure;

$$\bar{M}_I^{(1)} = [1^T \ \underline{V} \ \underline{M}_C^{(0)}] / [V \ \bar{C}(0)] \tag{98}$$

By carrying out the matrix multiplication in the denominator of equation (98) and using equation (82), we can obtain the final

expression of the mean age of the gaseous pollutants present in a ventilated enclosure;

$$\bar{M}_I = \sum_{i=1}^{n} \left[\frac{V_i \, C_i(0)}{V \, \bar{C}(0)} \right] M_{I_i}^{(1)} \tag{99}$$

That is, the system's average age is obtained by summing the mean-age in each space weighted by the fraction of gaseous pollutant content in the corresponding space of the total gaseous pollutant content in the system.

The Physical meaning of Q^{-1} and T matrix

The Q^{-1} matrix The inverse flow matrix, $\underline{Q}^{-1}$, can be written in terms of cofactors, A_{ij}, of the matrix $\underline{Q}$ as;

$$\underline{Q}^{-1} = \frac{1}{\text{Det } Q} \begin{bmatrix} A_{11} & A_{12} & \cdots & A_{1n} \\ \vdots & \vdots & & \vdots \\ A_{n1} & A_{n2} & \cdots & A_{nn} \end{bmatrix}$$

$$= \begin{bmatrix} B_{11} & B_{12} & \cdots & B_{1n} \\ \vdots & \vdots & & \vdots \\ B_{n1} & B_{n2} & \cdots & B_{nn} \end{bmatrix} \tag{100}$$

The elements in $\underline{Q}^{-1}$ are nonnegative (see equation (43)).

Assume that the equilibrium emission rate of a gaseous pollutant released in space i, denoted by $m_i(s,s)$, gives rise to a gaseous

pollutant concentration in space p, according to equation (53) is equal to;

$$C_p(s,s) = B_{pi}\, m_i(s,s) \tag{101}$$

By using equation (101) the elements in $\underline{Q}^{-1}$ can be written as;

$$B_{pi} = C_p/\dot{m}_i = T_{pi} \tag{102}$$

Here, T_{pi} can be defined as a transfer index.

The concept of local purging flow rate has been introduced by Zvirin and Shinnar (1979). The meaning of the local purging flow rate is the net flow rate at which gaseous pollutants are driven toward the exhaust duct. Consider an equilibrium emission rate of gaseous pollutant released in space i, then apply equations (37) and (53), during a continuous released, a mass balance in space i, is given;

$$\dot{m}_i(s,s) = Q\, C_e(s,s) = U_i\, C_i(s,s) \tag{103}$$

or,

$$1 / U_i = C_i(s,s) / \dot{m}_i(s,s) = B_{ii} = A_{ii} / \text{Det}\, \underline{Q} \tag{104}$$

where

U_i = local purging flow rate in space i.

Expressed in terms of the local purging flow rate, U_i, and the transfer index T_{pi}, the $\underline{Q}^{-1}$ becomes;

$$\underline{Q}^{-1} = \begin{bmatrix} 1/U_i & T_{12} & \cdots & T_{1n} \\ \vdots & \vdots & & \vdots \\ T_{n1} & T_{n2} & \cdots & 1/U_n \end{bmatrix} \tag{105}$$

According to Zvirin and Shinnar's study (1979) of internal tracer experiment and local retention time distribution, the final expression for the local purging flow rate can be obtained as follows;

$$U_p = m_i \; / \; [\int_0^\infty C_p(t)\, dt]\; P_{pi} \tag{106}$$

in which m_i is the amount of tracer injected in space i, and P_{pi} is the transition probability of tracer in space i passing through space p. The P_{pi} in words may be expressed as the ratio of amount of gaseous pollutant passing p per unit of time to amount of gaseous pollutant released in p per unit of time.

Now, if we consider the total time integrated exposure by gaseous pollutants in a ventilated enclosure, from equation (106) we know that the probability P_{pi}, can be expressed as;

$$P_{pi} = [U_p \int_0^\infty C_p(t)dt] \; / \; m_i \tag{107}$$

By using equation (103), equation (107) can be written as;

$$P_{pi} = [U_p \, M_{C_p}^{(0)}] \; / \; m_i = [U_p \, M_{C_p}^{(0)}] \; / \; [Q \, M_{C_e}^{(0)}] \tag{108}$$

From the statistical concepts, we can obtain the upper bound for the transition probability as follows:

$$P_{pi} \leq 1 \tag{109}$$

Again, differentiating equation (106) with respect to t and applying the relation of equation (103) and rearranging it, we can obtain the following important relationship,

$$\dot{m}_p = P_{pi} \, \dot{m}_i \tag{110}$$

Equation (110) implies that the emission rate of gaseous pollutants at

an arbitrary space $\dot{p}$, m_p, can be expressed as the proportional to the emission rate of pollutants released in space i, $\dot{m}_i$. In other words, the emission rate vector is not a unique set of variables, any other set $\underline{\dot{m}}'(t)$ related to $\underline{\dot{m}}(t)$ by a nonsingular transformation, $\underline{\dot{m}}'(t) = \underline{P}\ \underline{\dot{m}}(t)$, can fulfill the requirement of equation (110).

According to equation (102) and equation (110) the T_{pi} can be expressed as;

$$T_{pi} = C_p(s,s) / \dot{m}_i = C_p(s,s) / [\dot{m}_p / P_{pi}]$$
$$= P_{pi} / U_p \qquad (111)$$

In terms of the local purging flow rate, U_p, and the transition probability, P_{pi}, the inverse flow matrix $\underline{Q}^{-1}$ becomes;

$$\underline{Q}^{-1} = \begin{bmatrix} 1/Ui & P_{12}/U_1 & \cdots\cdots & P_1n/U_1 \\ \vdots & \vdots & & \vdots \\ Pn_1/Un & Pn_2/Un & \cdots\cdots & 1/Un \end{bmatrix} \qquad (112)$$

The T matrix By carrying out the matrix multiplication in definition of the matrix $\underline{T}$, using expression (112) of the matrix $\underline{Q}^{-1}$, then;

$$\underline{T} = \underline{Q}^{-1} \ \underline{V} = \begin{bmatrix} \frac{V_1}{U_1} & \frac{V_2}{U_1} P_{12} & \cdots\cdots & \frac{V_n}{U_1} P_{1n} \\ \vdots & \vdots & & \vdots \\ \frac{V_1}{U_n} P_{n1} & \frac{V_2}{U_n} P_{n2} & \cdots\cdots & \frac{V_n}{U_n} \end{bmatrix} \quad (113)$$

From equation (85) that the sum elements in an arbitrary row p in $\underline{T}$ is equal to the mean age of airflow in space p, $M_{I_p}^{(1)}$ that is,

$$M_{I_p}^{(1)} = \frac{1}{U_p} \sum_{j=1}^{n} V_j P_{pj}$$

$$= \left(\frac{V_p}{U_p} \right) + \frac{1}{U_p} \sum_{\substack{j=1 \\ (j \neq p)}}^{n} V_j P_{pj} \quad (114)$$

We know that $P_{pj} \leq 1$ and therefore we obtain the following upper bound of the local mean age of the airflow in space p;

$$M_{I_p}^{(1)} \leq \frac{1}{U_p} \sum_{j=1}^{n} V_j = \frac{V}{U_p} \quad (115)$$

or,

$$U_p \ M_{I_p}^{(1)} \leq V \quad (116)$$

Relation in equation (116) connected with two important quantities, the local purging flow rate and the local mean age of air. Equation (116) can be rewritten as;

$$U_p \leq [t_n / M_{I_p}^{(1)}] \ Q \quad (117)$$

When $M_{I_p}^{(1)} > t_n$, i.e., when the local mean-age of airflow is larger than

the mean-holding time of the system at the airspace p, relation (117) gives rise to the following restriction to the local purging flow rate;

$$Q > U_p \text{ (when } M_{I_p}^{(1)} > t_n) \tag{118}$$

Model Simulation

Comparison with research literature

Model case description A model case will be studied in some detail to give insight into the meanings of the concepts of the multiple airflow regions model and residence time distribution of polluted air. The model example is chosen from the paper "The Influence of Ventilation on Distribution and Dispersal of Atmospheric Gaseous Contaminants" by Brannigan and McQuitty (1971). That study was carried out in an environmental chamber, of which the dimensions and general outline are given in Figure 18. The dimensions were such as to simulate one pen of a piggery. Estimated capacity of a pen of this size is 20 pigs, each weighing approximately 55 kg. The data for ventilation rates (typical of commerical swine units), air-exchange rates and mean-holding time of air and the total emission rates of CO_2 and NH_3 are illustrated in Table 17. The layout of the sampling point is shown in Figure 19.

The procedure of model verification Brannigan and McQuitty's study discussed two kinds of ventilation systems, i.e., two different locations of outlet. One is mounted near the ceiling, the other mounted near the floor of the test chamber. Therefore, in the study of the model case, two kinds of ventilation systems will be included, i.e., (1) short-circuiting system (outlet height is equal to 2 m above floor

TABLE 17. The system parameters from model case by Brannigan and McQuitty (1971)

ventilation rate (m^3/hr)	air-exchange rate (1/hr)	mean-holding time (hr)	emission rate of gases (1/hr)	
			NH_3	CO_2
280	7.8	0.128	27	480
443	12.3	0.0813	27	480
932	25.8	0.0388	27	480

level), (2) displacement system (outlet height is equal to 0.5 m above floor level). There were 55 sampling points measured by Brannigan and McQuitty, the number of sampling points was reduced to 25 points in this simulation study. The multiple airflow regions models for the two ventilation systems is shown schematically in Figure 20. The x-z coordination of the test chamber was divided into 25 lumped forms of control volumes. The control volume P in Figure 20 is in a grid in which the distance between grid lines in the x- and z- direction are dx and dz, respectively. Assume, for simplicity, that the airflow and recirculation airflow is directed in the x- and z- direction. The flow patterns of the two ventilation systems are schematically shown in Figure 21.

The input data for the simulation model shall be included:

1. the entrainment ratio, r value,
2. the airflow matrix, $\underline{Q}$,
3. the air volume matrix, $\underline{V}$, and
4. the vector of total emission rates of gaseous pollutants,

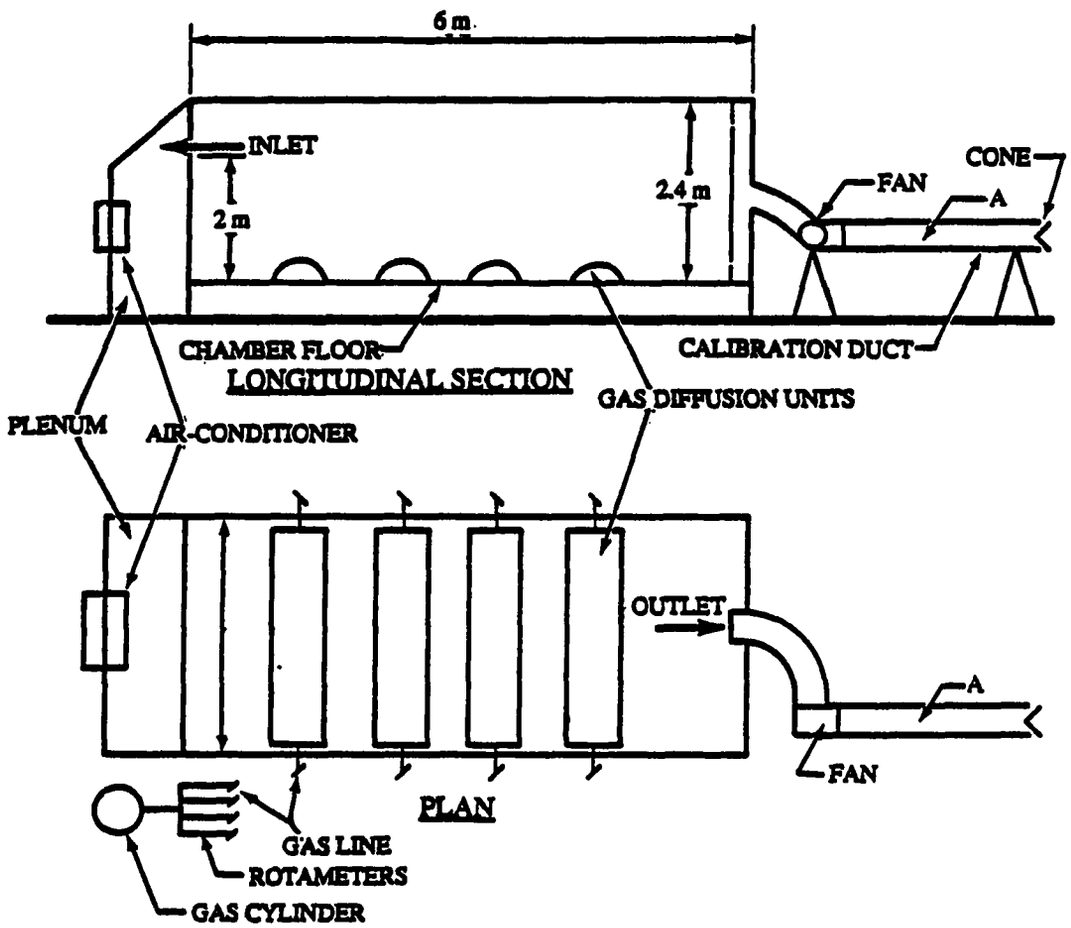

FIGURE 18. A section and plan of the environmental chamber with exhaust fan (Brannigan and McQuitty, 1971)

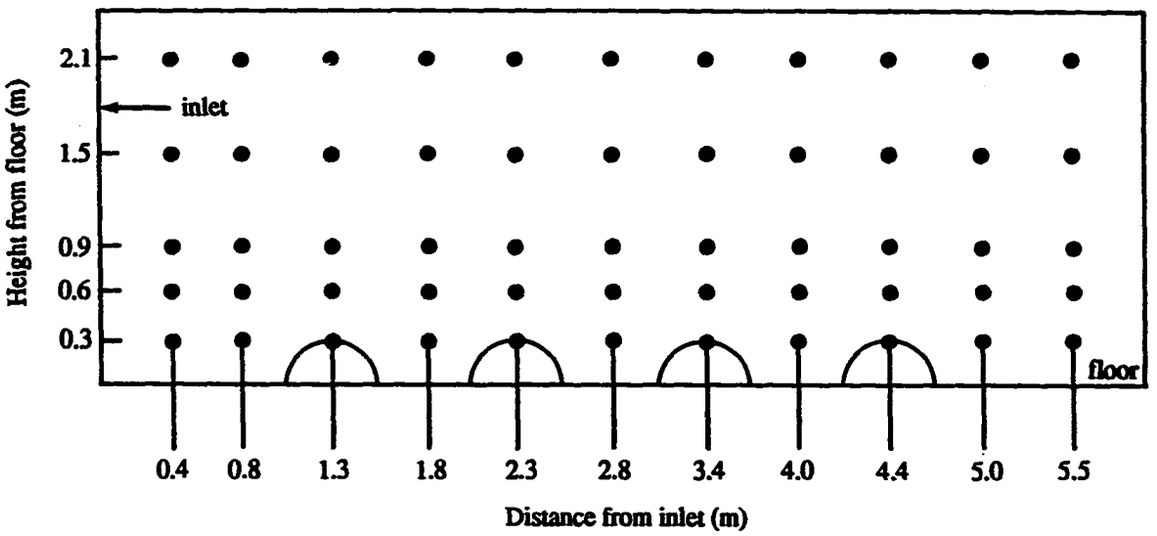

FIGURE 19. A longitudinal section of the environmental chamber showing the location of the sampling points (Brannigan and McQuitty, 1971)

$\underline{\dot{m}}(s,s)$.

The output of this simulation model including:

1. the dimensionless local purging flow rate, $U_i^* = U_i/Q$,
2. the dimensionless equilibrium concentration of gaseous pollutants, $C_i(s,s)^* = C_i(s,s)/(\dot{m}/Q)$,
3. the transition probability between each space, P_{ij},
4. the dimensionless local mean-age of airflow,

$$M_{I_i}^{(1)*} = M_{I_i}^{(1)} / t_n, \text{ and}$$

5. the general solution of the concentration of gaseous pollutants in each space, $\underline{C}(t)$.

The information flow diagram of the model case study is in Figure 22. Now, the detailed explanation of input data is as follows.

1. The entrainment ratio, r: Practically, the lower bound for r is much greater than 1. The actual value depends to some extent on the relative position between the supply and exhaust position, and size, shape (circular or slot, etc.) of the nozzle or air jet, etc. Some estimations of the entrainment ratio, r, are possible on the basis of a simple entrainment concept. It has been assumed that the secondary flow rate rQ in a ventilated enclosure is entirely induced by the primary flow rate, i.e., by the entrainment in the inlet jets.

   Equations for the entrainment of circular jets and jets from long slots have been mathematically presented in ASHRAE Handbook of Fundamentals (1985). They are

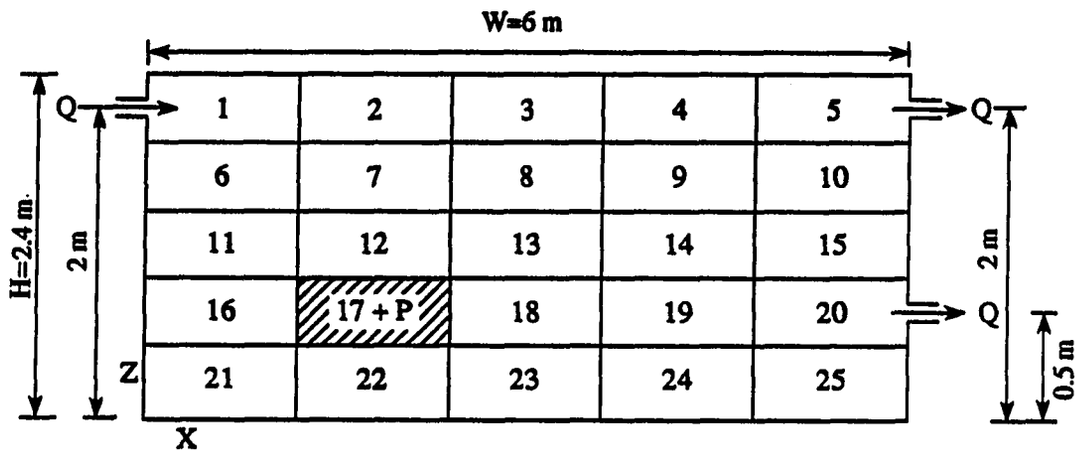

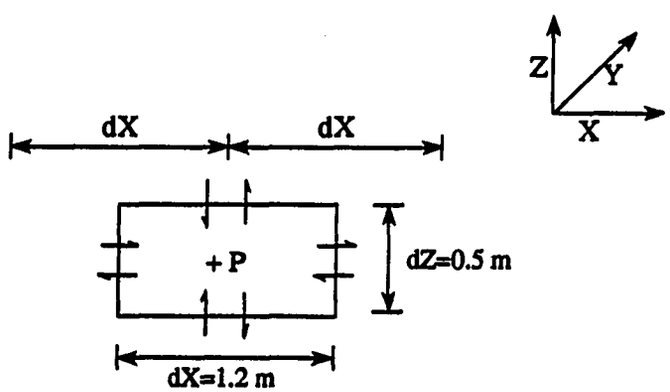

CONTROL VOLUME P

FIGURE 20. The multiple airflow regions model and control volume for ventilation systems described in research literature by Brannigan and McQuitty (1971)

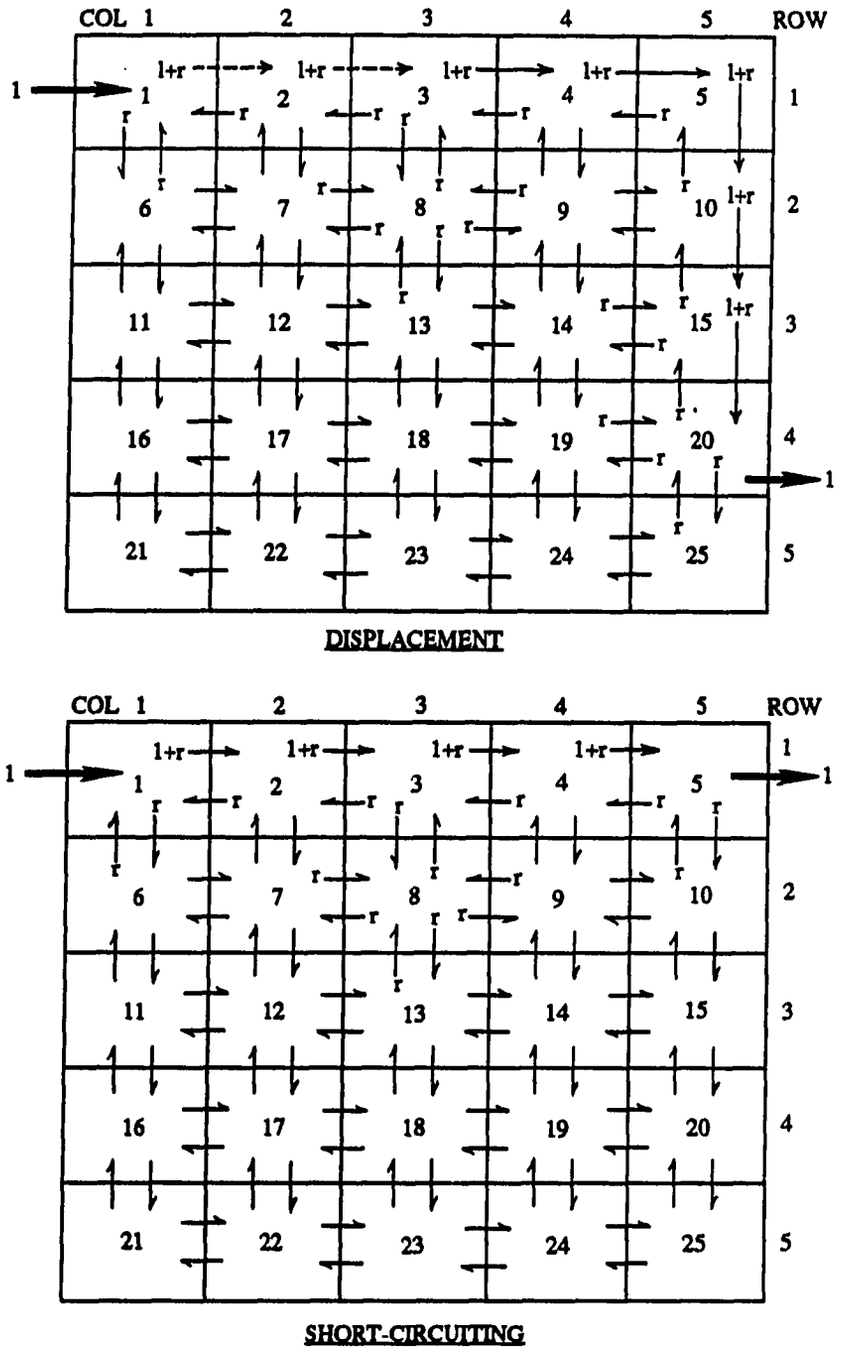

FIGURE 21. The air flow patterns for two ventilation systems in simulation model in the case of Brannigan and McQuitty, (1971)

(1) For circular jets:

$$r = rQ/Q = \text{entrained flow/initial flow}$$
$$= (2/K')(X/A_o^{0.5}) \quad (119a)$$

(2) For long slot:

$$r = rQ/Q = \text{entrained flow/initial flow}$$
$$= [(2/K')(X/H_o)]^{1/2} \quad (119b)$$

where

X = distance from face of outlet, m

A_o = effective area of the stream at discharge from an open end duct or at contracted section, m^2

H_o = width of slot, m

K' = proportionality constant, approximately 7.

In this model example, the air entered the chamber through a 2364 mm x 51 mm long slot. Therefore, the value for X, H_o, and K' are: X = 6 m, H_o = 51 mm, and K' = 7. Inserting all those values into equation (119b) shows the value of r is equal to 5.8.

2. The airflow matrix Q: The input data of the flow matrix, Q, is determined using equation (38) for the flow patterns that are shown in Figure 21. Figure 21 indicated that the solution of the airflow matrix is by 2-D lumped form of control volumes represented the conservation of air mass. The input data of the flow matrix are listed in Appendix D (Figures D-1 and D-2).

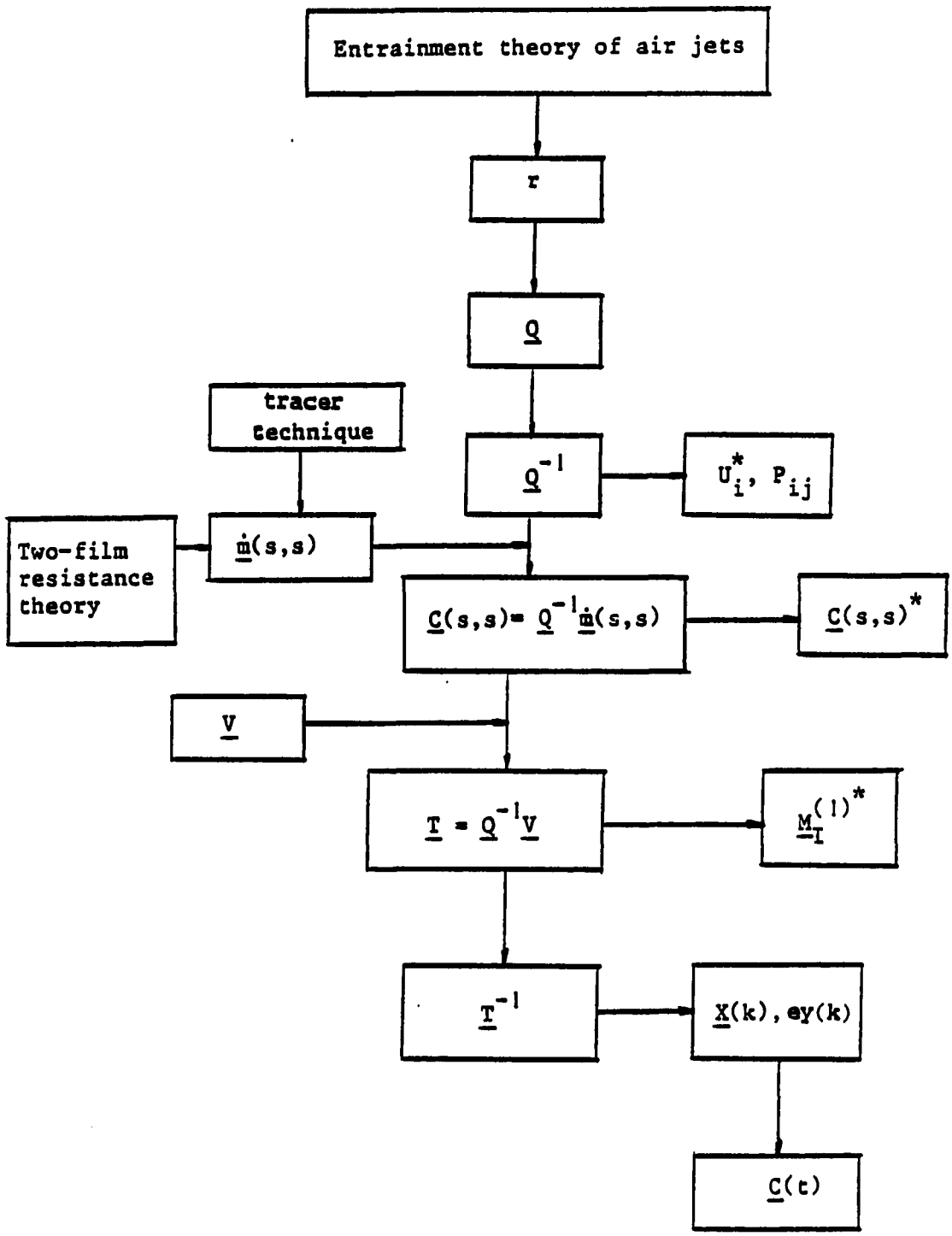

FIGURE 22. The information flow diagram for the simulation model case study

3. The air volume matrix, $\underline{V}$: In this simulation, the fraction of air volume, K_i, assume equal, i.e., $K_i = 1/25$, i = 1, 2, 3, ..., 25.

4. The steady-state emission rate matrix, $\dot{m}(s,s)$: According to Table 17, the total steady-state emission rate of gaseous pollutants for NH_3 and CO_2 are as follows, $\dot{m}(s,s)$ of NH_3 = 27 l/hr = 20.4 g/hr, and $\dot{m}(s,s)$ of CO_2= 480 l/hr = 942 g/hr (the ambient air condition assumes under 25°C, 1 atm). And, from Figure 19, the location of gas diffusion units are at spaces 22, 23, 24, and 25 in the multiple airflow regions model. Therefore, in calculating the equilibrium concentrations of gaseous pollutants in each space, the gas emission rates in spaces 22,

   23, 24, and 25 are the same and are equal to $\dot{m}(s,s)/4$.

Comparison with chamber test

Experimental procedure and equipment The test facility employed in this field study was composed of (1) an environmental chamber, (2) an air delivery system, (3) a gas charging system, and (4) a gas sampling and analyzing system. All components were housed in a laboratory that had controlled air conditioning equipment. An attempt was made to control the laboratory ambient temperature at 25°C. However, temperature gradients did exist because of cycling of the cooling equipment. The relative humidity generally ranged between 60% and 70% in the laboratory.

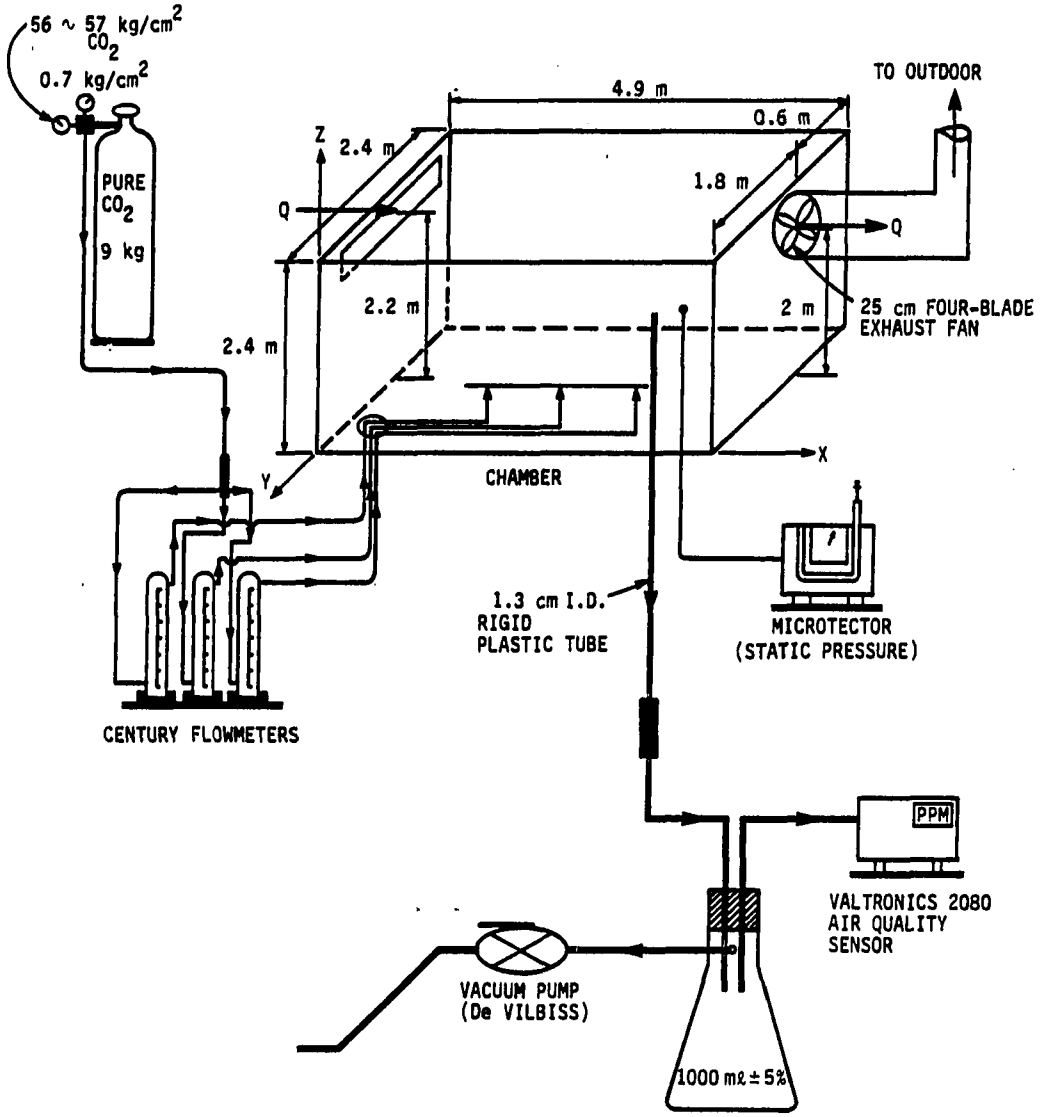

FIGURE 23. The layout of the experimental equipment and the dimensions of environmental chamber

1. Environmental chamber: The dimensions and general outline of the environmental chamber are given in Figure 23. The dimensions were such as to simulate one pen of a piggery. Estimated capacity of a pen of this size is 15 pigs, each weighing approximately 55 kg.
2. Air delivery system: The air entered the chamber from the laboratory through a long slot (2440 mm x 0-127 mm) inlet. A 25 cm diameter, 4-blade centrifugal fan was used for exhausting air from the chamber. The exhaust location was 2 m from floor level measured to the center of the outlet. Adjustment of ventilation rates was achieved by changing the width of the slot inlet and fan velocity. The static pressure was measured by a Dwyer microtector. The ventilation rate calculated for three setting of slot width were for Q=995 m^3/hr at 3.8 cm width, for Q=430 m^3/hr at 1.3 cm width, for Q=281 m^3/hr at 0.3 cm width. Assuming a chamber capacity of 15 pigs, three rates were equivalent to 66, 29, and 19 m^3/hr per pig. The three ventilation rates corresponded to air-exchange rates per hour of 35, 15, and 10 respectively.
3. Gas charging system: The gas charging system consisted of a high pressure cylinder of carbon dioxide, a two-stage pressure regulator, Tygon plastic tubing, and three CENTURY flowmeters (model 100H, catalog #450-015). The discharge from the cylinder of pure carbon dioxide was divided into three for the charging operation.

The CENTURY 100H flowmeter had a millimeter scale which could be converted to a volume flow scale for air with aid of calibration charts. Adjustment factors associated with the calibration charts were used to calculate the gas flow rate for gases other than air. According to manufacturer's information, the adjustment factor is equal to the square root of the specific gravity of air divided by the specific gravity of carbon dioxide. The value is equal to 0.818. The carbon dioxide was used at a rate of 24 l/pig/hr (i.e., a total of 360 l/hr), this being approximately equivalent to the carbon dioxide production of a 55 kg pig (Anderson et al. 1987). To investigate the variation of gas concentrations influenced by the location of pollution sources, the gas charging points were laid out as shown in Figure 24. Figure 24 shows that the gas charging points were near the sampling points 1A, 3A, 5A, and 5B.

4. Gas sampling and analyzing system: Measurements of carbon dioxide gas concentration were taken using a Valtronics 2080 Air Quality Sensor. The gas sample was drawn out through a 2 m length of 1.3 cm i.d. rigid plastic pipe by a vacuum pump and delivered via a 1000ml jar to the sensor. To detect concentration variation in both longitudinal and vertical direction, sampling was carried out in two planes, 0.8 m and 1.6 m from one side wall, which is away from the exhaust fan location. The layout of the sampling points is shown in Figure

24. In all, 12 sampling points were chosen. The rigid plastic pipe was inserted 0.8 m and 1.6 m horizontally into the chamber through sampling holes. Before and after sampling, the holes were closed with tape. Equilibration was assumed to be 10 min. to 15 min. after a constant gas concentration was reached in the exhaust air. Sampling of the 12 points was carried out in random order and three subsample collections were made at each sampling point.

The procedure of model verification The basic procedure of model verification for the chamber test is the same as the algorithm outline in Figure 22. The detailed explanation of input data is as follows;

1. The entrainment ratio, r: The chamber test has three ventilation rate levels which were adjusted by chamber inlet slot width. According to equation (119b) and based on the three values of width of slot, the entrainment ratios can be calculated for each ventilation rate. The results were: r=6.8 for Q=995 m^3/hr (H_o=3.8 cm), r=10.5 for Q=430 m^3/hr (H_o=1.3 cm), and r=23.4 for Q=281 m^3/hr (H_o=0.3 cm).
2. The airflow matrix, Q: The input data of the flow matrix is followed by equation (38) and the airflow patterns which are shown in Figure 25. Figure 25 indicated that the solution of the airflow matrix is by 3-D lumped form of control volumes representing the conservation of air mass. The input data of the flow matrix are listed in Appendix D (Figure D-2).

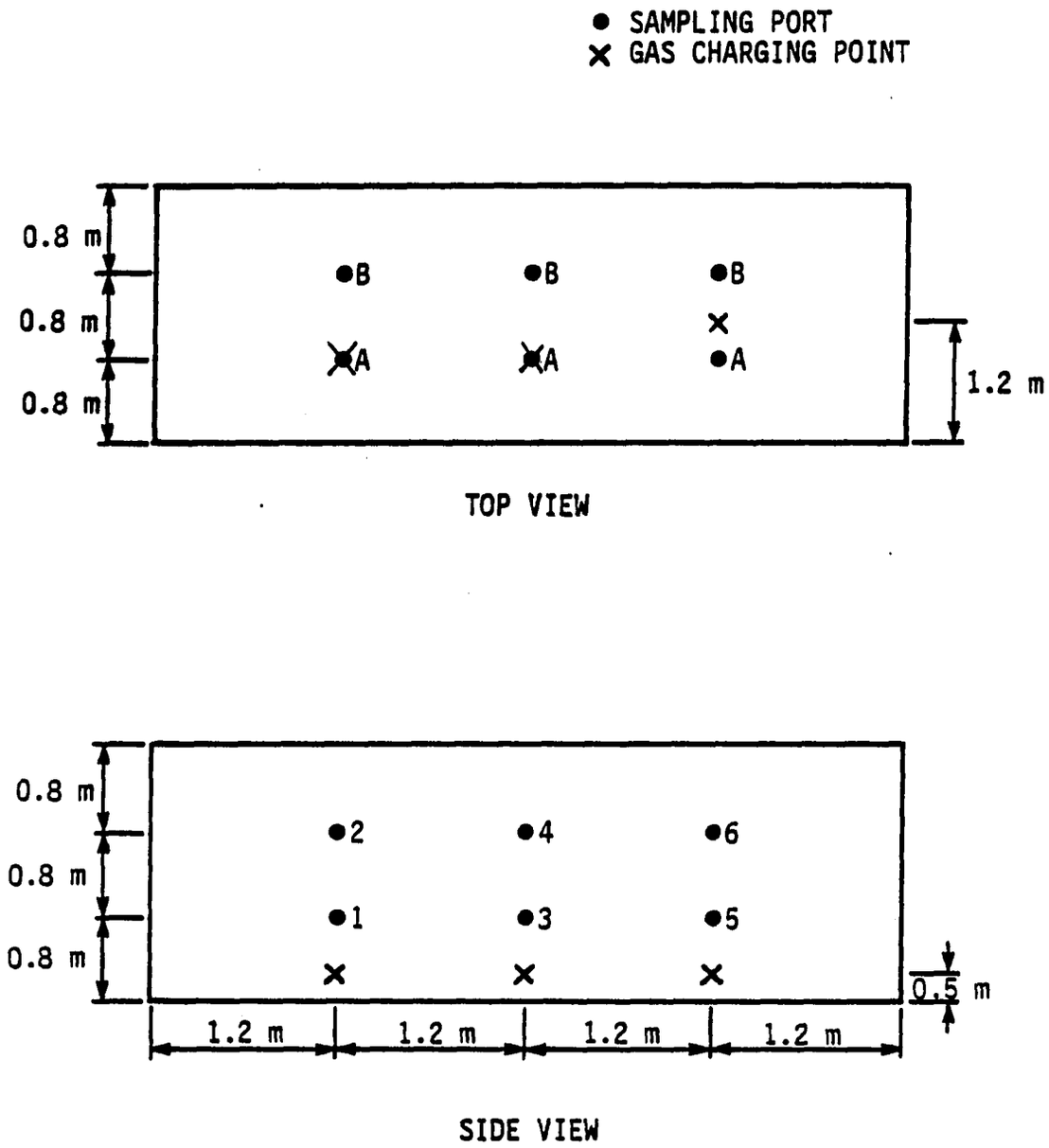

FIGURE 24. A top and side view of the environmental chamber showing the location of the sampling points

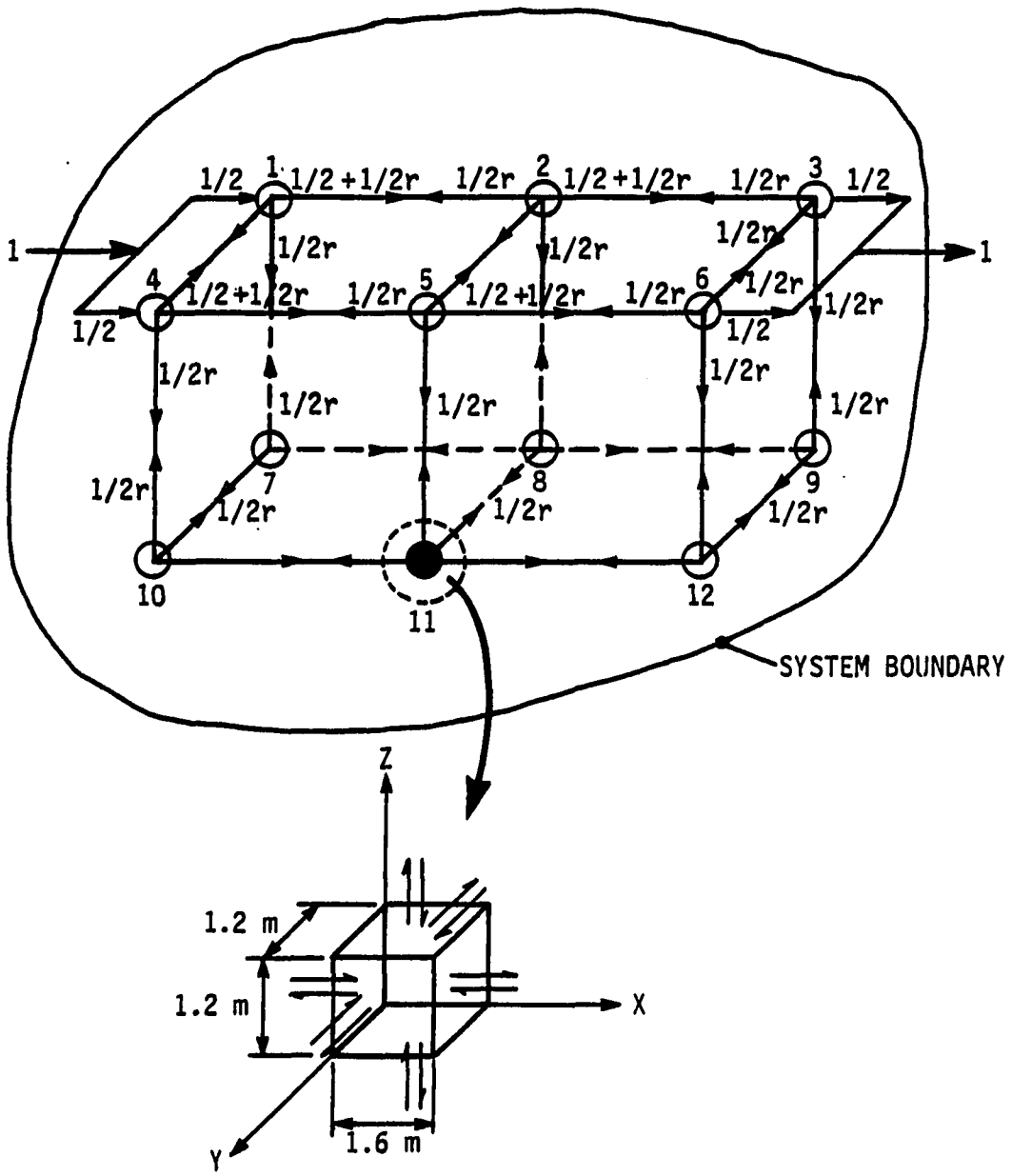

FIGURE 25. The airflow patterns and control volume for the model simulation in chamber test case

3. The air volume matrix, $\underline{V}$: In this chamber test case, the fraction of air volume K_i is assumed equal, i.e., $K_i=1/12$, i=1, 2, 3, ..., 12.

4. The equilibrium CO_2 emission rate matrix, $\dot{m}(s,s)$: The total equilibrium CO_2 emission rate is 360 l/hr which is equal to 767 g/hr (the ambient air condition assumes under 25°C, 1 atm). Figure 24 shows that the gas charging points were released near the range of sampling points 1A, 3A, 5A, and 5B. Thus, in calculating the equilibrium concentration of CO_2 in each space, we may assume that the CO_2 gases were emitted from spaces 9, 10, 11, and 12 which are shown in Figure 25. Here, the emission rate for each charging point is assumed equal and uniformly distributed among spaces 9, 10, 11, and 12 in Figure 25. Therefore, the values of emission rates in the emission rate column matrix are: the beginning eight row values are zero, and the last four row values are equal to $\dot{m}(s,s)/4$.

Discussion of Results

Comparison with research literature

The dimensionless local purging flow rate, dimensionless local mean- age of airflow, and dimensionless local equilibrium concentration are shown in Figure 26. Figure 26 indicated that the local purging flow rate in the displacement system is higher than that of the short-circuiting system, while the local mean-age of airflow and local

COL 1	2	3	4	5	ROW
1.00	.97	.95	.93	.89	1
Q → .84	.90	.94	.97	.98	
.80	.86	.90	.92	.94	
.96	.97	.97	.96	.93	2
.91	.94	.96	.98	.99	
.88	.90	.92	.94	.95	
.93	.96	.96	.97	.96	3
.94	.97	.98	.99	.99	
.93	.94	.95	.97	.97	
.91	.93	.95	.96	1.00	4
.98	.98	.99	.99	1.00	
.96	.97	.99	.99	1.00 → Q	
.86	.90	.92	.93	.92	5
.99	.99	1.00	1.00	1.00	
.98	1.01	1.02	1.03	1.04	

u_i^*
$M_{ii}^{(1)*}$
$Ci(s,s)^*$

(a) Displacement system

COL 1	2	3	4	5	ROW
1.00	.98	.97	.98	1.00	1
Q → .86	.93	.97	.99	1.00 → Q	
.85	.92	.96	.99	1.00	
.95	.97	.97	.97	.95	2
.93	.96	.98	.99	1.01	
.93	.96	.98	1.01	1.01	
.91	.94	.94	.94	.92	3
.97	.98	.99	1.01	1.01	
.99	1.00	1.02	1.03	1.04	
.88	.91	.92	.91	.88	4
1.00	1.002	1.01	1.02	1.02	
1.02	1.04	1.05	1.06	1.07	
.84	.87	.88	.87	.84	5
1.007	1.01	1.02	1.02	1.03	
1.05	1.07	1.09	1.10	1.106	

(b) Short-circuiting system

FIGURE 26. The simulation results of dimensionless of local purging flow rate, local mean-age of airflow, and local equilibrium concentration of gaseous pollutants for (a) displacement and (b) short-circuiting ventilation systems

equilibrium concentration of gaseous pollutants in displacement are lower than that of the short-circuiting system.

The calculated mean equilibrium concentration of ammonia and carbon dioxide at both levels of outlet height is illustrated in Table 18. In

TABLE 18. The calculated mean equilibrium concentration of ammonia and carbon dioxide at both levels of outlet height

outlet height(m)	equilibrium gaseous pollutants(ppm) ammonia	carbon dioxide
0.5 (displacement)	58(49)[a]	1037(910)
2.0 (short-circuiting)	62(53)	1104(980)

[a] The number in the parentheses is the measured results of Brannigan and McQuitty (1971).

concentration calculations, to convert from units of g/m^3 to ppm (volume), it is assumed that the ideal gas law is accurate under ambient condition. The model assumed the ambient temperature to be 25°C and 1 atm. Therefore, the conversion factors for CO_2 and NH_3 from units g/m^3 to ppm are 560 and 1440, respectively. In Table 18, it is shown that the simulated results of total mean equilibrium concentration of ammonia and carbon dioxide are close to the measured values. Table 18 also indicated that the short-circuiting system has higher mean concentration than that of the displacement system.

The mean equilibrium concentration of ammonia and carbon dioxide at

different ventilation rates changing with height-from-floor and distance- from-inlet are illustrated in Figures 27, 28, 29, and 30. Figures 27, 28, 29, and 30 show the comparison of model predicted concentration of ammonia and carbon dioxide at three different ventilation rates changing with height-from-floor and distance-from-inlet with that measured by Brannigan and McQuitty (1971). Figures 27, 28, 29, and 30 indicated that at higher ventilation rates, the predicted and measured values are consistent, while a clear discrepancy was observed at low ventilation rates. The discrepancy may have the following explanations;

1. The NH_3 and CO_2 are extremely soluble compounds (from the results of chemical-biochemical experiment it is shown that the overall transfer coefficient Ko, for NH_3 and CO_2 are 2.3×10^{-8} and 3.5×10^{-5} gmole/cm^2-s, respectively). Therefore, at low ventilation rate conditions, it has longer mean internal age which can make NH_3 and CO_2 have enough time to react rapidly with water vapor in the air and to yield more than one secondary chemical compound, such as H_2CO_3, NO_2, and MNO_3 (denote general nitrate compounds); and then NH_3 and CO_2 detected by gas analyzer was fluctuated. However, it is assumed that all the gaseous pollutants are dynamically passive, i.e., no chemical interactions occur between primary pollutants and normal atmospheric conditions in the multiple airflow region model.
2. In this simulation model study, it is assumed that the same entrainment ratio and the same airflow patterns are present in

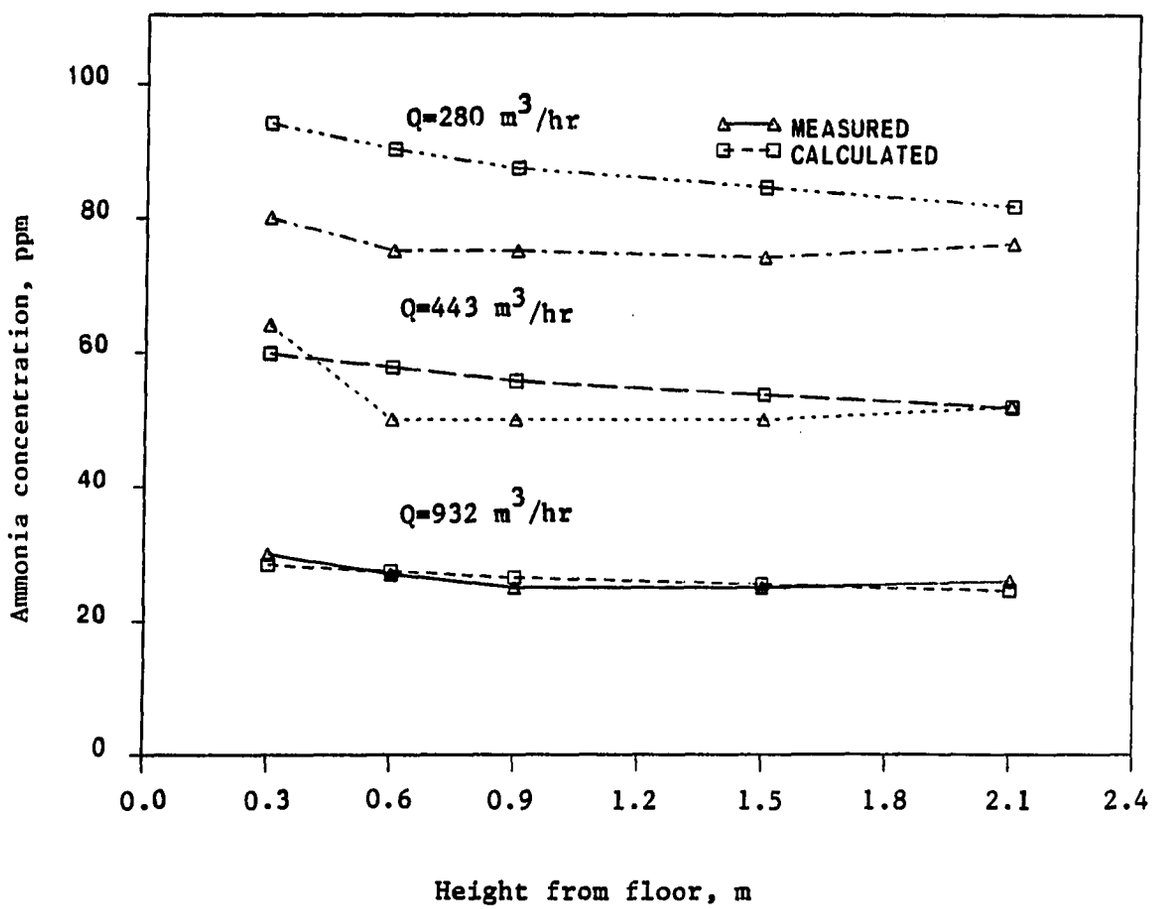

FIGURE 27. The comparison of model predicted of ammonia interacted with height-from-floor and different ventilation rates with that measured by Brannigan and McQuitty (1971)

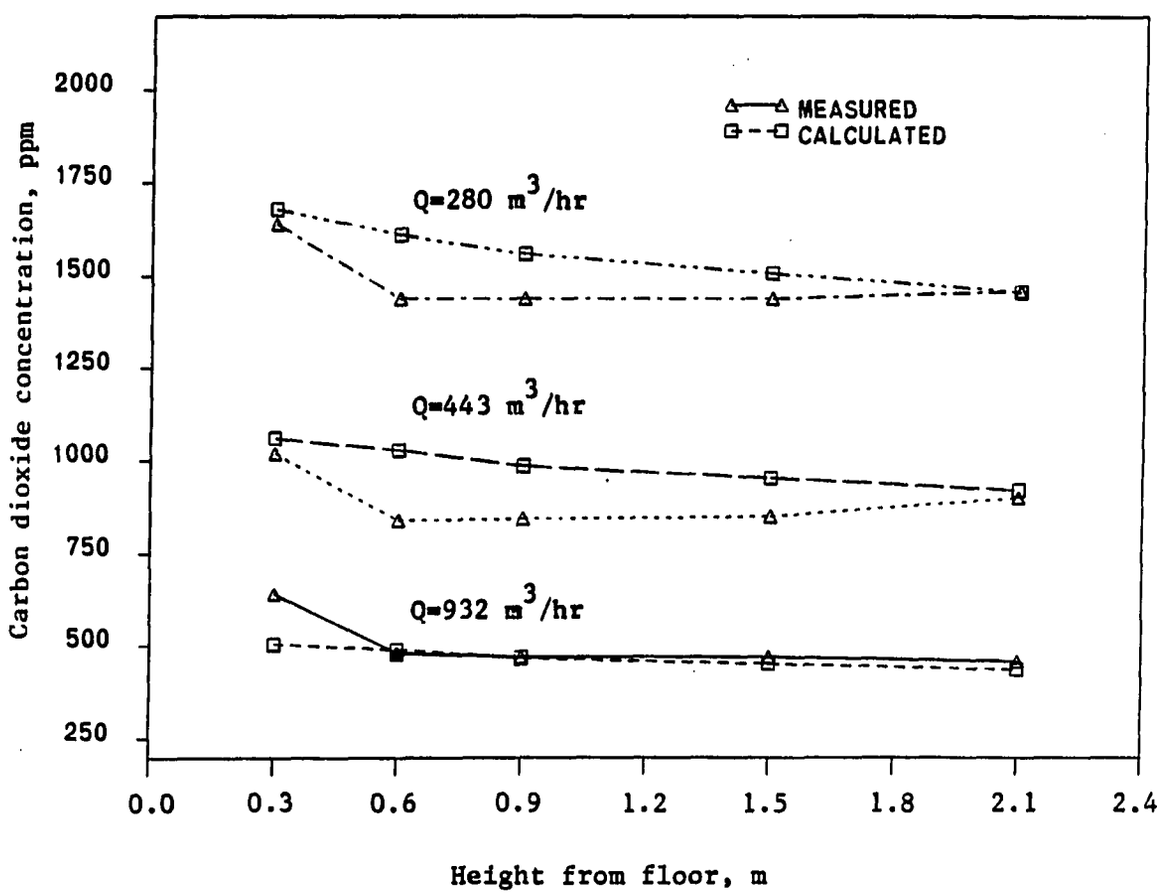

FIGURE 28. The comparison of model predicted of carbon dioxide interacted with height-from-floor and different ventilation rates with that measured by Brannigan and McQuitty (1971)

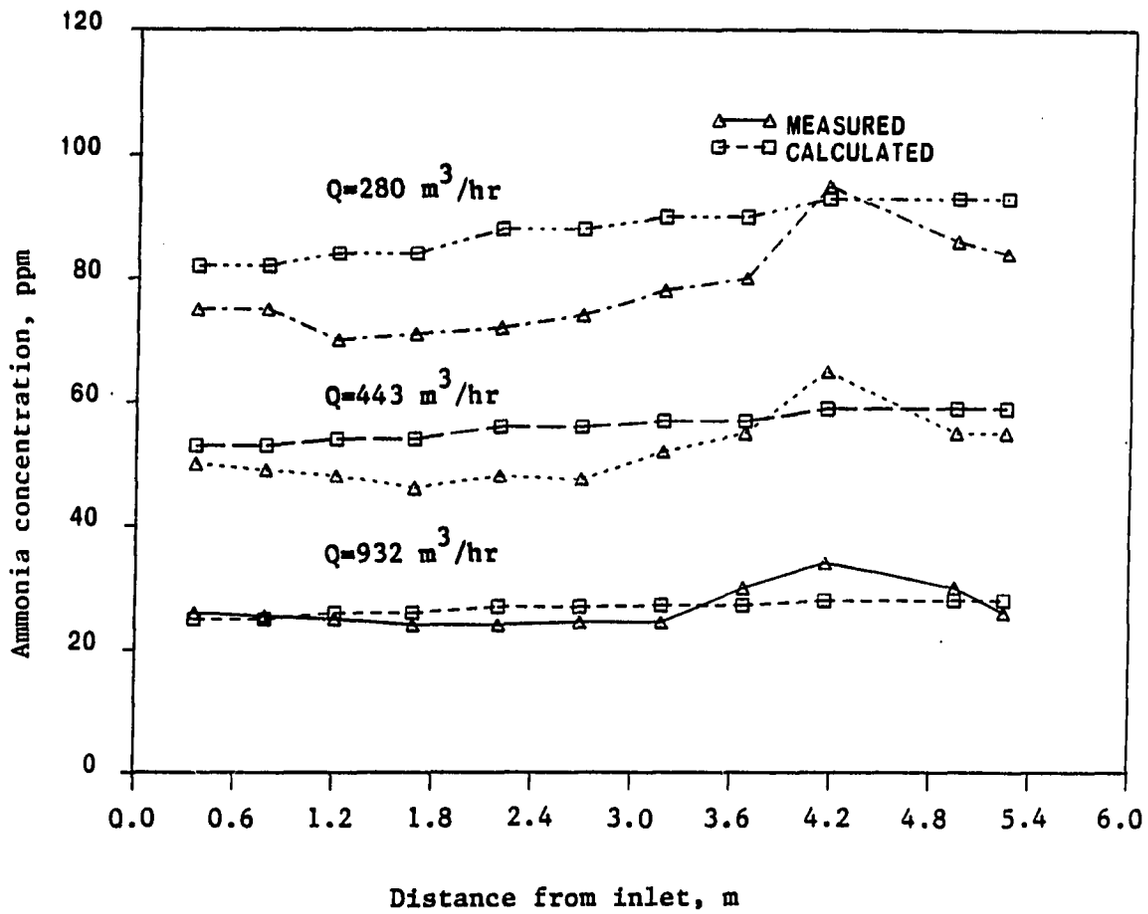

FIGURE 29. The comparison of model predicted of ammonia interacted with distance-from-inlet and different ventilation rates with that measured by Brannigan and McQuitty (1971)

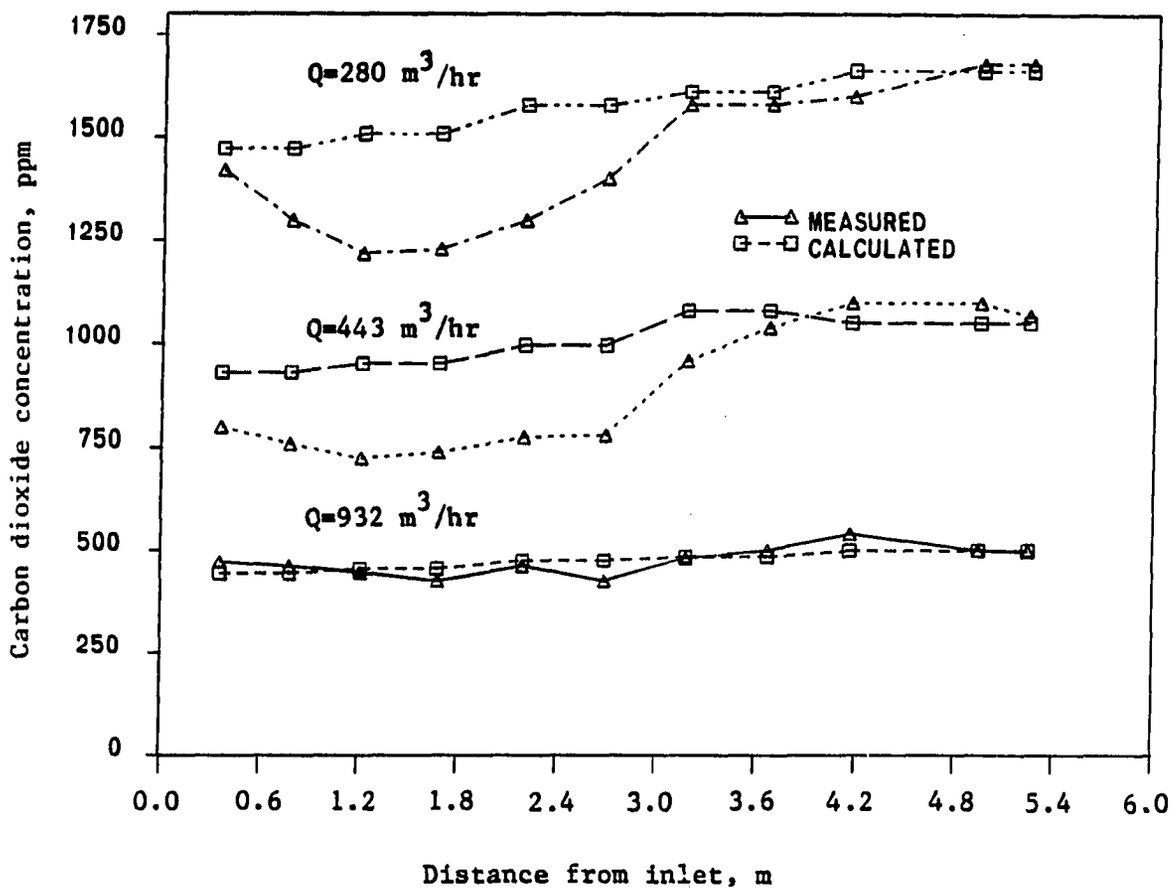

FIGURE 30. The comparison of model predicted of carbon dioxide interacted with distance-from-inlet and different ventilation rates with that measured by Brannigan and McQuitty (1971)

three different ventilation rates. However, at the actual conditions, the recirculation of airflow and its patterns will change in different ventilation rates. The simulation results show that the airflow patterns in multiple airflow regions model better match measured results as the ventilation rate increases.

3. Because of density difference with regard to the ambient air, the gaseous pollutant sets up its own motion independent of local airflow motion. Thus, a dynamically passive pollutant becomes a dynamically active pollutant. Therefore, the transportation for an active gaseous pollutant is not necessarily related to the airflow motion, and subsequently, neither is it directly related to the flow matrix $\underline{Q}$, used in this model approach.

In this model case study, the 3-compartmental airflow regions model (regions in parallel) was selected to study the transient behavior of the two ventilation systems. The 3-compartment model is illustrated in Figure 31. The simulation results of transient behavior of gaseous pollutants in the two ventilation systems for different ventilation rates are shown in Figures 32, 33, 34, and 35. Figures 32, 33, 34, and 35 indicated that:

1. Complete mixing is the best feasible operative mode for the short-circuiting system at higher ventilation rate conditions. (The detailed theoretical interpretation of mixing factor is discussed in Appendix E.)

2. In the transient phase, the displacement system approaches the steady-state concentration faster than the short-circuiting system.
3. Different points have different concentration profiles, even at the same ventilation system. The displacement system for point 2 and point 3 have the same trend of concentration histories for NH_3 and CO_2 at both high and low ventilation rates, while for the short-circuiting system point 1 and point 2 have the same trend of concentration histories at both ventilation rates. It means the air movements in a ventilated enclosure are turbulent and the predominant and distinctive feature of turbulence is its randomness. An inevitable consequence of the randomness is that the concentration field is also random. And from Figures 32, 33, 34, and 35, the results indicated that the distributions of gaseous pollutants with the same conditions at different times will be different from one another. Therefore, the concentration field must be described in a statistical sense, i.e., in terms of mean concentration, variance, etc.
4. Generally speaking, at the point at the ceiling for the displacement system and the point at the floor for the short-circuiting system, the concentration profiles rapidly reach their maximum concentrations, then smoothly start to decay to their equilibrium concentration.

Comparison with chamber test

The overall mean value of measured and calculated carbon dioxide concentration for three ventilation rates is listed in Table 19 (the results of data analysis are listed in Appendix F Table F-1). Table 19 shows that the measured and calculated carbon dioxide concentrations followed a similar trend for three ventilation rate levels. Table 19 also indicated that the error between measured and calculated values ranged between 3.02 percent and 5.6 percent. The most significant sources of error may be included:

1. Homogeneous mixing: The assumptions of local uniform mixing space and dynamically passive pollutants are used in deriving the system equations, but in the actual condition, the local convective accelerations and the density difference between CO_2 and air do not vanish. Therefore, any significant departure from homogeneity might be expected.

TABLE 19. Mean carbon dioxide concentrations for measured and calculated at three ventilation rate levels

ventilation rate m^3/hr	CO_2 concentration ppm		error %
	measured	calculated	
995	411.56	437.70	5.6
430	960.67	989.63	3.02
281	1452.75	1530.87	5.4

2. Carbon dioxide charging rate: To investigate the effect of the error in the carbon dioxide charging rate, runs were performed with the value increased by 25 percent and decreased by 25

1. Short-circuiting ventilation system

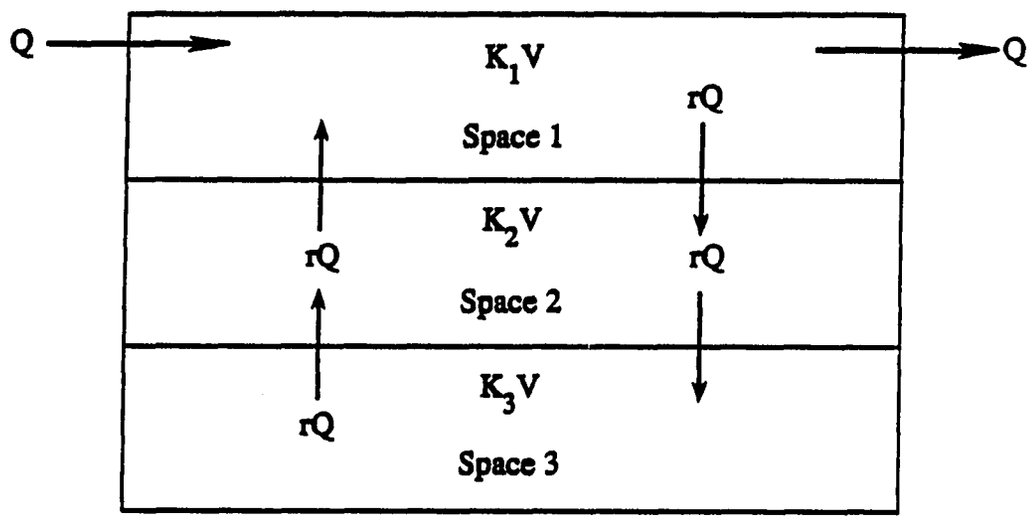

2. Displacement ventilation system

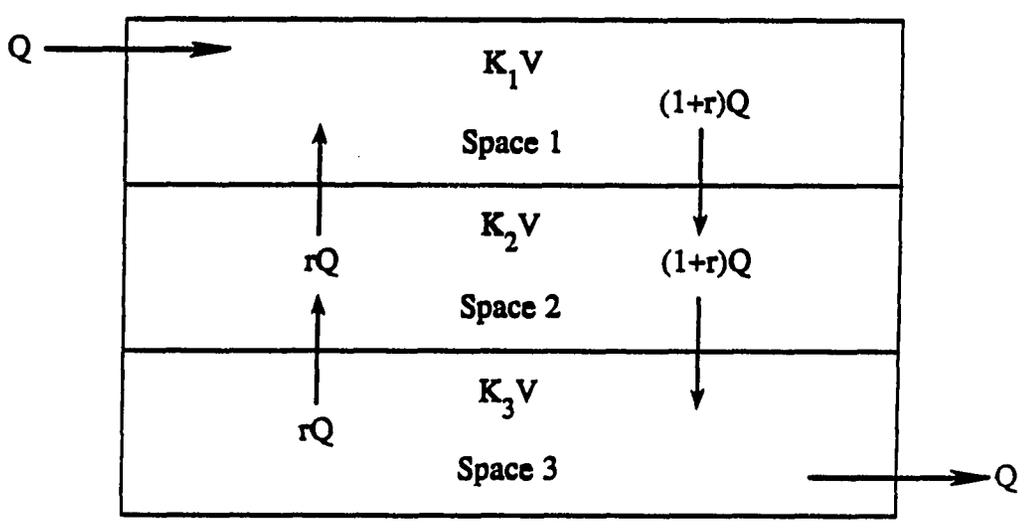

FIGURE 31. The three-compartment airflow model for two different ventilation systems in the model case study

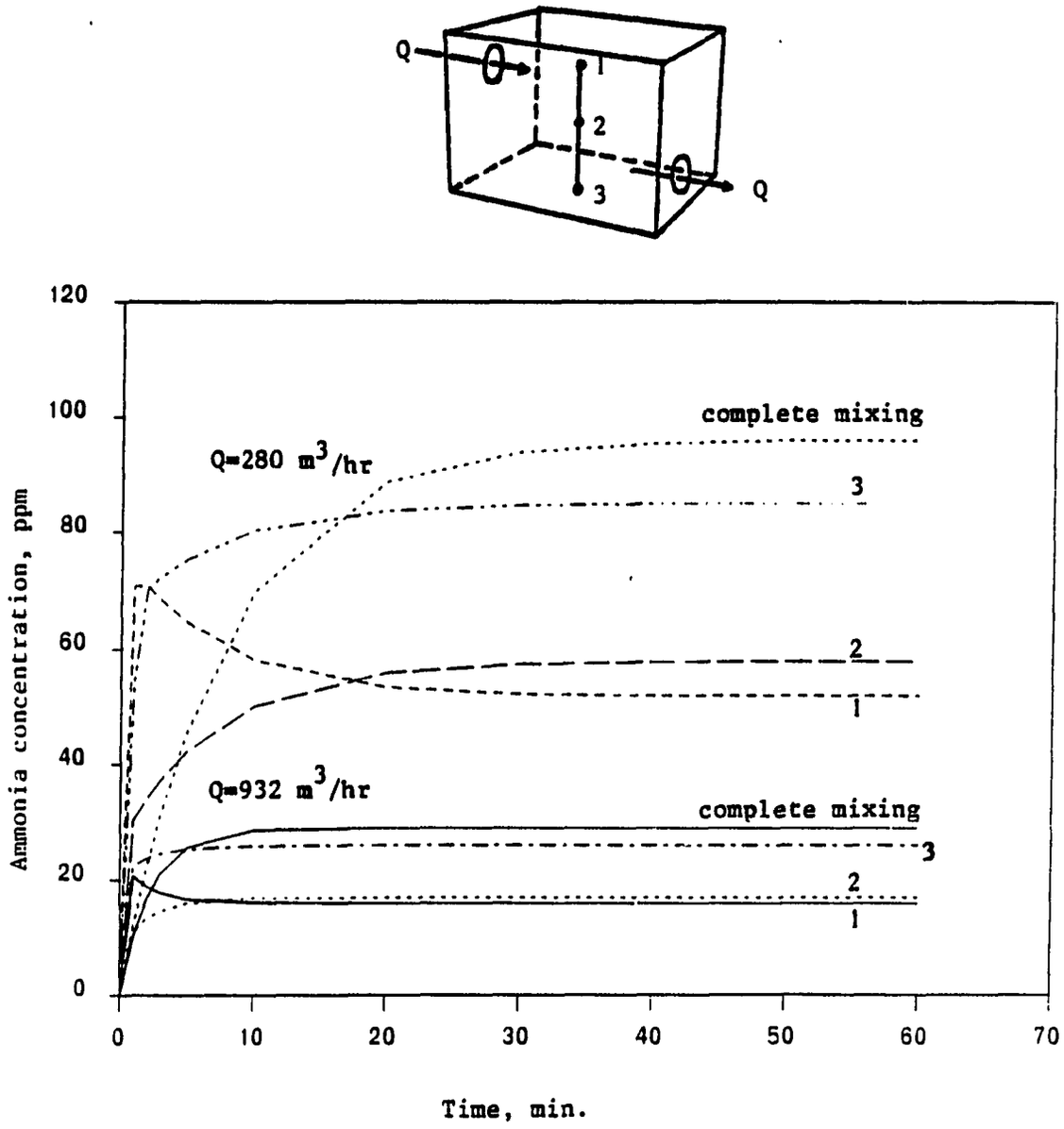

FIGURE 32. The transient behavior of an ammonia of the displacement system at different ventilation rates for complete mixing and different airspaces

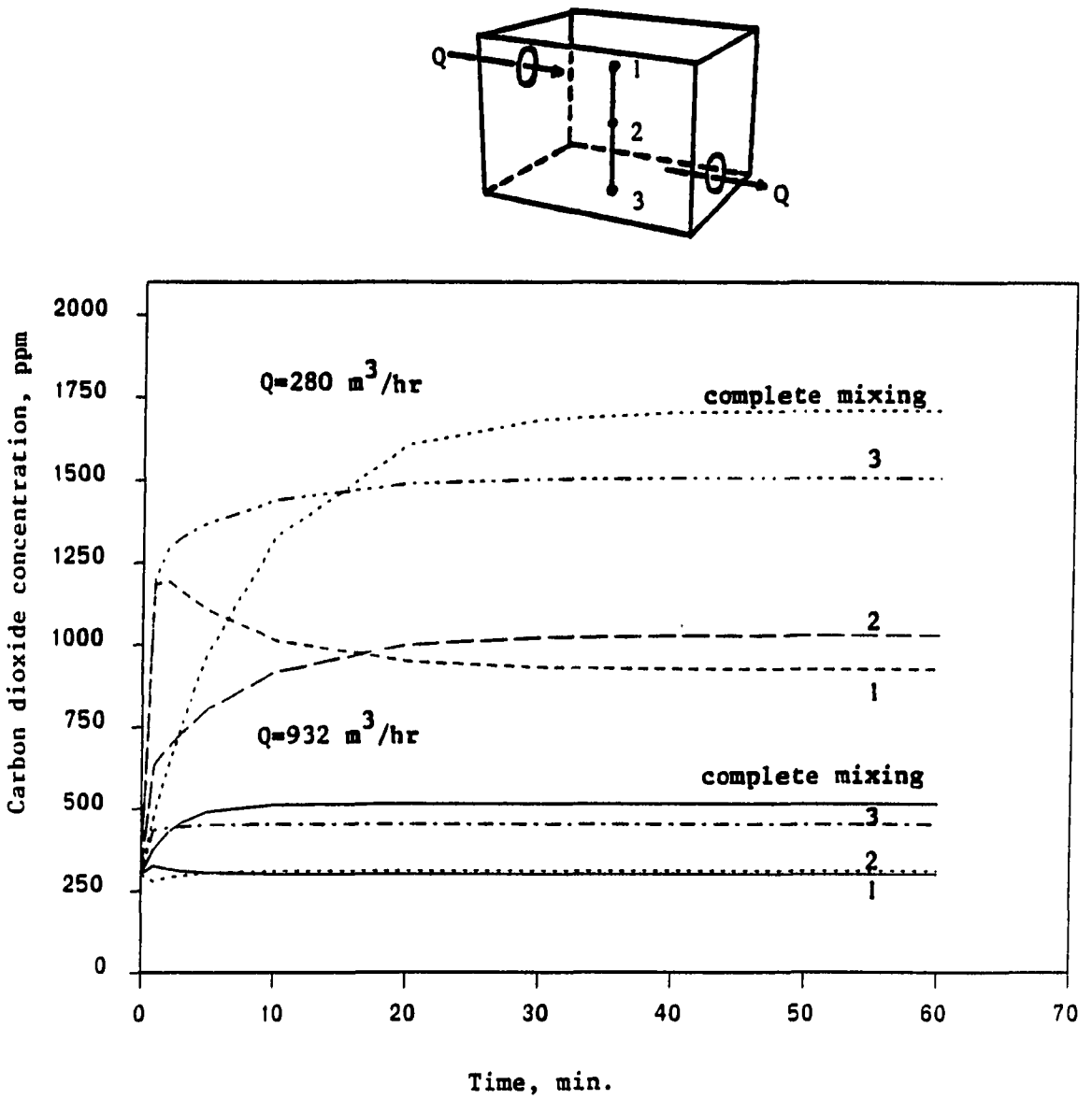

FIGURE 33. The transient behavior of carbon dioxide of the displacement system at different ventilation rates for complete mixing and different airspaces

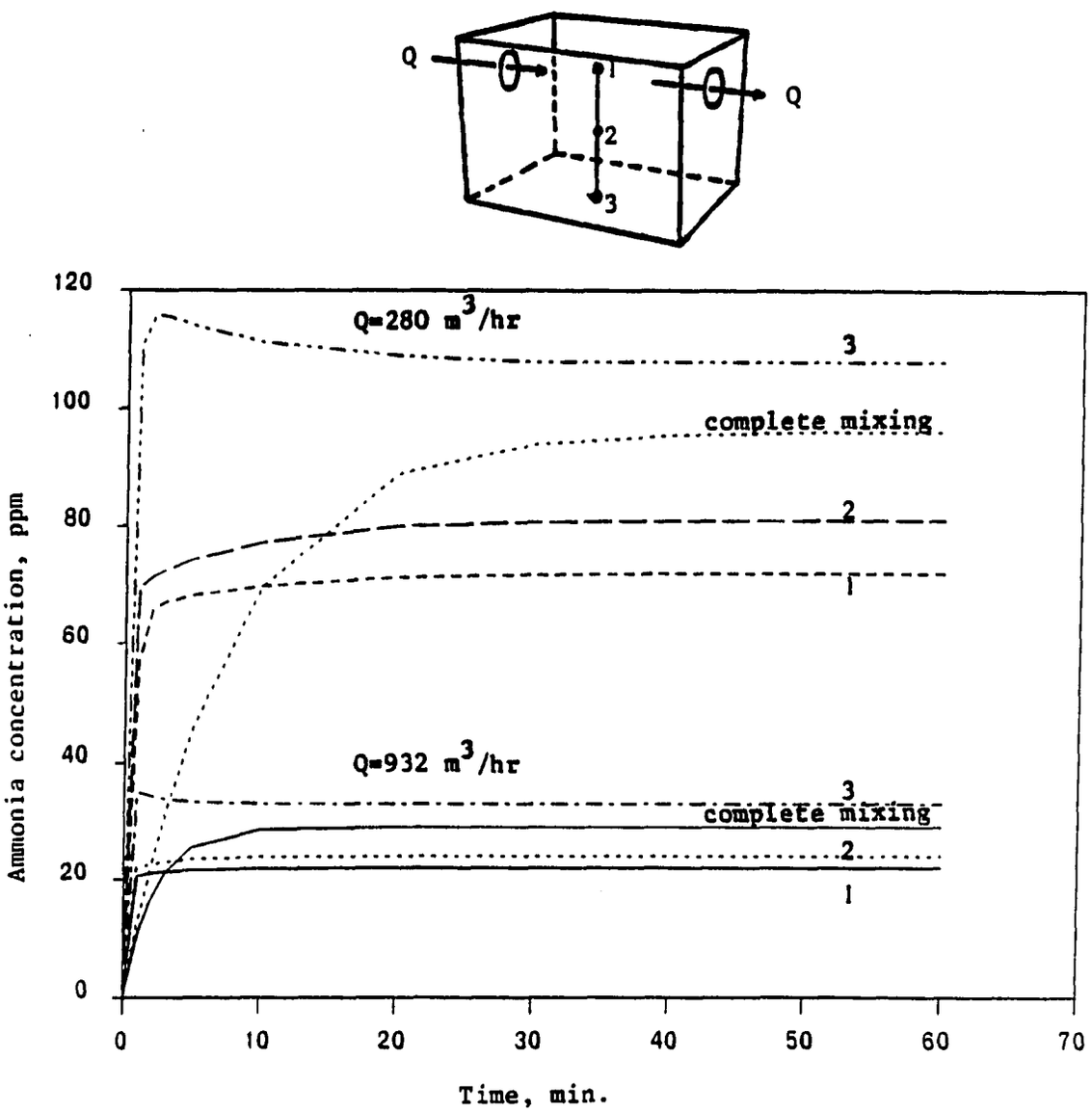

FIGURE 34. The transient behavior of an ammonia of the short-circuiting system at different ventilation rates for complete mixing and different airspaces

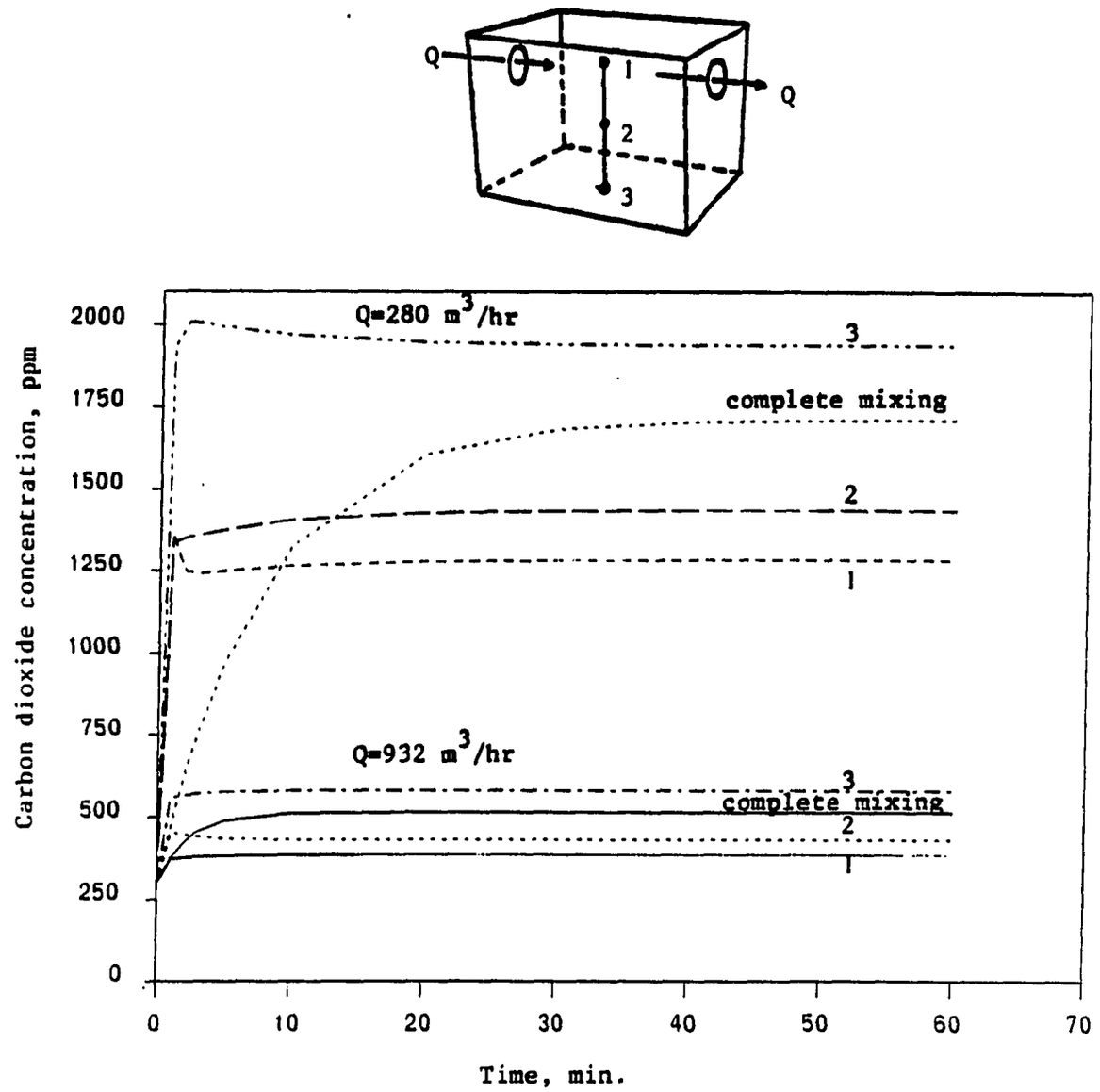

FIGURE 35. The transient behavior of carbon dioxide of the short-circuiting system at different ventilation rates for complete mixing and different airspaces

percent (i.e., one scale of flowmeter) at the condition of ventilation rate equal to 281 m^3/hr (the detailed data analysis is listed in Appendix F, Table F-1). The resulting changes in the measured carbon dioxide are listed in Table 20. Table 20 indicated there is roughly a 25 percent to 31 percent change in the estimated values and the error in output is roughly equal to the error in the input in this particular case.

3. Measured carbon dioxide concentration: The measuring device must be calibrated against a gas mixture of known CO_2 concentration, but in this field chamber test we neglected the calibration. Had the calibration been performed, then some calibration error would have been introduced. This error causes us to read $\underline{C}'(t) = e\underline{C}(t)$ instead of $\underline{C}(t)$, and equation (49) becomes;

$$d\underline{C}(t)/dt = -\underline{T}^{-1}\ \underline{C}(t) + 1/e\ \underline{V}^{-1}\ \underline{m}(t) \qquad (120)$$

So we see that this has the same effect as an error of 1/e in the CO_2 charging rate. Hence, the analysis above applies in this case. From the manufacturer's specification, we expect the CO_2 concentration reading to be accurate to within 25 percent to 30 percent. So random error uniformly distributed between $\pm$ 25 percent to 30 percent was applied to the CO_2 concentration.

Some of the more interesting interactions occurred in the chamber test and model simulation. From the viewpoint of distance from inlet, distance from one side wall which is away from the exhaust fan, and height from floor level, the response surfaces of measured and

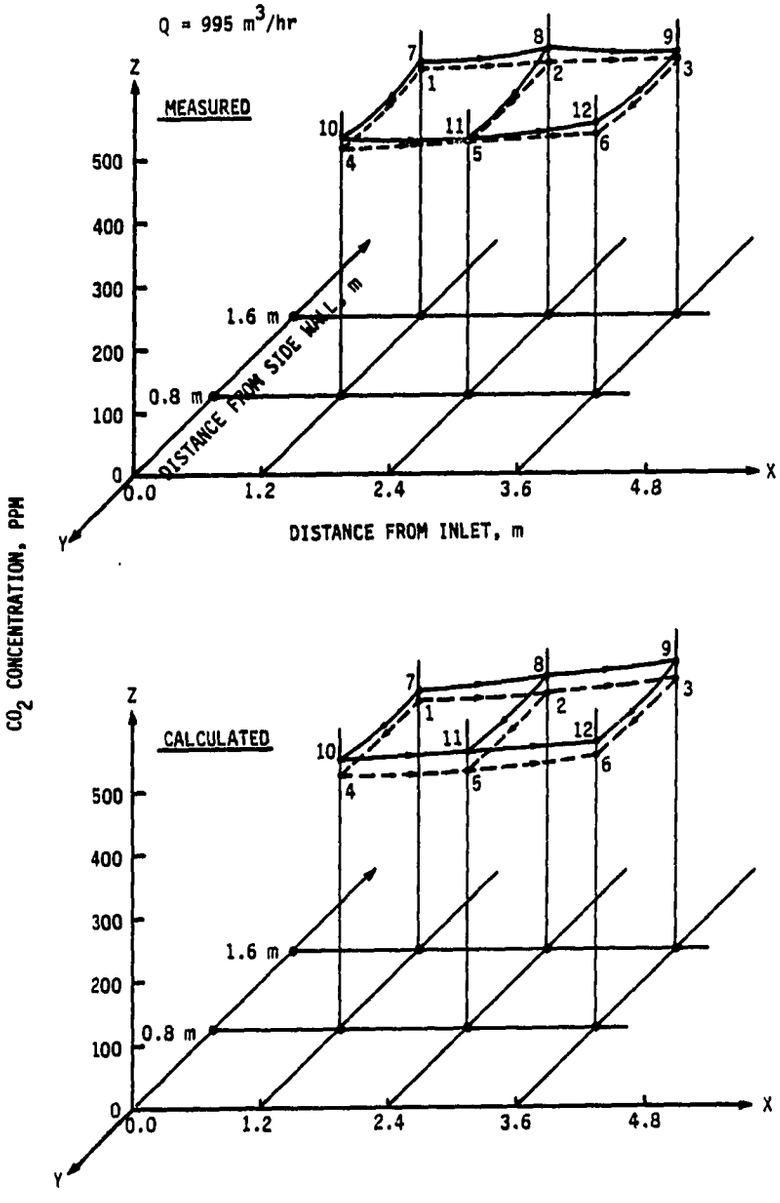

FIGURE 36. The response surfaces of CO_2 concentration at Q=995 m^3/hr in ventilated chamber

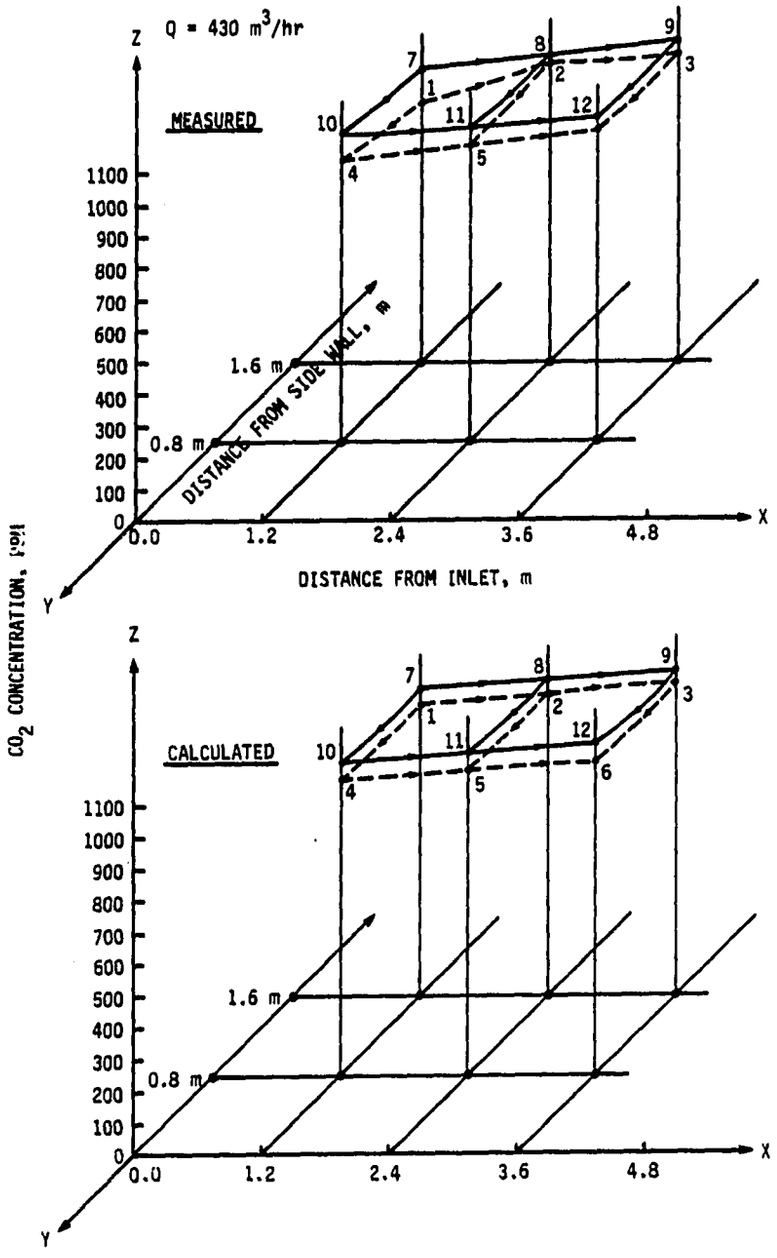

FIGURE 37. The response surfaces of CO_2 concentration at Q=430 m^3/hr in ventilated chamber

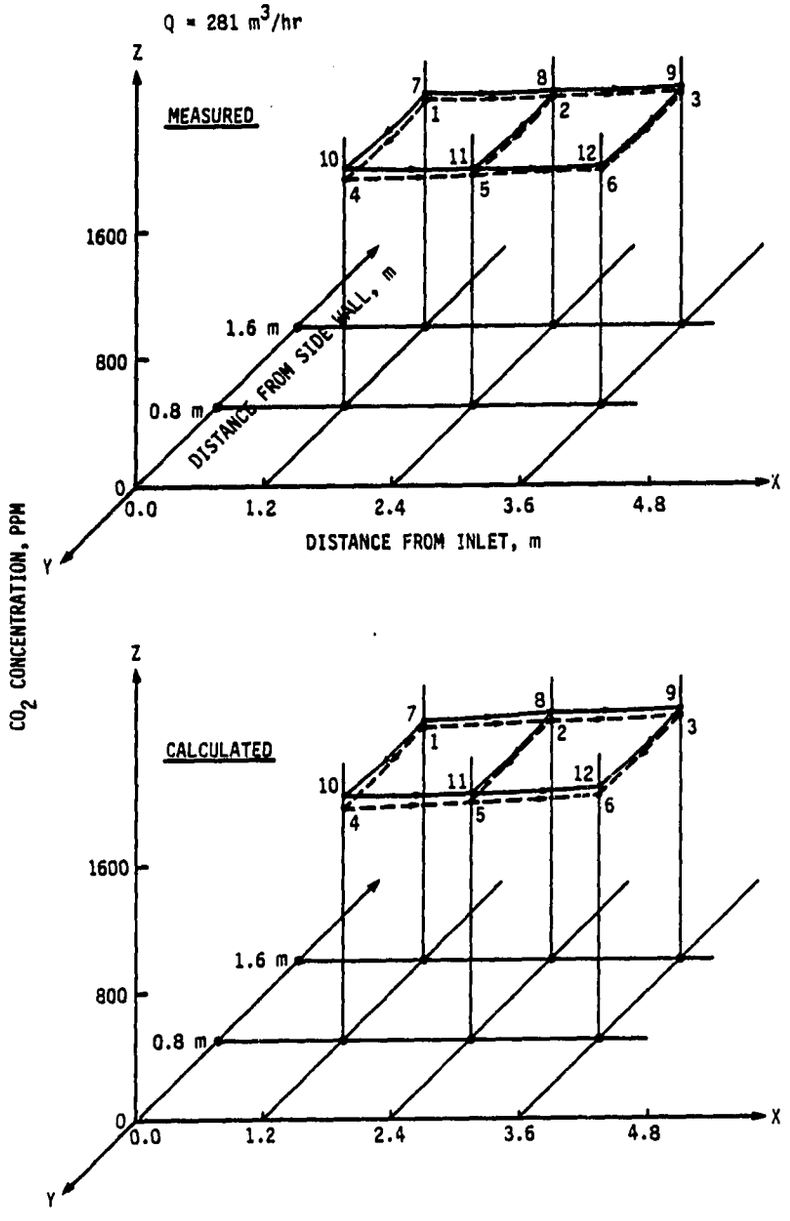

FIGURE 38. The response surfaces of CO_2 concentration at Q=281 m^3/hr in ventilated chamber

TABLE 20. Sensitivity analysis of carbon dioxide charging rate ($Q=281\ m^3/hr$)

charging rate l/min	measured mean concen. ppm	output error %
6	1452.75	
7.5(+25%)	1818.93	25.21
4.5(-25%)	1009.25	-30.54

calculated carbon dioxide concentrations are shown in Figures 36, 37, and 38 in which the coordination of the environmental chamber is followed by Figure 23 (the detailed data analysis is listed in Appendix F, Table F-2). In those figures, the surfaces that are connected by solid lines and by dotted lines represent the sampling points near the floor and the ceiling respectively. The arrows in each solid and dotted line show the gas concentration for each sampling point from lower to higher value. Figures 36, 37, and 38 do not indicate much variation between the three ventilation rate levels. However, they have been included to show the general trend of concentration variations that existed for both measured and calculated carbon dioxide concentrations over the range of distance-from-inlet, height-from-floor, and distance-from-side wall.

CONCLUSIONS

Chemical-biochemical Process Study

From a statistical standpoint, the overall performance of the chemical-biochemical gaseous pollutants control was disappointing. And none of these additives have proved to be completely effective in controlling gaseous pollutants released from swine manure. The chemical- bacteria additives slightly reduced the CH_4 and CO_2 released from swine manure, while the same additives did not have an effect on the NH_3 reduction. The hydrogen sulfide content of the swine manure was initially low. The concentration of NH_3, CO_2, and CH_4 was increased rapidly during storage in the column after additives treatment in about 21 days.

Generally speaking, most of these chemical-bacteria additives must be used in large amounts and must be applied frequently for effective gaseous pollutants control, which make them costly. Therefore, the circumstances should be carefully evaluated before making a decision to use chemical-bacteria additives for control of gaseous pollutants. These should be employed after all other control alternatives have failed.

A two-film resistance model was re-examined. The gases for which the liquid phase resistance appears to control are O_2, N_2, CO_2, H_2S and CH_4, while NH_3 is controlled by gas phase resistance. The weakness of this two-film model seems to be the use of data obtained when the liquid was a simple liquid and not manure. Hence, there remains some doubt about the applicability of existing gas and liquid transfer coefficients

to actual field conditions. Nevertheless, this emission model has some merits:

1. Supplements highly variable data obtained from typical air sampling in livestock building.
2. Can describe the magnitude and distribution of pollution sources, concentrations and health effects in the whole ventilated enclosure.
3. Optimizes manure pit design and operating criteria.

On the whole, the method has been simplified from equations of several researchers by reducing the input requirements to data which are generally readily available. Therefore, the method presented becomes fairly simple and straightforward; however, it should be used with care. A good knowledge of the swine waste compositions and the prevailing physical situation of the swine waste pit is necessary.

Ventilation Process Study

The dynamic behavior of gaseous pollutants in ventilated swine buildings is mainly caused by molecular diffusion, turbulent movement, and circulation of air flow. Also, the problems of determination of space air distribution for ventilation systems with multiple inlets and outlets are more difficult, and there does not exist any definition of a local flow rate which would describe the local flow situation. Velocity profiles can answer the problem, but these are usually hard to obtain. Therefore, at any airspace or at any point, air and gaseous pollutants can be presented by age distribution, and a statistical moment concept

is used to quantify a ventilation system's performance to remove gaseous pollutants.

The key concepts in the multiple airflow regions model are purging flow rates to present the local transport phenomena, and the mean-age of both air and gaseous pollutants to justify the pig's maximum exposure time to toxic gases. The starting point in the model formulation is the flow matrix $\underline{Q}$ consisting of the total flow rates of air between each air space. At last, the net flow rates (purging flow rate) are also contained in the inverse of the flow matrix, $\underline{Q}^{-1}$.

Comparison with research literature

From this simulation study, the inverse matrix $\underline{Q}^{-1}$ governing the equilibrium concentration was obtained. The results were consistent with those reported by Brannigan and McQuitty (1971). In this experimental study, ventilation rate was the independent variable of primary importance in determining the concentrations of CO_2 and NH_3. From Figures 32 to 35, it is shown that the matrix $\underline{T}^{-1}$ governs the response when step inputs of CO_2 and NH_3 are use to excite the system. The sum of the elements in a row of the matrix $\underline{T}$, say row i, is equal to the local mean-age of air, $M_{I_i}^{(1)}$, in the corresponding airspace.

This model case study proposes that four system variables (t_n, $M_{I_i}^{(1)}$, U_i, r) can describe a multiple airflow regions model with short-circuiting and displacement ventilation systems. It is also shown that the model can be partially justified on the basis of the entrainment theory of air jets. From Table 18, and Figures 27 to 30, it

can be shown that the simulation results are consistent with the measured results.

Simulation results also show that the effect of the outlet location would be more significant as a change in the steady state concentration of gaseous pollutants within the airspace rather than by an increase in the rate of removal of gaseous pollutants in the exhaust air. Therefore, from the energy conservation point of view, this model can provide assistance in developing energy strategies.

Comparison with chamber test

The model calculation in the case of the chamber test is by the solution in three-dimensional lumped form of control volumes which represent the conservation of airflow mass. The model verification shows that the simulation results of the response surfaces of CO_2 concentration are consistent with the measured data.

From this chamber test, it is seen that the error did exist in the measuring and predicting procedure. The difficulties that may arise from the CO_2 charging system being so sensitive to the flowmeter accuracy to the system's prediction equations being sensitive to errors in input data or to the assumptions made in deriving the system equations. Some possible errors are:

1. Departures from homogeneous mixing which is assumed in all spaces.
2. Errors in measured CO_2 concentrations.
3. Errors in the CO_2 charging rate.

The type 1 error can be largely avoided by measuring the CO_2 concentration at more locations in a given space and checking that the readings do not differ significantly and by improving the quantitative and qualitative representation of airflow patterns in ventilated airspaces. The effect of errors 2 and 3 can be reduced to an acceptable level by improved instrumentation and procedures.

On the whole, the model is thought to be useful because the model parameters are closely related to the physical quantities of the system. The entrainment ratio, r, is useful in understanding the mixing characteristics in airspaces. The local mean-age of polluted air accounts for the mean time polluted air must spend in each airspace of the ventilation systems. Furthermore, from the theoretical analysis, which is based on fundamental physical and mathematical concepts, modeling the diffusion of air and knowing the ability of a ventilation system to remove gaseous pollutants at any airspace in a swine confinement building can be articulately described by the local purging flow rates and local age distribution. The state-of-the-art at present is known as the nature of, and how to characterize by lumped-parameter model, the flow of ventilation air and gaseous pollutants through a ventilated swine building. This model also can compensate for the ambiguities deduced from multiple regression analyses which can show the tendencies of the system model and cannot articulate the true relationships between gaseous pollutants and ventilation systems in swine confinement buildings.

SUMMARY

The purpose of this dissertation was to understand the effect of chemical-bacteria additives on the production of gaseous pollutants from swine manure, and to study the dynamic behavior of gaseous pollutants in ventilated airspaces. The chemical analysis consisted of sampling ammonia, methane, hydrogen sulfide, and carbon dioxide by gas chromatography/mass spectrometry (GC/MS). The results of chemical-biochemical control experiment show that: (1) the chemical-bacteria additives slightly reduced the methane and carbon dioxide release, (2) the same additives did not show any effect on the reduction of ammonia, and (3) the hydrogen sulfide contents of the swine manure continued to be low. The concentration of ammonia, carbon dioxide, and methane increased rapidly during storage in the experimental column after additives treatment in about 21 days. Methane, ammonia, and carbon dioxide generated from stored swine manure gave average values of 3.76 and 2.2 ppm of methane, 0.35 and 0.11 ppm of ammonia, and 1000 and 470 ppm of carbon dioxide for treated and untreated manure, respectively.

Based on the two-film resistance theory, a model capable of predicting the emission rate of the gaseous pollutants from swine manure in a simple and quick manner was developed. According to the emission rate model, the gases liquid phase resistance appears to control are carbon dioxide, hydrogen sulfide and methane, while ammonia is controlled by gas phase resistance. The average emission rate of methane, ammonia, and carbon dioxide at 15°C are 0.02, 1.52, and 0.50

g/min, for untreated samples and 0.04, 3.91, and 1.06 g/min for treated samples, respectively.

A multiple airflow regions model is presented and explored from the viewpoint of the matrix method for dynamic systems analysis. The model includes the local flow rate and the internal mean-age of polluted air. The starting point in the model formulation is the flow matrix $\underline{Q}$ consisting of the total flow rates among the component airspaces. The net flow rates are contained in the inverse of the flow matrix, $\underline{Q}^{-1}$. The model calculation is by the solution in 3-D lumped form of control volume representing conservation of airflow rate. The model shows that the gaseous pollutants' distributions are similar to the measured data from the research literature and field chamber test. The results also show that the precision of calculation is adequate for design purposes, although at low ventilation rates, some mismatch between calculated and measured results occurred. The model also shows the displacement ventilation system is the best flow principle in a ventilated enclosure. The results indicated that mean-holding time, local mean-age, local purging flow rate, and entrainment ratio of airflow are useful descriptions of the dynamic behavior of gaseous pollutants in ventilated airspaces.

SUGGESTIONS FOR FUTURE RESEARCH

1. To develop an exposure model which quantifies swine exposure to volatile compounds. The model incorporates the mass transfer from swine manure pit to indoor air by combining a two-film resistance model with both the multiple airflow regions model and the residence time distribution theory. This exposure model will enable engineers to describe the magnitude and distribution of pollution sources, concentrations and health effects in the whole ventilation system.

2. To develop an environmental control system for gaseous pollutants in a ventilated enclosure. This will be straightforward in two ways: (1) applying the Laplace transform techniques to the known age distribution function of each gaseous pollutant will result in a transfer function which can be used in a closed loop automatic control system of enclosure gases; (2) applying the modern time-domain control theory to the linear dynamics equation, i.e., equation (49) will result in a control model equation which can be used directly for the automatic control of enclosure gases. This state-space approach to system description has been regarded as an advanced modeling technique compared with any of the frequency-oriented transfer techniques. The state-space approach is particularly useful in providing statistical description of system behavior.

BIBLIOGRAPHY

Adamson, J. A., A. J. Francis, J. M. Duxbury, and M. Alexander. 1975. Formation of volatile organic products in soil under anaerobiosis --- I. Metabolism of glucose. Soil Biol. Biochem. 7:45-50.

American Conference of Government Industrial Hygienists. 1982. Threshold limit values for chemical substances in the work environment with intended change for 1982. American Conference of Governmental Health Hygienists, Cincinnati, Ohio.

Anderson, G. A., R. J. Smith, D. S. Bundy, and E. G. Hammond. 1987. Model to predict gaseous contaminants in swine confinement buildings. J. Agric. Engng. Res. 37(4):235-253.

ASHRAE Handbook of Fundamentals. 1985. American Society of Heating, Refrigrating, and Air Conditioning Engineers, New York.

Avery, G. L., G. E. Merva, and J. B. Gerrish. 1975. Hydrogen sulfide production in swine confinement units. Transactions of the ASAE 18(1): 149-151.

Balch, W. E., S. Schoberth, B. S. Tanner, and R. S. Wolfe. 1977. Acetobacterium a new genus of hydrogen-oxidizing, carbon dioxide-reducing, anaerobic bacteria. Int. J. Syst. Bacteriol. 25: 377-382.

Banwart, W. L., and J. M. Bremner. 1975a. Formation of volatile sulfur compounds by microbial decomposition of sulfur containing amino acids in soils. Soil Biol. Biochem. 7: 359-364.

Banwart, W. L., and J. M. Bremner. 1975b. Detection of carbonyl sulfide and other gases emanating from beef cattle manure. Soil Sci. Am. Proc. 37: 700-702.

Barber, E. M., and J. R. Ogilvie. 1982. Incomplete mixing in ventilated airspaces. Part I. Theoretical considerations. Canada Agric. Engng. 24(1): 25-29.

Bergdoll, J. F. 1975. The use of dried bacteria cultures and enzymes control odor and liquify organic waste found in hog, dairy and poultry producing units as well as lagoons. Pp. 372-373. In Managing livestock wastes. Proceedings, the 3rd International Symposium on Livestock Wastes. Amer. Soc. Agric. Eng. Publ. PROC-275. ASAE, St. Joseph, Michigan.

Bethea, R. M., and R. S. Narayan. 1972. Identification of beef cattle feedlot odors. Transactions of the ASAE 15(6): 1135-1137.

Brannigan, P. G., and J. B. McQuitty. 1971. The influence of ventilation on distribution and dispersal of atmospheric gaseous contaminants. Canada Agric. Engng. 13(2): 69-75.

Bremner, J. M., and W. L. Banwart. 1976. Sorption of sulfur gases by soils. Soil Biol. Biochem. 8: 79-83.

Bundy, D. S. 1984. Rate of dust decay as affected by relative humidity, ionization and air movement. Transactions of the ASAE 27:865-870.

Burnett, W. E. 1969. Air pollution from animal wastes. Determination of malodors by chromatographic and organoleptic techniques. Environ. Sci. Technol. 3(8): 744-747.

Cholette, A., and L. Cloutier. 1959. Mixing efficiency determinations for continuous flow systems. The Canadian Journal of Chemical Engng. 37:105-112.

Cohen, Y., W. Cocchio, and D. Mackay. 1978. Laboratory study of liquid-phase controlled volatilization rates on presence of wind waves. Environ. Sci. Technol. 12(5): 553-558.

Cole, C. A., H. D. Bartlett, D. H. Buckner, and D. E. Younkin. 1975. Odor control of liquid dairy and swine manure using chemical and biological treatments. Pp. 374-377. In Managing livestock wastes. Proceedings, 3rd International Symposium on Livestock Wastes. Amer. Soc. Agric. Eng. Publ. PROC-275. ASAE, St. Joseph, Michigan.

Cooper, P., and I. S. Cornforth. 1978. Volatile fatty acids in stored animal slurry. J. Sci. Food Agric. 29: 19-27.

Cornu, A., and R. Massot. 1975. Compilation of mass spectral data. 2nd ed. Heyden and Sons, Ltd., London.

Csanady, G. T. 1973. Turbulent diffusion in the environment. D. Reidel Publishing Company, Boston, Mass.

Curtis, S. E., C. R. Anderson, J. Simon, A. H. Jensen, D. L. Day, and K. W. Kelley. 1975. Effects of aerial ammonia, hydrogen sulfide and swine- house dust on rate of gain and respiratory-tract structure in swine. J. Anim. Sci. 41(3): 735-739.

Danckwerts, P. V. 1953. Continuous flow systems. Distribution and residence times. Chem. Engng. Sci. 2: 1-18.

Daniels, F., and R. A. Alberty. 1966. Physical chemistry. John Wiley, New York.

Day, D. L. 1966. Liquid hog manure can be deodorized by treatment with chlorine or lime. Ill. Res. 8(3): 16.

Day, D. L., E. L. Hasen, and S. Anderson. 1965. Gases and odors in confinement swine buildings. Transactions of the ASAE 8(1): 118-121.

Donham, K. J. 1982. Respiratory disease hazards of swine confinement works. Termination report for National Institute of Occupational Safety and Health Grant, National Institute of Health, Washington, D.C.

Donham, K. J., M. Rubino, T. D. Thedell, and J. Kammermeyer. 1977. Potential health hazards to agricultural workers in swine confinement buildings. J. Occupational Medicine 19(6): 383-387.

Drummond, J. G., S. E. Curtis, J. Simon, and H. W. Norton. 1980. Effects of aerial ammonia on growth and health of young pigs. J. Anim. Sci. 50(6): 1085-1091.

Elliot, L. F., and T. A. Travis. 1973. Detection of carbonyl sulfide and other gases emanating from beef cattle manure. Soil Sci. Am. Proc. 37: 700-702.

Faith, W. L. 1964. Odor control in cattle feed yards. J. Air Pollution Control Assoc. 14: 459-460.

Fiedler, M., and V. Ptak. 1962. On matrices with non-diagonal elements and positive principal minors. Czechoslovak Mathematical Journal 12(87): 382-400.

Francis, A. J., J. M. Duxbury, and M. Alexander. 1975. Formation of volatile organic products in soils under anaerobiosis. II. Metabolism of amino acid. Soil Biol. Biochem. 7: 51-56.

Freney, J. R. 1967. Sulfur-containing organics. Pp. 229-259. In A. D. Mclaren and G. H. Peterson Eds. Soil biochemistry. Marcel Dekker, New York, N. Y.

Furry, R. B. 1965. Similitude study of the change in CO_2 concentration in a ventilated enclosure. Unpublished Ph.D. Thesis. Iowa State University, Ames, IA.

Graham, A. 1987. Nonnegative matrices and applicable topics in linear algebra. John Wiley & Sons, New York.

Grub, W., E. P. Foerster, and L. F. Tribble. 1974. Swine building air contaminant control with pit ventilation. ASAE, St. Joseph, Michigan. Mimeographed Paper ASAE 74-4532.

Hammond, E. G., C. Fedler, and G. Junk. 1979. Identification of dust-borne odors in swine confinement facilities. Transactions of the ASAE 22(6): 1186-1192.

Hartung, L. D., E. G. Hammond, and J. R. Miner. 1971. Identification of carbonyl compounds in a swine-building atmosphere. Pp. 105-106. In Proceedings of the International Symposium on Livestock Wastes. ASAE, St. Joseph, Michigan.

Himmelblau, D. M., and K. B. Bischoff. 1968. Process analysis and simulation. Deterministic systems. John Wiley & Sons, New York.

Hoff, J. D., W. Nelson, and A. L. Sutton. 1981. Ammonia volatilization from liquid swine manure applied to cropland. J. Environ. Qual. 10(1): 90-95.

Hutchinson, G. L., A. R. Mosier, and C. E. Andre. 1982. Ammonia and amine emissions from a large cattle feedlot. J. Environ. Qual. 11(2): 288-293.

Iowa Bureau of Labor. 1981. Iowa occupational safety and health standards for general industry. Iowa Bureau of Labor, Des Moines, IA.

Janni, K. A., J. C. Nye, D. D. Jones, and V. L. Anderson. 1980. Change in gas release rates and component concentrations during storage of swine manure. Pp. 402-404, 409. In Proceedings, the 4th International Symposium on Livestock wastes. ASAE Publication 2-81.

Jennings, B. H., and J. A. Armstrong. 1971. Ventilation theory and practice. ASHRAE Trans. 77(I):50-60.

Jensen, R. A. 1977. Control of nuisance odors from fecal pounds by the use of bacteria cultures. Paper presented at 83rd National Meeting American Institute of Chemical Engineers, New York, N. Y.

Kadota, H., and Y. Ishida. 1972. Production of volatile sulfur 1591 by microorganism. Ann. Rev. Microbiology 26: 127-138.

Kovacs, F., A. Nagy, and J. Sallai. 1967. Effects of environmental factors on health and productivity of pigs. II. Dust, microorganisms and chemical pollution of the air in piggeries. Magy Allotow Lap. 22:496. (Abstracted in Vet. Bull. 38:727, 1968).

Lancaster, P. 1969. Theory of matrices. Academic Press, New York, N.Y.

Lebeda, D. L., D. Day, and T. Hayakawa. 1964. Air pollution in swine buildings with fluid waste handling. ASAE, St. Joseph, Michigan. Mimeographed paper ASAE 64-940.

Levenspiel, O., and K. B. Bischoff. 1963. Patterns of flow in chemical process vessels. Pp. 95-198. In Advances in chemical engineering. Vol. 4. Academic Press, New York, N.Y.

Lewis, W. K., and W. G. Whitman. 1924. Principles of gas absorption. Industrial and Engng. Chemistry 16(12): 1215-1220.

Liss, P. S., and P. J. Slater. 1974. Flux of gases across the air-sea interface. Nature 247: 181-184.

Loehr, R. C. 1974. Agricultural waste management. Academic Press, New York, N.Y. 567 pp.

Lunney, P. D., C. Springer and L. J. Thibodeaux. 1985. Liquid-phase mass transfer coefficients for surface impoundments. Environmental Progress 4(3): 203-211.

Mackay, D., and P. J. Leinonen. 1975. Rate of evaporation of low-solubility contaminants from water bodies to atmosphere. Environ. Sci. Technol. 9(13): 1178-1180.

Mackay, D., and R. S. Matsugu. 1973. Evaporation rates of liquid hydrocarbon spilled on land and water. The Canada J. of Chemical Engng. 51(8): 434-439.

Mackay, D., and A. W. Wolkoff. 1973. Rate of evaporation of law-solubility contaminants from water bodies to atmosphere. Environ. Sci. Technol. 7(7): 611-614.

Mackay, D., and T. K. Yuen. 1981. Volatilization rates of organic contaminants from rivers. Water Pollut. Res. J. of Canada 5: 83-98.

Malmstrom, T. G., and A. Ahlgren. 1982. Aspect of ventilation in office room. In International Symposium on Indoor Air Pollutions. Health, and Energy Conservation, Amherst, Mass.

McAllister, J. S. V., and J. B. McQuitty. 1965. Release of gas from slurry. Records of Agricultural Research, North Ireland 14(2): 73-78.

McGill, A. E. J., and N. Jackson. 1977. Change in the shortchain carboxylic acid content and chemical oxygen demand of stored pig slurry. J. Sci. Food Agric. 28: 424-430.

Merkel, J. A., T. E. Hazen, and J. R. Miner. 1969. Identification of gases in a confinement building atmosphere. Transactions of the ASAE 12(3): 310-313.

Miner, J. R. 1974. Odor from confined livestock production. EPA Publication EPA-660. 12-74-023. EPA Research and Development Office, Washington, D.C.

Miner, J. R., and T. E. Hazen. 1969. Ammonia and amines: Components of swine-building odor. Transactions of the ASAE 12(4): 772-774.

Miner, J. R., and R. C. Stroh. 1976. Controlling feedlot surface odor emission rate by application of commercial products. Transactions of the ASAE 19: 533-538.

Miner, J. R., M. D. Kelley, and A. W. Anderson. 1975. Identification and measurement of volatile compounds within a swine building and measurement of ammonia evolution rates from manure-covered surface. Pp. 351-355. In International Symposium on Livestock Wastes. ASAE, St. Joseph, Michigan.

Mosier, A. R., C. E. Anderson, and F. G. Viets, Jr. 1973. Identification of alipnatic amines volatilized from cattle feedyard. Environ. Sci. Technol. 7(7): 642-644.

Muehling, A. J. 1969. Gases and odors from stored swine waste. J. Anim. Sci. 30: 526-530.

National Research Council. 1981. Indoor pollutants. National Academic Press, Washington, D.C.

Nauman, E. B. 1981. Residence time distributions and micromixing. Chem. Eng. Commun. 8: 53-131.

Owens, M. R., W. Edwards, and J. W. Gibs. 1964. Some reaeration studies in stream. Int. J. Air Water Pollut. 8: 469-486.

Parr, J. F. 1974. Organic-matter-- the decomposition and oxygen relationship. Pp. 121-139. In Factors involved in land application of agricultural municipal wastes. USDA-ARS, Beltsville MD.

Plemmons, R. J. 1977. M-Matrix characterizations. I--Nonsingular M-Matrices. Linear Algebra and Its Applications 18: 175-188.

Randall, J. M. 1977. The prediction of airflow pattern in livestock buildings. J. Agric. Engng. Res. 20(2): 199-215.

Randall, J. M., and V. A. Battans. 1979. Stability criteria for airflow patterns in livestock buildings. J. Agric. Engng. Res. 24: 361-374.

Ritter, W. F., N. E. Collin, and P. R. Eastburn. 1975. Chemical treatment of liquid dairy manure to reduce malodors. Pp. 381-384. In Managing livestock wastes. Proceedings, 3rd International symposium on Livestock Wastes. ASAE Publ. PROC-275. ASAE, St. Joseph, Michigan.

Riviere, J., J. C. Subtil, and G. Latroux. 1974. Etude de levolution physico-chimcque et microbiologique du lisier de porce pendant le stockage anaerobie. Ann. Agron. 25: 383-401.

Robertson, A. M., and H. Galbraith. 1971. Effect of ventilation on the gas concentration in a part-slatted piggery. Farm Building R & D Studies 1: 17-28.

Sallvik, K. 1974. Manure gases and their effect on livestock health. In Proceedings, International Livestock Environment Symposium. ASAE Publication SP-01-74: 373-377.

Sandberg, M. 1981. What is ventilation efficiency? Building and Environ. 16(2): 123-135.

Sandberg, M. 1983. Ventilation efficiency as a guide to design. ASHRAE Trans. 89(IIb): 455-479.

Schuetzle, D. 1980. Air pollutions (and mass spectrometry). In Biochemical application of mass spectrometry. First supplementary volume. John Wiley & Sons, New York.

Schuetzle, D., and C. V. Hampton. 1985. Gas chrometagraph/mass spectrometry in air pollution studies. Pp. 159-193. In Karasek, F. W., O. Hutzinger, and S. Safe, Eds. Mass spectrometry in environmental science. Plenum Press, New York.

Seinfeld, J. H. 1975. Air pollution. Physical and chemical fundamentals. McGraw-Hill Inc., New York.

Seltzer, W., S. G. Moum, and T. M. Goldhaft. 1969. A method for the treatment of animal wastes to control ammonia and other odors. Poult. Sci. 48: 1912-1918.

Seneta, E. 1973. Non-negative martices. An introduction to theory and applications. John Wiley & Sons, New York.

Skaaret, E. 1986. Contaminants removal performance in terms of ventilation effectiveness. Environ. Int. 12: 419-427.

Skaaret, E., and H. M. Mathisen. 1982. Ventilation efficiency. Environ. Int. 8: 473-481.

Skaaret, E., and H. M. Mathisen. 1983. Ventilation efficiency-- A guide to efficient ventilation. ASHRAE Trans. 89(IIb): 480-495.

Skarp, S.-U. 1975. Manure gases and air currents in livestock housing. Pp. 363-365. In Proceedings, 3rd International Symposium on Livestock Wastes. ASAE Publication PROC-275.

Smith, J. H., D. C. Bomberger, Jr., and D. L. Hayhen. 1980. Prediction of the volatilization of high-volatility chemicals from natural water bodies. Environ. Sci. Technol. 14(11): 1332-1337.

Stumm, W., and J. J. Morgan. 1981. Aquatic chemistry. An introduction emphasizing chemical equilibria in natural waters. John Wiley, New York.

Sweeten, J. M., D. R. Reddell, Schake, and B. Garner. 1977. The odors intensities at cattle feedlots. Transactions of the ASAE 20: 502-508.

Taiganides, E. P., and R. K. White. 1969. The menace of noxious gases in animal units. Transactions of the ASAE 12(3): 359-362, 367.

Therasse, R., and L. Sine. 1974. Determination d'une methode de mesure du remouvellement de l'air daus les batimemts. Bull. Rech. Agron. Gembloux 9(2): 165-187.

Thibodeaux, L. J. 1979. Chemodynamic. Environmental movement of chemical in air, water, and soil. John Wiley, New York.

Ulich, W. L., and J. P. Ford. 1975. Malodor reduction in beef cattle feedlot. Pp. 369-371. In Managing livestock wastes. Proceedings, 3rd International Symposium on Livestock Wastes. ASAE Publ. PROC-275. ASAE, St. Joseph, Michigan.

Wadden, R. A., and P. A. Scheff. 1983. Indoor air pollution -- characterization, prediction and control. John Wiley, New York.

Warburton, D. J., J. N. Scarborough, D. L. Day, A. J. Mueling, A. H. Jensen, and S. E. Curtis. 1980. Evaluation of commerical products for odor control and solids reduction of liquid swine manure. Pp. 309-313. In Proceedings, 4th International Symposium on Livestock Wastes. ASAE Publ. 2-81.

Water Pollution Control Federation. 1967. Safety in wastewater works. Manual of Practice No. 1. Water Pollution Control Federation, Washington, D. C.

White, R. K., E. P. Taigandies, and D. Cole. 1971. Chromatographic identification of malodors from dairy animal waste. Pp. 110-113. In Livestock waste management and pollution abaement. Proceedings, International symposium on livestock wastes. ASAE publ. PROC-271. ASAE, St. Joseph, Michigan.

Yasuhara, A., and K. Fuwa. 1977a. Odor and volatile compounds in liquid swine manure. I. Carboxylic acids and phenols. Bull. Chem. Soc. Jpn. 50(3): 731-733.

Yasuhara, A., and K. Fuwa. 1977b. Odor and volatile compounds in liquid swine manure. II. Steam-distillable substances. Bull. Chem. Soc. Jpn. 50(11): 3029-3032.

Zvirin, Y., and R. Shinnar. 1979. Interpretation of internal tracer experiments and local sojourn time distributions. Int. J. Multiphase Flow 2: 495-520.

Zwietering, Th. N. 1959. The degree of mixing in continuous flow systems. Chem. Engng. Sci. 11(1): 1-15.

ACKNOWLEDGEMENTS

The author would like to express his appreciation to:

Dr. Dwaine S. Bundy for serving as major professor and for guidance, advice and support throughout this study.

Dr. Carl E. Anderson, Dr. Earl G. Hammond, Professor Alfred W. Joensen, and Dr. Richard J. Smith, for being committee members and for their suggestions concerning this study.

Dr. Lujsan, a post-doctoral fellow in the Food Technology Department, for helping me to operate the GC/MS.

Mr. Marc Lott, the lab technician.

Mrs. Jan Leslie, the section secretary.

Graduate colleagues in the Bull Pen and Davidson Hall for making my graduate studies a learning and enjoyable experience.

Tehsin Kuan, Shuchwen Peng, and Changhsin Cheng for their special friendships.

My parents and three sisters for their continual support throughout my entire life.

APPENDIX A: THE TYPICAL MASS SPECTRA AND TOTAL ION CHROMATOGRAM (TIC) OF HEADSPACE FROM AIR SAMPLE AND EIGHT WASTE TREATMENT SAMPLES

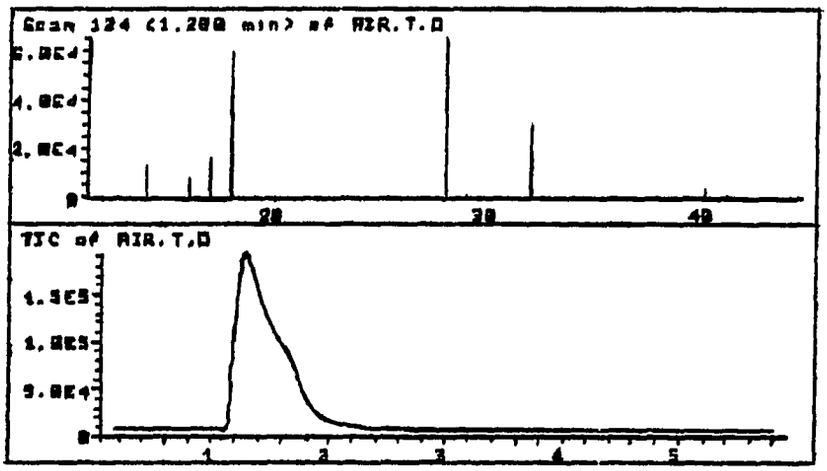

FIGURE A-1. The typical mass spectra and TIC results for air sample

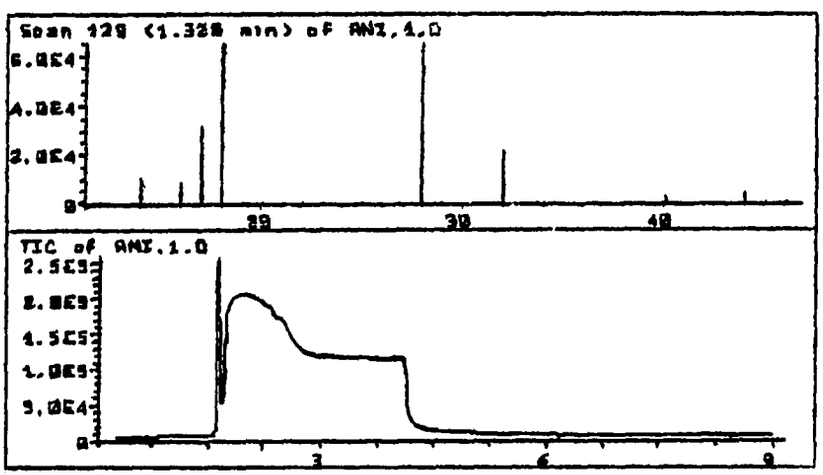

FIGURE A-2. The typical mass spectra and TIC results for waste treatment #1

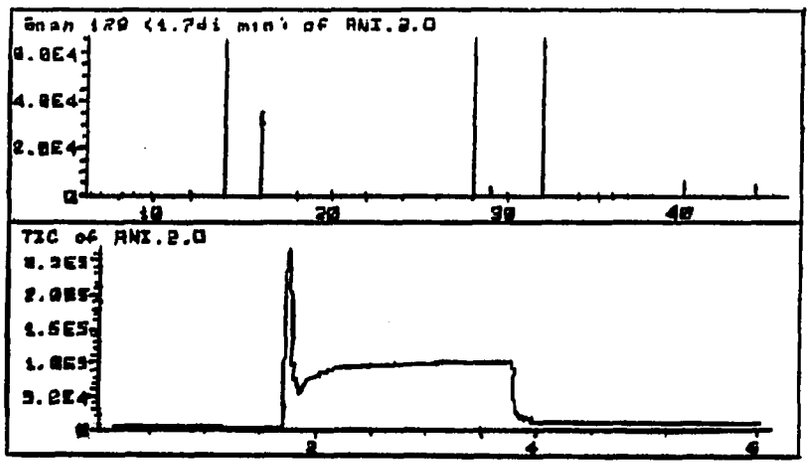

FIGURE A-3. The typical mass spectra and TIC results for waste treatment #2

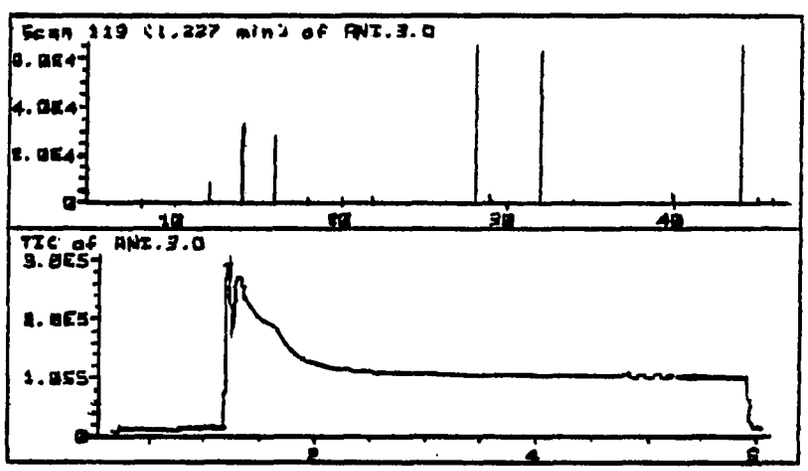

FIGURE A-4. The typical mass spectra and TIC results for waste treatment #3

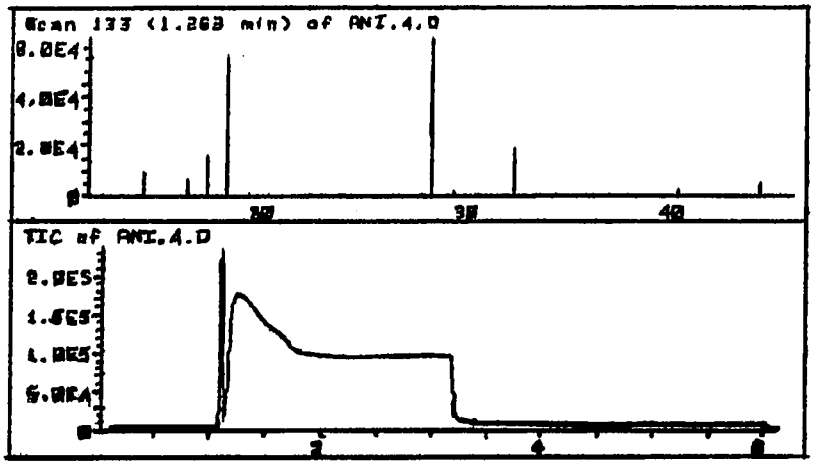

FIGURE A-5. The typical mass spectra and TIC results for waste treatment #4

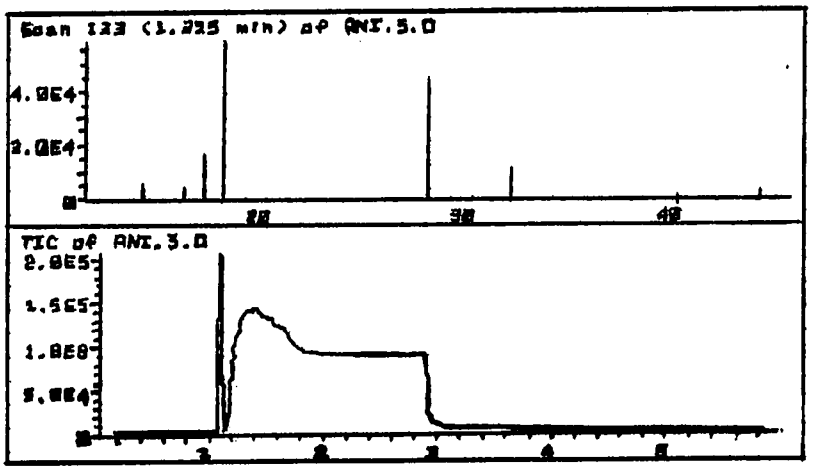

FIGURE A-6. The typical mass spectra and TIC results for waste treatment #5

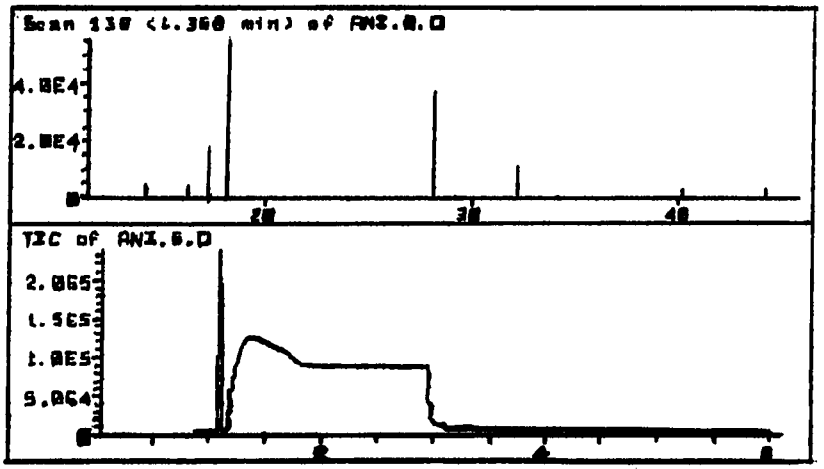

FIGURE A-7. The typical mass spectra and TIC results for waste treatment #6

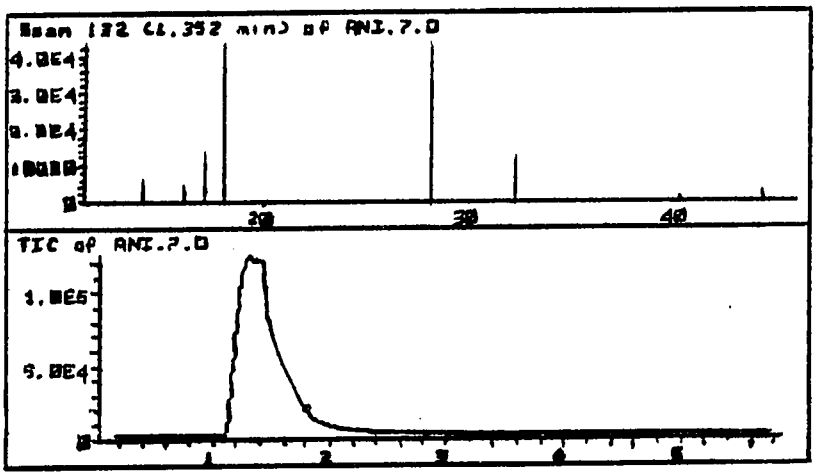

FIGURE A-8. The typical mass spectra and TIC results for waste treatment #7

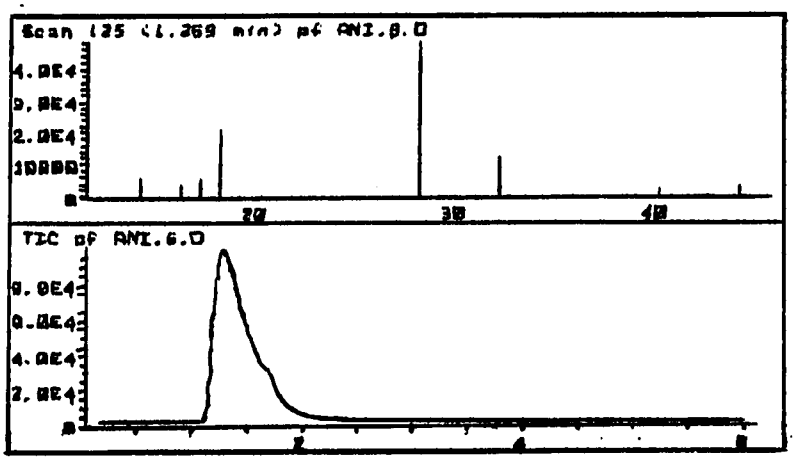

FIGURE A-9. The typical mass spectra and TIC results for waste treatment #8

APPENDIX B: OVERALL QUANTITATIVE RESULTS (PEAK AREAS) OF CHEMICAL-BIOCHEMICAL CONTROL EXPERIMENT

TABLE B-1. Relative quantitative of selected Compounds in headspace screening by GC/MS

Gases	Date	Gas samples analyzed by GC/MS								
	(1987)	Air	1	2	3	4	5	6	7	8
		Peak areas ($x10^6$)								
O_2	2/23	7.8	8.6	8.1	10.3	9.5	8.1	8.1		
	3/04	8.0	7.6	7.9	13.8	9.9	8.1	8.1		
	3/12	7.7	8.9	7.2	10.2	14.9	8.2	1.1		
	3/19	---	6.1	3.2	13.5	10.3	1.2	8.8		
	4/09	7.4	3.9	5.2	8.7	2.7	3.5	4.4	1.1	3.1
	4/16	7.5	4.1	4.5	8.8	3.5	3.8	4.6	3.8	4.4
	4/23	7.4	6.4	3.1	7.5	4.2	3.2	2.8	2.7	.35
	4/30	7.5	4.2	3.2	7.4	4.4	3.6	3.5	2.6	1.5
	5/28	7.5	4.3	4.2	8.5	3.6	3.4	4.4	3.8	3.7
	6/11	7.5	4.2	3.3	7.5	3.6	3.5	4.2	4.4	3.5
	6/18	7.5	4.2	3.2	6.9	3.3	3.3	4.6	4.2	4.4
	7/02	4.7	5.1	5.3	3.6	3.0	3.6	3.3	3.5	2.9
CO_2	2/23	---	3.6	4.1	4.0	6.1	5.1	1.3		
	3/04	.0001	3.4	3.8	3.9	5.9	4.8	1.6		
	3/12	.0001	3.7	3.6	3.9	6.1	4.9	1.5		
	3/19	.0001	.84	3.2	.84	2.7	.29	1.4		
	4/09	.0001	1.5	2.6	5.5	2.4	1.4	1.2	.01	.01
	4/16	.0001	1.2	2.4	2.6	2.1	1.2	1.3	.03	.07
	4/23	.0001	.54	.84	2.4	1.1	.32	.38	.04	.08
	4/30	.0001	1.4	1.9	2.4	1.4	0.9	1.1	.03	.07
	5/28	.0001	1.5	1.6	2.6	1.7	0.8	1.2	.03	.07
	6/11	.0001	1.4	1.5	2.6	1.5	1.0	1.3	.45	.08
	6/18	.0001	1.2	1.6	2.4	1.6	0.9	1.2	.39	.07
	7/02	.0001	1.5	1.4	3.4	2.5	0.8	0.9	.40	.08
H_2S	2/23	0	0	0	0	0	0	0		
	3/04	0	0	0	0	0	0	0		
	3/12	0	0	0	0	0	0	0		
	3/19	0	0	0	0	0	0	0		
	4/09	0	0	0	0	0	0	0	0	0
	4/23	0	0	0	0	0	0	0	0	0
	4/23	0	0	0	0	0	0	0	0	0
	4/30	0	0	0	0	0	0	0	0	0
	5/28	0	0	0	0	0	0	0	0	0
	6/11	0	0	0	0	0	0	0	0	0
	6/18	0	0	0	0	0	0	0	0	0
	7/02	0	0	0	0	0	0	0	0	0

Table B-1 (Continued)

Gases	Date	Gas samples analyzed by GC/MS								
	(1987)	Air	1	2	3	4	5	6	7	8
		Peak areas ($x10^6$)								
NH_3	2/23	---	.17	.14	.12	.12	.12	.09		
	3/04	.96	2.9	4.8	4.9	5.4	4.5	1.5		
	3/12	.96	2.2	4.9	4.9	5.4	4.5	1.5		
	3/19	3.9	2.2	5.8	5.1	5.7	.11	1.6		
	4/09	.5	19.5	.96	6.1	2.7	8.8	1.7	1.7	3.1
	4/16	.62	4.6	1.5	6.5	4.2	7.4	1.6	1.6	3.2
	4/23	2.1	34.1	6.0	6.5	8.4	8.4	3.9	1.9	.76
	4/30	1.5	8.5	5.5	6.4	7.5	7.5	1.5	1.7	1.4
	5/28	0.8	5.7	4.6	6.1	5.2	7.3	1.7	1.6	1.1
	6/11	.68	5.4	4.3	5.6	4.6	6.9	1.6	1.7	1.2
	6/18	.56	5.7	4.2	5.1	4.2	6.5	1.5	1.6	1.3
	7/02	.5	2.4	7.9	8.7	3.6	6.4	1.5	1.5	1.2
CH_4	2/23	1.5	1.2	3.1	3.1	4.5	3.0	1.3		
	3/04	3.9	.2	2.9	3.3	4.6	3.2	1.0		
	3/12	1.4	1.6	3.2	3.1	4.6	3.2	1.2		
	3/19	4.2	1.5	3.1	3.7	2.4	1.4	1.1		
	4/09	1.3	.44	.90	2.8	.62	.54	1.4	.04	.33
	4/16	.46	.32	.62	2.3	.52	.49	1.4	.12	.35
	4/23	.86	1.4	1.1	3.2	.86	.52	.53	.48	.31
	4/30	.56	1.5	1.2	2.4	.54	.51	.54	.45	.32
	5/28	1.4	.9	1.0	2.2	.52	.54	1.4	.39	.33
	6/11	1.3	.88	.90	2.5	.49	.51	1.1	.49	.36
	6/18	1.4	.85	.86	2.3	.51	.49	.68	.44	.34
	7/02	0.2	.26	.60	.85	.62	.50	.40	.40	.66
H_2O	2/23	---	.94	.75	.66	.52	.55	.48		
	3/04	12.9	.15	.67	2.6	4.7	4.1	4.6		
	3/12	5.1	9.3	10.1	7.2	4.7	4.1	2.1		
	3/19	13.0	44.2	7.2	2.4	6.7	4.6	41.7		
	4/09	2.2	0	3.9	2.6	5.9	3.5	1.9	6.3	11.6
	4/16	6.4	8.6	4.3	6.4	6.2	3.2	2.3	3.5	6.8
	4/23	7.9	0	13.9	4.7	4.7	17.2	16.3	7.1	2.6
	4/30	8.6	7.5	10.6	5.6	5.5	5.6	6.2	6.4	5.5
	5/28	5.3	7.7	4.8	5.2	4.3	4.6	2.3	3.8	5.9
	6/11	9.8	9.2	7.6	7.0	6.7	5.9	4.3	4.6	6.2
	6/18	8.9	9.7	6.6	6.2	5.4	6.8	5.3	6.2	5.7
	7/02	.05	9.6	3.8	6.4	6.0	2.9	.07	.12	.1

APPENDIX C: THE MASS SPECTRA, TOTAL ION CHROMATOGRAM, AND THE RESULTS OF PEAK PROCESSING FOR EACH SELECTED GAS COMPOUND OF THE EXTERNAL QUANTITATIVE STANDARD FOR CHEMICAL-BIOCHEMICAL CONTROL EXPERIMENT

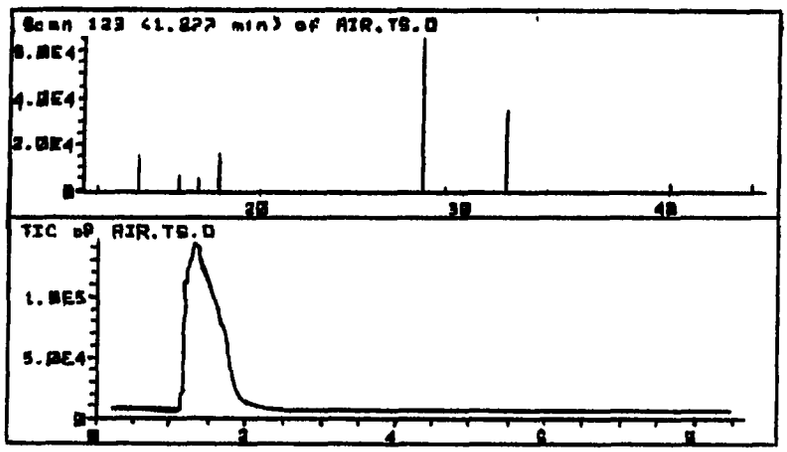

TIC of AIR.TS.D
ANIMAL WASTE GASES SAMPLES - AIR TEST SAMPLE -50ul

peak#	ret time	area	start time	end time
1	1.280	32928218	1.092	1.659
2	1.659	5992059	1.659	2.165

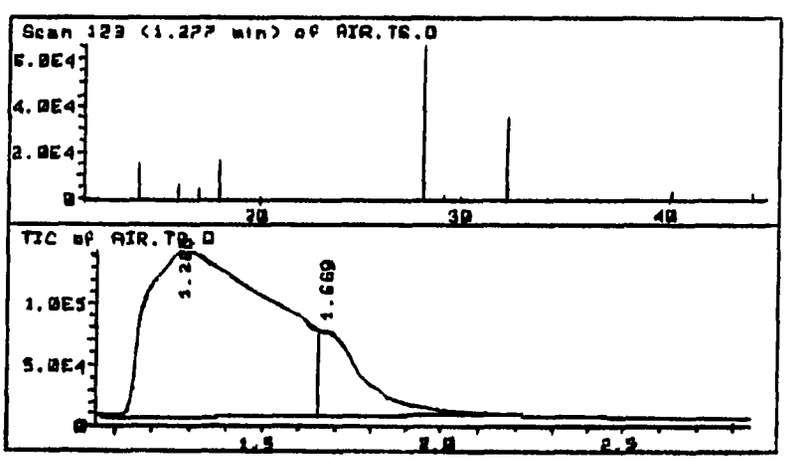

FIGURE C-1. Total ion chromatogram and mass spectra of air sample

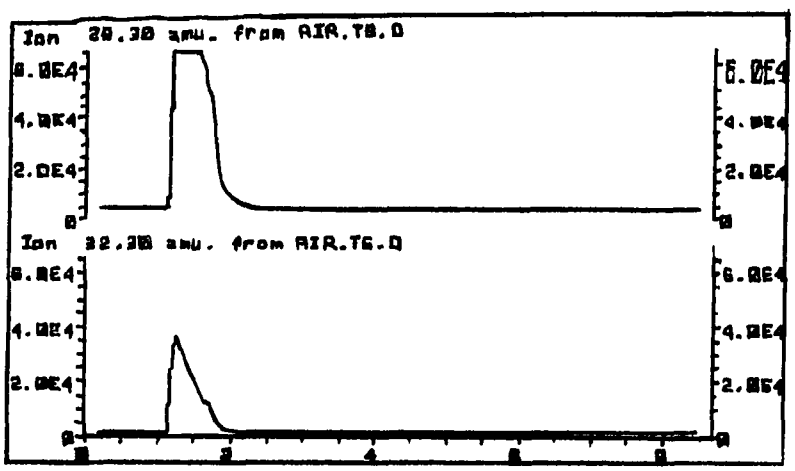

Ion 32.30 amu. from AIR.TS.D
ANIMAL WASTE GASES SAMPLES - AIR TEST SAMPLE -50ul

peak#	ret time	area	start time	end time
1	1.246	6810370	1.094	1.668
2	1.685	579512	1.668	1.883

FIGURE C-2. The selected ion monitor for N_2 and O_2

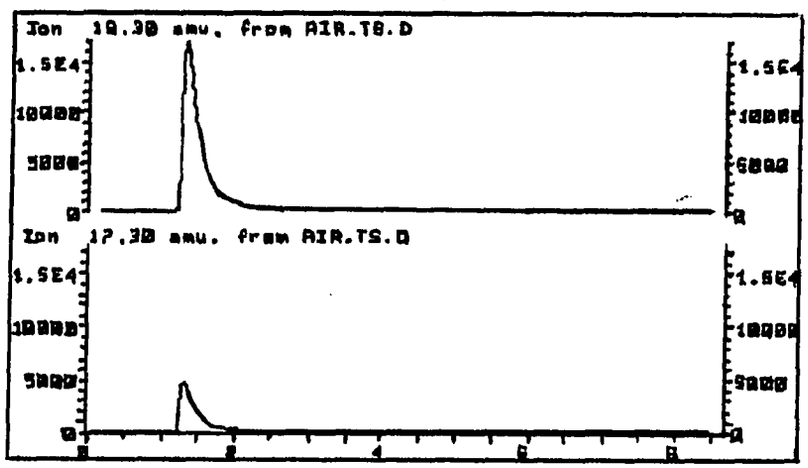

Ion 18.30 amu. from AIR.T8.D
ANIMAL WASTE GASES SAMPLES - AIR TEST SAMPLE -50ul

peak#	ret time	area	start time	end time
1	1.314	2183331	1.139	1.661
2	1.667	58555	1.661	1.800

FIGURE C-3. The selected ion monitor for H_2O and NH_3

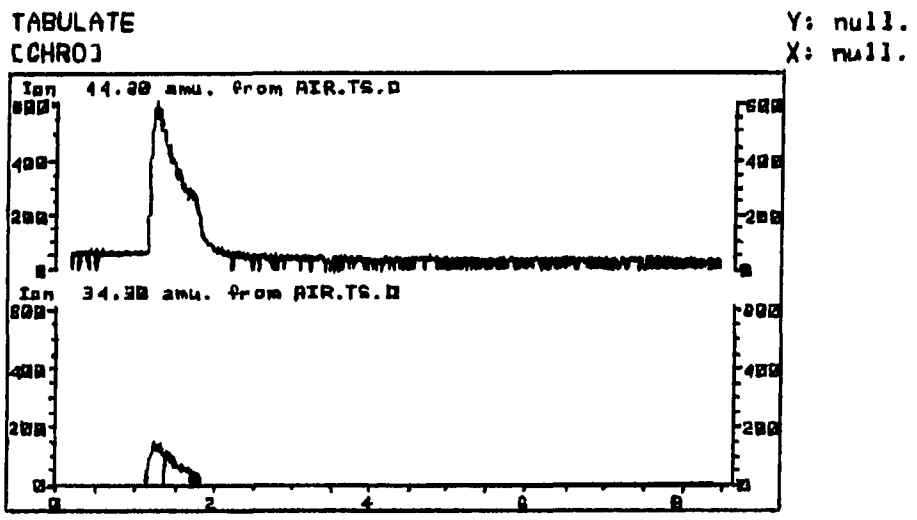

FIGURE C-4. The selected ion monitor for CO_2 and H_2S

TABULATE
[CHRO]

Y: null.
X: null.

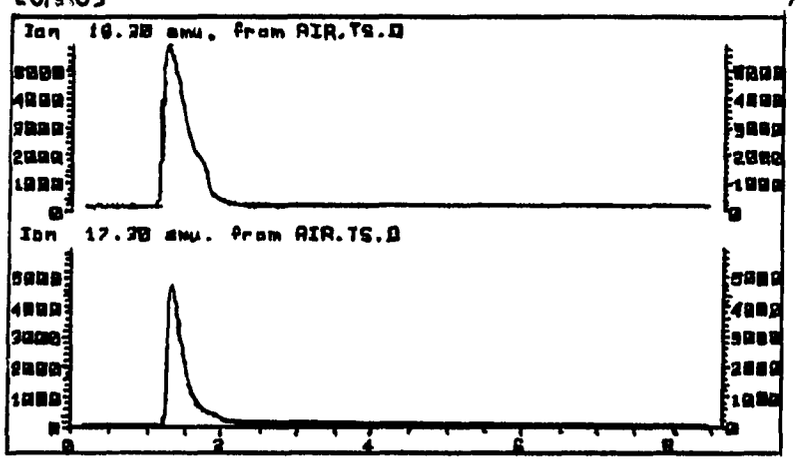

Ion 16.30 amu. from AIR.TS.D
ANIMAL WASTE GASES SAMPLES - AIR TEST SAMPLE -50ul

peak#	ret time	area	start time	end time
1	1.257	1265265	1.094	1.990

TABULATE
[CHRO]

Y: null.
X: null.

Ion 17.30 amu. from AIR.TS.D
ANIMAL WASTE GASES SAMPLES - AIR TEST SAMPLE -50ul

peak#	ret time	area	start time	end time
1	1.316	495934	1.175	1.598

FIGURE C-5. The selected ion monitor for CH_4 and NH_3

APPENDIX D: THE INPUT DATA OF FLOW MATRICES IN MULTIPLE AIRFLOW REGIONS MODEL SIMULATION STUDY

GIVEN MATRIX

12.6000	-5.8000	0.0000	0.0000	0.0000	-5.8000	0.0000
0.0000	0.0000	0.0000	0.0000	0.0000	0.0000	0.0000
0.0000	0.0000	0.0000	0.0000	0.0000	0.0000	0.0000
0.0000	0.0000	0.0000	0.0000			
-5.8000	18.4000	-5.8000	0.0000	0.0000	0.0000	-5.8000
0.0000	0.0000	0.0000	0.0000	0.0000	0.0000	0.0000
0.0000	0.0000	0.0000	0.0000	0.0000	0.0000	0.0000
0.0000	0.0000	0.0000	0.0000			
0.0000	-6.8000	18.4000	-5.8000	0.0000	0.0000	0.0000
-5.8000	0.0000	0.0000	0.0000	0.0000	0.0000	0.0000
0.0000	0.0000	0.0000	0.0000	0.0000	0.0000	0.0000
0.0000	0.0000	0.0000	0.0000			
0.0000	0.0000	-5.8000	18.4000	-5.8000	0.0000	0.0000
0.0000	-5.8000	0.0000	0.0000	0.0000	0.0000	0.0000
0.0000	0.0000	0.0000	0.0000	0.0000	0.0000	0.0000
0.0000	0.0000	0.0000	0.0000			
0.0000	0.0000	0.0000	-6.8000	12.6000	0.0000	0.0000
0.0000	0.0000	-5.8000	0.0000	0.0000	0.0000	0.0000
0.0000	0.0000	0.0000	0.0000	0.0000	0.0000	0.0000
0.0000	0.0000	0.0000	0.0000			
-5.8000	0.0000	0.0000	0.0000	0.0000	17.4000	-5.8000
0.0000	0.0000	0.0000	-5.8000	0.0000	0.0000	0.0000
0.0000	0.0000	0.0000	0.0000	0.0000	0.0000	0.0000
0.0000	0.0000	0.0000	0.0000			
0.0000	-5.8000	0.0000	0.0000	0.0000	-5.8000	23.2000
-5.8000	0.0000	0.0000	0.0000	-5.8000	0.0000	0.0000
0.0000	0.0000	0.0000	0.0000	0.0000	0.0000	0.0000
0.0000	0.0000	0.0000	0.0000			
0.0000	0.0000	-5.8000	0.0000	0.0000	0.0000	-5.8000
23.2000	-5.8000	0.0000	0.0000	0.0000	-5.8000	0.0000
0.0000	0.0000	0.0000	0.0000	0.0000	0.0000	0.0000
0.0000	0.0000	0.0000	0.0000			
0.0000	0.0000	0.0000	-5.8000	0.0000	0.0000	0.0000
-5.8000	23.2000	-5.8000	0.0000	0.0000	0.0000	-5.8000
0.0000	0.0000	0.0000	0.0000	0.0000	0.0000	0.0000
0.0000	0.0000	0.0000	0.0000			
0.0000	0.0000	0.0000	0.0000	-5.8000	0.0000	0.0000
0.0000	-5.8000	17.4000	0.0000	0.0000	0.0000	0.0000
-5.8000	0.0000	0.0000	0.0000	0.0000	0.0000	0.0000
0.0000	0.0000	0.0000	0.0000			
0.0000	0.0000	0.0000	0.0000	0.0000	-5.8000	0.0000
0.0000	0.0000	0.0000	17.4000	-5.8000	0.0000	0.0000
0.0000	-5.8000	0.0000	0.0000	0.0000	0.0000	0.0000
0.0000	0.0000	0.0000	0.0000			
0.0000	0.0000	0.0000	0.0000	0.0000	0.0000	-5.8000
0.0000	0.0000	0.0000	-5.8000	23.2000	-5.8000	0.0000
0.0000	0.0000	-5.8000	0.0000	0.0000	0.0000	0.0000
0.0000	0.0000	0.0000	0.0000			
0.0000	0.0000	0.0000	0.0000	0.0000	0.0000	0.0000
-5.8000	0.0000	0.0000	0.0000	-5.8000	23.2000	-5.8000
0.0000	0.0000	0.0000	-5.8000	0.0000	0.0000	0.0000
0.0000	0.0000	0.0000	0.0000			
0.0000	0.0000	0.0000	0.0000	0.0000	0.0000	0.0000
0.0000	-5.8000	0.0000	0.0000	0.0000	-5.8000	23.2000
-5.8000	0.0000	0.0000	0.0000	-5.8000	0.0000	0.0000
0.0000	0.0000	0.0000	0.0000			
0.0000	0.0000	0.0000	0.0000	0.0000	0.0000	0.0000
0.0000	0.0000	-5.8000	0.0000	0.0000	0.0000	-5.8000
17.4000	0.0000	0.0000	0.0000	0.0000	-5.8000	0.0000

FIGURE D-1. The flow matrix for short-circuiting system in the case of comparison with research literature

0.0000	0.0000	0.0000	0.0000			
0.0000	0.0000	0.0000	0.0000	0.0000	0.0000	0.0000
0.0000	0.0000	0.0000	-5.8000	0.0000	0.0000	0.0000
0.0000	17.4000	-5.8000	0.0000	0.0000	0.0000	-5.8000
0.0000	0.0000	0.0000	0.0000			
0.0000	0.0000	0.0000	0.0000	0.0000	0.0000	0.0000
0.0000	0.0000	0.0000	0.0000	-5.8000	0.0000	0.0000
0.0000	-5.8000	23.2000	-5.8000	0.0000	0.0000	0.0000
-5.8000	0.0000	0.0000	0.0000			
0.0000	0.0000	0.0000	0.0000	0.0000	0.0000	0.0000
0.0000	0.0000	0.0000	0.0000	0.0000	-5.8000	0.0000
0.0000	0.0000	-5.8000	23.2000	-5.8000	0.0000	0.0000
0.0000	-5.8000	0.0000	0.0000			
0.0000	0.0000	0.0000	0.0000	0.0000	0.0000	0.0000
0.0000	0.0000	0.0000	0.0000	0.0000	0.0000	-5.8000
0.0000	0.0000	0.0000	-5.8000	23.2000	-5.8000	0.0000
0.0000	0.0000	-5.8000	0.0000			
0.0000	0.0000	0.0000	0.0000	0.0000	0.0000	0.0000
0.0000	0.0000	0.0000	0.0000	0.0000	0.0000	0.0000
-5.8000	0.0000	0.0000	0.0000	-5.8000	17.4000	0.0000
0.0000	0.0000	0.0000	-5.8000			
0.0000	0.0000	0.0000	0.0000	0.0000	0.0000	0.0000
0.0000	0.0000	0.0000	0.0000	0.0000	0.0000	0.0000
0.0000	-5.8000	0.0000	0.0000	0.0000	0.0000	11.6000
-5.8000	0.0000	0.0000	0.0000			
0.0000	0.0000	0.0000	0.0000	0.0000	0.0000	0.0000
0.0000	0.0000	0.0000	0.0000	0.0000	0.0000	0.0000
0.0000	0.0000	-5.8000	0.0000	0.0000	0.0000	-5.8000
17.4000	-5.8000	0.0000	0.0000			
0.0000	0.0000	0.0000	0.0000	0.0000	0.0000	0.0000
0.0000	0.0000	0.0000	0.0000	0.0000	0.0000	0.0000
0.0000	0.0000	0.0000	-5.8000	0.0000	0.0000	0.0000
-5.8000	17.4000	-5.8000	0.0000			
0.0000	0.0000	0.0000	0.0000	0.0000	0.0000	0.0000
0.0000	0.0000	0.0000	0.0000	0.0000	0.0000	0.0000
0.0000	0.0000	0.0000	0.0000	-5.8000	0.0000	0.0000
0.0000	-5.8000	17.4000	-5.8000			
0.0000	0.0000	0.0000	0.0000	0.0000	0.0000	0.0000
0.0000	0.0000	0.0000	0.0000	0.0000	0.0000	0.0000
0.0000	0.0000	0.0000	0.0000	0.0000	-5.8000	0.0000
0.0000	0.0000	-5.8000	11.6000			

FIGURE D-1. Continued

GIVEN MATRIX

12.6000	-5.8000	0.0000	0.0000	0.0000	-5.8000	0.0000
0.0000	0.0000	0.0000	0.0000	0.0000	0.0000	0.0000
0.0000	0.0000	0.0000	0.0000	0.0000	0.0000	0.0000
0.0000	0.0000	0.0000	0.0000			
-6.8000	18.4000	-5.8000	0.0000	0.0000	0.0000	-5.8000
0.0000	0.0000	0.0000	0.0000	0.0000	0.0000	0.0000
0.0000	0.0000	0.0000	0.0000	0.0000	0.0000	0.0000
0.0000	0.0000	0.0000	0.0000			
0.0000	-6.8000	18.4000	-5.8000	0.0000	0.0000	0.0000
-5.8000	0.0000	0.0000	0.0000	0.0000	0.0000	0.0000
0.0000	0.0000	0.0000	0.0000	0.0000	0.0000	0.0000
0.0000	0.0000	0.0000	0.0000			
0.0000	0.0000	-6.8000	18.4000	-5.8000	0.0000	0.0000
0.0000	-5.8000	0.0000	0.0000	0.0000	0.0000	0.0000
0.0000	0.0000	0.0000	0.0000	0.0000	0.0000	0.0000
0.0000	0.0000	0.0000	0.0000			
0.0000	0.0000	0.0000	-6.8000	12.6000	0.0000	0.0000
0.0000	0.0000	-5.8000	0.0000	0.0000	0.0000	0.0000
0.0000	0.0000	0.0000	0.0000	0.0000	0.0000	0.0000
0.0000	0.0000	0.0000	0.0000			
-5.8000	0.0000	0.0000	0.0000	0.0000	17.4000	-5.8000
0.0000	0.0000	0.0000	-5.8000	0.0000	0.0000	0.0000
0.0000	0.0000	0.0000	0.0000	0.0000	0.0000	0.0000
0.0000	0.0000	0.0000	0.0000			
0.0000	-5.8000	0.0000	0.0000	0.0000	-5.8000	23.2000
-5.8000	0.0000	0.0000	0.0000	-5.8000	0.0000	0.0000
0.0000	0.0000	0.0000	0.0000	0.0000	0.0000	0.0000
0.0000	0.0000	0.0000	0.0000			
0.0000	0.0000	-5.8000	0.0000	0.0000	0.0000	-5.8000
23.2000	-5.8000	0.0000	0.0000	0.0000	-5.8000	0.0000
0.0000	0.0000	0.0000	0.0000	0.0000	0.0000	0.0000
0.0000	0.0000	0.0000	0.0000			
0.0000	0.0000	0.0000	-5.8000	0.0000	0.0000	0.0000
-5.8000	23.2000	-5.8000	0.0000	0.0000	0.0000	-5.8000
0.0000	0.0000	0.0000	0.0000	0.0000	0.0000	0.0000
0.0000	0.0000	0.0000	0.0000			
0.0000	0.0000	0.0000	0.0000	-6.8000	0.0000	0.0000
0.0000	-5.8000	18.4000	0.0000	0.0000	0.0000	0.0000
-5.8000	0.0000	0.0000	0.0000	0.0000	0.0000	0.0000
0.0000	0.0000	0.0000	0.0000			
0.0000	0.0000	0.0000	0.0000	0.0000	-5.8000	0.0000
0.0000	0.0000	0.0000	17.4000	-5.8000	0.0000	0.0000
0.0000	-5.8000	0.0000	0.0000	0.0000	0.0000	0.0000
0.0000	0.0000	0.0000	0.0000			
0.0000	0.0000	0.0000	0.0000	0.0000	0.0000	-5.8000
0.0000	0.0000	0.0000	-5.8000	23.2000	-5.8000	0.0000
0.0000	0.0000	-5.8000	0.0000	0.0000	0.0000	0.0000
0.0000	0.0000	0.0000	0.0000			
0.0000	0.0000	0.0000	0.0000	0.0000	0.0000	0.0000
-5.8000	0.0000	0.0000	0.0000	-5.8000	23.2000	-5.8000
0.0000	0.0000	0.0000	-5.8000	0.0000	0.0000	0.0000
0.0000	0.0000	0.0000	0.0000			
0.0000	0.0000	0.0000	0.0000	0.0000	0.0000	0.0000
0.0000	-5.8000	0.0000	0.0000	0.0000	-5.8000	23.2000
-5.8000	0.0000	0.0000	0.0000	-5.8000	0.0000	0.0000
0.0000	0.0000	0.0000	0.0000			
0.0000	0.0000	0.0000	0.0000	0.0000	0.0000	0.0000
0.0000	0.0000	-6.8000	0.0000	0.0000	0.0000	-5.8000
18.4000	0.0000	0.0000	0.0000	0.0000	-5.8000	0.0000

FIGURE D-2. The flow matrix for displacement system in the case of comparison with research literature

0.0000	0.0000	0.0000	0.0000			
0.0000	0.0000	0.0000	0.0000	0.0000	0.0000	0.0000
0.0000	0.0000	0.0000	-5.8000	0.0000	0.0000	0.0000
0.0000	17.4000	-5.8000	0.0000	0.0000	0.0000	-5.8000
0.0000	0.0000	0.0000	0.0000			
0.0000	0.0000	0.0000	0.0000	0.0000	0.0000	0.0000
0.0000	0.0000	0.0000	0.0000	-5.8000	0.0000	0.0000
0.0000	-5.8000	23.2000	-5.8000	0.0000	0.0000	0.0000
-5.8000	0.0000	0.0000	0.0000			
0.0000	0.0000	0.0000	0.0000	0.0000	0.0000	0.0000
0.0000	0.0000	0.0000	0.0000	0.0000	-5.8000	0.0000
0.0000	0.0000	-5.8000	23.2000	-5.8000	0.0000	0.0000
0.0000	-5.8000	0.0000	0.0000			
0.0000	0.0000	0.0000	0.0000	0.0000	0.0000	0.0000
0.0000	0.0000	0.0000	0.0000	0.0000	0.0000	-5.8000
0.0000	0.0000	0.0000	-5.8000	23.2000	-5.8000	0.0000
0.0000	0.0000	-5.8000	0.0000			
0.0000	0.0000	0.0000	0.0000	0.0000	0.0000	0.0000
0.0000	0.0000	0.0000	0.0000	0.0000	0.0000	0.0000
-6.8000	0.0000	0.0000	0.0000	-5.8000	18.4000	0.0000
0.0000	0.0000	0.0000	-5.8000			
0.0000	0.0000	0.0000	0.0000	0.0000	0.0000	0.0000
0.0000	0.0000	0.0000	0.0000	0.0000	0.0000	0.0000
0.0000	-5.8000	0.0000	0.0000	0.0000	0.0000	11.6000
-5.8000	0.0000	0.0000	0.0000			
0.0000	0.0000	0.0000	0.0000	0.0000	0.0000	0.0000
0.0000	0.0000	0.0000	0.0000	0.0000	0.0000	0.0000
0.0000	0.0000	-5.8000	0.0000	0.0000	0.0000	-5.8000
17.4000	-5.8000	0.0000	0.0000			
0.0000	0.0000	0.0000	0.0000	0.0000	0.0000	0.0000
0.0000	0.0000	0.0000	0.0000	0.0000	0.0000	0.0000
0.0000	0.0000	0.0000	-5.8000	0.0000	0.0000	0.0000
-5.8000	17.4000	-5.8000	0.0000			
0.0000	0.0000	0.0000	0.0000	0.0000	0.0000	0.0000
0.0000	0.0000	0.0000	0.0000	0.0000	0.0000	0.0000
0.0000	0.0000	0.0000	0.0000	-5.8000	0.0000	0.0000
0.0000	-5.8000	17.4000	-5.8000			
0.0000	0.0000	0.0000	0.0000	0.0000	0.0000	0.0000
0.0000	0.0000	0.0000	0.0000	0.0000	0.0000	0.0000
0.0000	0.0000	0.0000	0.0000	0.0000	-5.8000	0.0000
0.0000	0.0000	-5.8000	11.6000			

FIGURE D-2. Continued

ROW \ COL	1	2	3	4	5	6	7	8	9	10	11	12
1	1/2+3/2r	-1/2r	0	-1/2r	0	0	-1/2r	0	0	0	0	0
2	-1/2-1/2r	1/2+2r	-1/2r	0	-1/2r	0	0	-1/2r	0	0	0	0
3	0	-1/2-1/2r	1/2+3/2r	0	0	-1/2r	0	0	-1/2r	0	0	0
4	-1/2r	0	0	1/2+3/2r	-1/2r	0	0	0	0	-1/2r	0	0
5	0	-1/2r	0	-1/2-1/2r	1/2+2r	-1/2r	0	0	0	0	-1/2r	0
6	0	0	-1/2r	0	-1/2-1/2r	1/2+3/2r	0	0	0	0	0	-1/2r
7	-1/2r	0	0	0	0	0	3/2r	-1/2r	0	-1/2r	0	0
8	0	-1/2r	0	0	0	0	-1/2r	2r	-1/2r	0	-1/2r	0
9	0	0	-1/2r	0	0	0	0	-1/2r	3/2r	0	0	-1/2r
10	0	0	0	-1/2r	0	0	-1/2r	0	0	3/2r	-1/2r	0
11	0	0	0	0	-1/2r	0	0	-1/2r	0	-1/2r	2r	-1/2r
12	0	0	0	0	0	-1/2r	0	0	-1/2r	0	-1/2r	3/2r

FIGURE D-3. The general flow matrix in the case of comparison with chamber test

APPENDIX E: THE CONCEPT OF MIXING FACTOR IN A VENTILATED ENCLOSURE

In view of equation (54) and equation (55) at the condition of no pollution source term, the decay of gaseous concentration can be given by:

$$\underline{C}(t) = \sum_{k=1}^{j-1} A(k)\ \underline{X}(k)\ \exp(-ey(k)\ t) \qquad \text{(E-1)}$$

After a sufficiently long time has passed (say $t > t_o$), the right-hand side of equation (E-1) is dominated by the component with the largest eigenvalue, thus equation (E-1) can be rewritten as an exponential decay equation,

$$\underline{C}(t) \tilde{} \exp(-ey_{max}t) \qquad (t > to) \qquad \text{(E-2)}$$

where ey_{max} is the maximum eigenvalue of the matrix $\underline{T}^{-1}$. Therefore, in a plot of logarithmic concentration vs. time, the linear logarithmic curves in different airspaces become parallel for $t > to$, with equal slope S_e and it holds that

$$S_e = ey_{max} \qquad \text{(E-3)}$$

From the theory of matrix, it is shown that the eigenvalues of the matrix $\underline{T}^{-1}$ are equal to the reciprocal of the eigenvalues of the matrix $\underline{T}$. Because the matrix $\underline{T}$ is a nonnegative and therefore can be applied by the Perron-Frobenius Theorem. The Perron-Frobenius Theorem states that the maximum eigenvalue is less than or equal to the maximum row sum, and greater than, or equal to the minimum row sum (Seneta, 1973; P. 6). The theorem applied on $\underline{T}$ and in view of the physical interpretation (85) of the row sum of $\underline{T}$ gives:

$$\min_p M_{Ip}^{(1)} \leq \frac{1}{s_e} \leq \max_p M_{Ip}^{(1)} \qquad \text{(E-4)}$$

This means the magnitude of the reciprocal of the slope of an exponential decay curve lies between the smallest mean-age of the air occurring in any airspaces and the largest mean-age of air occurring in any airspaces.

Another natural approach to characterizing the overall decay rate when mixing is not complete is to fit an expression of the type in terms of measurement data, and can be written as (Jennings and Armstrong, 1971; Cholette and Cloutier, 1959):

$$C(t) \simeq C(0) \exp(-e\ \tau\ t) \qquad \text{(E-5)}$$

where parameter τ is referred to as the mixing factor.

The value of this factor obtained is dependent on the period during which measurements have been made, and the longer the measuring time, the closer to y_{max} will be the value of τ obtained. Nevertheless, when the derivation from complete mixing is dominant it is presumably a satisfactory measure of the overall ventilation rate.

Therefore, from the model simulation study in the case of comparison with research literature, the mixing factor τ at $t > t_o$ can be calculated and illustrated as Table E-1, in which the maximum eigenvalues for short-circuiting and displacement ventilation systems are 50.54 and 54.32, respectively.

Table E-1 indicated that complete mixing is the best feasible operative mode for the short-circuiting system at a higher air-exchange rate.

TABLE E-1. The mixing factor, τ, in the different ventilation rates for the model case simulation study

Ventilation system	Air-exchange rate, e, 1/hr		
	7.80	12.30	25.80
Short-circuiting	0.15	0.24	0.51
Displacement	0.14	0.23	0.47

APPENDIX F: THE ANALYSIS RESULTS OF CARBON DIOXIDE CONCENTRATION FOR THE CHAMBER TEST

TABLE F-1. The analysis results of CO_2 concentration (ppm) for the chamber test (temperature =25°C, RH=65%-70%, and background CO_2=315ppm)

Sampling points											
1A	1B	2A	2B	3A	3B	4A	4B	5A	5B	6A	6B
(Q = 995 m^3/hr, m = 6 l/min)											
409	415	370	392	410	430	407	410	418	416	412	416
416	409	396	386	415	420	413	394	423	415	426	411
400	392	402	406	420	429	415	420	430	425	415	412
(Q = 430 m^3/hr, m = 6 l/min)											
979	935	885	896	998	978	932	955	1005	1002	989	985
980	945	874	889	1005	969	944	944	1012	1008	992	979
978	939	872	902	987	982	938	939	998	1005	985	978
(Q = 281 m^3/hr, m = 6 l/min)											
1478	1468	1428	1430	1452	1425	1450	1423	1435	1435	1426	1425
1498	1489	1393	1425	1462	1452	1452	1449	1465	1464	1466	1465
1479	1475	1430	1430	1455	1462	1464	1459	1498	1479	1457	1458
(Q = 281 m^3/hr, m = 7.5 l/min)											
1926	1875	1775	1756	1825	1842	1836	1826	1881	1797	1788	1785
1850	1877	1767	1769	1766	1863	1803	1797	1925	1768	1805	1805
(Q = 281 m^3/hr, m = 4.5 l/min)											
1015	1001	998	998	1017	1018	1000	1002	1018	1020	1000	1005
1009	1000	1000	997	1016	1010	1009	1001	1017	1018	1006	1002

TABLE F-2. The analysis results of CO_2 concentration (ppm) from theoretical calculation and measurement in the chamber test

	Sampling points											
	1A	1B	2A	2B	3A	3B	4A	4B	5A	5B	6A	6B
						$Q = 995\ m^3/hr$						
measured	405	408	398	395	415	426	412	408	424	419	418	411
cal'ed	413	425	388	392	438	428	418	415	449	446	431	427
						$Q = 430\ m^3/hr$						
measured	940	979	877	896	997	977	938	946	1005	1003	989	981
cal'ed	969	986	929	935	1006	992	977	973	1024	1019	998	996
						$Q = 281\ m^3/hr$						
measured	1446	1485	1417	1428	1456	1478	1455	1444	1466	1459	1450	1449
cal'ed	1497	1519	1482	1482	1534	1523	1514	1513	1546	1543	1528	1527

APPENDIX G: A MINIMAL MODEL FOR THE DESCRIPTION OF THE MEANING OF THE AIRFLOW MATRIX IN THE MULTIPLE AIRFLOW REGIONS MODEL

Minimal Model

1 subvolume receives outside air

1 subvolume receives only entrained air

1 subvolume discharges

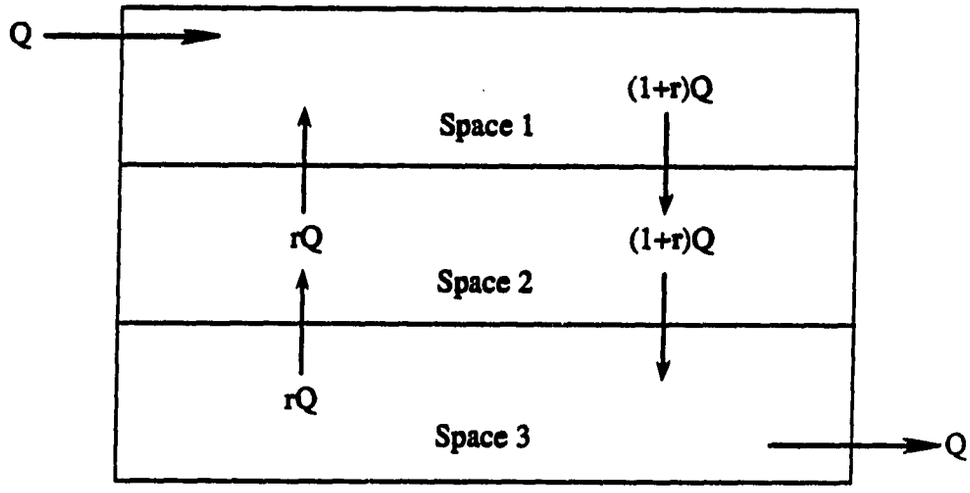

Displacement ventilation system

Notation: Q_{ij}: j=source , i=destination

$Q_{11} = (1+r)Q \quad Q_{12} = rQ \quad Q_{13} = 0$

$Q_{21} = (1+r)Q \quad Q_{22} = (1+2r)Q \quad Q_{23} = rQ$

$Q_{31} = 0 \quad Q_{32} = (1+r)Q \quad Q_{33} = (1+r)Q$

$$\underline{Q} = \begin{bmatrix} (1+r)Q & -rQ & 0 \\ -(1+r)Q & (1+2r)Q & -rQ \\ 0 & -(1+r)Q & (1+r)Q \end{bmatrix}$$

$$\underline{Q}_S = \begin{bmatrix} Q & 0 & 0 \\ 0 & 0 & 0 \\ 0 & 0 & 0 \end{bmatrix}$$

Noting

$$\underline{Q}\ \underline{1} = \begin{bmatrix} (1+r)Q - rQ + 0 \\ -(1+r)Q + (1+2r)Q - rQ \\ 0 - (1+r)Q + (1+r)Q \end{bmatrix} = \begin{bmatrix} Q \\ 0 \\ 0 \end{bmatrix}$$

$$\underline{Q}_S\ \underline{1} = \begin{bmatrix} Q + 0 + 0 \\ 0 + 0 + 0 \\ 0 + 0 + 0 \end{bmatrix} = \begin{bmatrix} Q \\ 0 \\ 0 \end{bmatrix}$$

Hence $\underline{Q}\ \underline{1} = \underline{Q}_s\ \underline{1}$

(but this does not imply $\underline{Q} = \underline{Q}_s$ because a column matrix has no inverse an $\underline{Q}\ \underline{1} \neq \underline{Q}$)

$$\underline{Q}^T = \begin{bmatrix} (1+r)Q & -(1+r)Q & 0 \\ -rQ & (1+2r)Q & -(1+r)Q \\ 0 & -rQ & (1+r)Q \end{bmatrix}$$

$$\underline{Q}^T\ \underline{1} = \begin{bmatrix} (1+r)Q - (1+r)Q + 0 \\ -rQ + (1+2r)Q - (1+r)Q \\ 0 - rQ + (1+r)Q \end{bmatrix} = \begin{bmatrix} 0 \\ 0 \\ Q \end{bmatrix} = \underline{Q}_e$$